

Spring 5-2009

RAFT Synthesis of Water-Soluble, Stimuli-Responsive (Co)polymers and Post-Polymerization End Group Modification Via the Thiol-ene Reaction

Bing Yu

University of Southern Mississippi

Follow this and additional works at: <https://aquila.usm.edu/dissertations>

 Part of the [Polymer Chemistry Commons](#)

Recommended Citation

Yu, Bing, "RAFT Synthesis of Water-Soluble, Stimuli-Responsive (Co)polymers and Post-Polymerization End Group Modification Via the Thiol-ene Reaction" (2009). *Dissertations*. 1049.
<https://aquila.usm.edu/dissertations/1049>

This Dissertation is brought to you for free and open access by The Aquila Digital Community. It has been accepted for inclusion in Dissertations by an authorized administrator of The Aquila Digital Community. For more information, please contact aquilastaff@usm.edu.

The University of Southern Mississippi

RAFT SYNTHESIS OF WATER-SOLUBLE, STIMULI-RESPONSIVE
(CO)POLYMERS AND POST-POLYMERIZATION END GROUP MODIFICATION
VIA THE THIOL-ENE REACTION

by

Bing Yu

Abstract of a Dissertation
Submitted to the Graduate Studies Office
of The University of Southern Mississippi
in Partial Fulfillment of the Requirements
for the Degree of Doctor of Philosophy

May 2009

COPYRIGHT BY

BING YU

2009

The University of Southern Mississippi


RAFT SYNTHESIS OF WATER-SOLUBLE, STIMULI-RESPONSIVE
(CO)POLYMERS AND POST-POLYMERIZATION END GROUP MODIFICATION
VIA THE THIOL-ENE REACTION

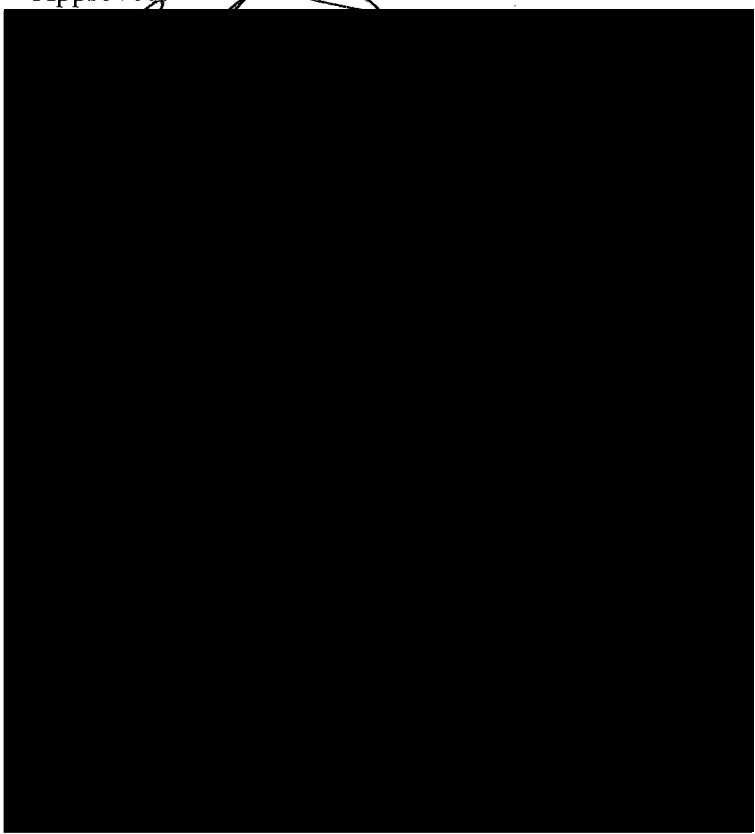
by

Bing Yu

A Dissertation

Submitted to the Graduate Studies Office
of The University of Southern Mississippi
in Partial Fulfillment of the Requirements
for the Degree of Doctor of Philosophy

Approved: 



May 2009

ABSTRACT

RAFT SYNTHESIS OF WATER-SOLUBLE, STIMULI-RESPONSIVE (CO)POLYMERS AND POST-POLYMERIZATION END GROUP MODIFICATION VIA THE THIOL-ENE REACTION

by Bing Yu

May 2009

A series of water-soluble, stimuli-responsive (co)polymers was synthesized via the reversible addition-fragmentation chain transfer (RAFT) polymerization. The end group of a RAFT polymer, poly(*N*-isopropylacrylamide), was modified to ene or yne function via thiol-ene click chemistry. The ene or yne end group subsequently underwent thiol-ene or thiol-yne addition affording mono- or di-functional end group.

First, three methacrylic monomers containing 2 or 3 pendent tertiary amine functional groups, 1,3-bis(dimethylamino)propan-2-yl methacrylate (**M1**), 1-(bis(3-(dimethylamino)propyl)amino)propan-2-yl methacrylate (**M2**), and 2-((2-(2-(dimethylamino)ethoxy)ethyl)methylamino)ethyl acrylate (**M3**), were synthesized via an acylation reaction between methacryloyl chloride and the corresponding aminoalcohol. All of these three monomers were successfully homopolymerized under RAFT conditions with 1-methyl-1-cyanoethyl dithiobenzoate (CPDB) as chain transfer agent (CTA). For each monomer, homopolymerization using two different CTA:Initiator ratio was conducted. The effect of the CTA:Initiator ratio on

the kinetics is in agreement with the prediction by RAFT mechanism. The stimuli-responsive properties of poly**M1**, poly**M2**, and poly**M3** in aqueous solution were tested and all the homopolymers shows reversible thermo-responsive and pH-responsive properties.

Second, a monomer with excellent biocompatibility, 2-(methacryloyloxy)ethyl phosphorylcholine (MPC), was homopolymerized in water via RAFT polymerization mediated by 4-cyanopentanoic acid dithiobenzoate (CTP). The prepared MPC homopolymer was used as a macro-CTA in the RAFT polymerization of four stimuli-responsive monomers, *N,N*-diethylacrylamide (**DEAm**), 4-vinylbenzoic acid (**VBZ**) *N*-(3-sulfopropyl)-*N*-methacrylooxyethyl-*N,N*-dimethylammonium betaine (**DMAPS**), and the newly synthesized *N,N*-di-*n*-propylbenzylvinylamine (**DnPBVA**), yielding a series of water-soluble, stimuli-responsive AB diblock copolymers. The stimuli-responsive properties of there copolymers were examined by a combination of ¹H NMR spectroscopy and dynamic light scattering. The results show that aggregates with varied sizes formed upon application of the corresponding stimulus (change of pH, temperature, or electrolyte concentration). And the removal of the stimulus caused the dissociation of the aggregates, proving the reversibility of the stimuli-responsive property.

Finally, a well-defined precursor homopolymer of *N*-Isopropylacrylamide (**NIPAm**) was prepared using RAFT polymerization in DMF at 70°C employing the CPDB as CTA. The dithiobenzoate end-groups were subsequently modified to give ene

or yne functional end groups via a thiol-ene click reaction catalyzed using a combination of octylamine and dimethylphenylphosphine to induce a thio-Michael reaction with either allyl methacrylate or propargyl acrylate. The conversion of the end-group was near quantitative according to ^1H NMR spectroscopy. The ene and yne groups were then reacted quantitatively via radical thiol-ene and radical thiol-yne reactions under UV-irradiation with three representative thiols yielding the mono and bis-end functional NIPAm homopolymers. The lower critical solution temperatures (LCST) were then determined for all NIPAm homopolymers using a combination of optical measurements and dynamic light scattering. Results show that the LCST varies depending on the chemical nature of the end-groups with measured values lying in the range 26-35°C.

To my wife and my parents
For their love and support

ACKNOWLEDGMENTS

I would like to thank my director, Dr. Andrew B. Lowe, and the other committee members, Dr. Mohamed O. Elasri, Dr. Charles E. Hoyle, Dr. Douglas S. Masterson and Dr. Hans J. Schanz, for their advice and support throughout my Ph.D. study.

I would like to thank all the members of the Lowe research group and all the members of the Department of Chemistry and Biochemistry.

I would like to thank the Cannon research group for the generous use of their dynamic light scattering instrument.

I would like to gratefully acknowledge the National Institutes of Health (NIH) for funding part of this research and MRSEC for also providing me financial support.

Deepest thanks are conveyed to my wife, Fei Cai, and my parents, for their selfless love and support.

TABLE OF CONTENTS

ABSTRACT	ii
DEDICATION	v
ACKNOWLEDGMENTS	vi
LIST OF TABLES	x
LIST OF FIGURES	xi
LIST OF SCHEMES.....	xv

CHAPTER

I. INTRODUCTION.....	1
1. Controlled Polymerization.....	1
1.1 The Criteria for Controlled Polymerization.....	2
1.2 Conventional Controlled Polymerizations.....	4
1.2.1 Living Anionic Polymerization (LAP).....	5
1.2.2 Living Cationic Polymerization (LCP).....	8
1.2.3 Ring-Opening Metathesis Polymerization (ROMP).....	11
1.3 Controlled Radical Polymerizations.....	13
1.3.1 Nitroxide-Mediated Polymerization	14
1.3.2 Atom Transfer Radical Polymerization (ATRP).....	17
1.3.2.1 Initiator.....	18
1.3.2.2 Transition-Metal Catalyst	19
1.3.2.3 Monomer.....	20
1.3.2.4 Reverse ATRP.....	21
1.3.3 Reversible Addition-Fragmentation Chain Transfer (RAFT) Polymerization	22
1.3.3.1 Introduction.....	22
1.3.3.2 Mechanism of RAFT polymerization	23
1.3.3.3 Kinetics of RAFT polymerization	25
1.3.3.4 MW control of RAFT polymerization	30
1.3.3.5 Chain Transfer Agent (CTA) for RAFT polymerization..	31

1.3.3.6	Synthetic Routes to RAFT CTAs.....	37
1.3.3.7	Monomers suitable for RAFT.....	41
1.3.3.8	Advanced macromolecular architecture via RAFT polymerization	45
1.3.3.9	Removal of the end group of RAFT polymer.....	53
1.3.4	Tellurium-Mediated Radical Polymerization (TERP).....	53
2.	Stimuli-Responsive Water-Soluble (Co)Polymers.....	56
2.1	Water-Soluble Polymers	56
2.1.1	Non-Ionic Water-Soluble Polymers	56
2.1.2	Ionic Water-Soluble Polymers	57
2.2	Polymeric Micelles	64
2.3	Self-Assembly of Stimuli-Responsive Copolymers	66
2.4	Experimental Technique to Study Self-Assembly.....	68
2.4.1	NMR Spectroscopy.....	70
2.4.2	DLS and SLS	71
2.4.3	Fluorescence Spectroscopy.....	72
3.	Thiol-Ene Chemistry.....	73
3.1	Conventional Thiol-Ene Chemistry.....	73
3.2	Applications of Thiol-Ene Reaction in Polymer Synthesis	75
II.	OBJECTIVES OF RESEARCH	80
III.	SYNTHESIS OF DI- AND TRI- TERTIARY AMINE CONTAINING METHACRYLIC MONOMERS AND THEIR (CO)POLYMERIZATION VIA RAFT	84
1.	Introduction.....	84
2.	Experimental.....	87
3.	Results and Discussion	93
4.	Summary and Conclusions	108
IV.	RAFT SYNTHESIS AND STIMULUS-INDUCED SELF-ASSEMBLY IN WATER OF COPOLYMERS BASED ON THE BIOCOMPATIBLE MONOMER 2-(METHACRYLOYLOXY)ETHYL PHOSPHORYLCHOLINE	109
1.	Introduction.....	109
2.	Experimental.....	112
3.	Results and Discussion	116
4.	Summary and Conclusions	135
V.	SEQUENTIAL THIOL-ENE/THIOL-ENE AND THIOL-ENE/THIOL-YNE REACTIONS AS A ROUTE TO WELL-DEFINED MONO AND BIS END-FUNCTIONALIZED POLY(N-ISOPROPYLACRYLAMIDE).....	136

1. Introduction.....	136
2. Experimental.....	142
3. Results and Discussion	145
4. Summary and Conclusions	166
VI. SUMMARY AND CONCLUSIONS.....	168
VII. FUTURE WORK	171
REFERENCES.....	173

LIST OF TABLES

Table I-1 Experimental techniques for micelle characterization.	69
Table III-1. Summary of composition, conversion, M_n theory, M_n experimental and polydispersity index for a series of M1 -lauryl methacrylate statistical copolymers.	102
Table III-2. Summary of composition, conversion, M_n theory, M_n experimental and polydispersity index for a series of M3 -hexyl methacrylate and M3 -lauryl methacrylate statistical copolymers.	103
Table IV-1. Summary of M_n experimental, M_p experimental, polydispersity index, and composition of synthesized AB diblock copolymers based on MPC.	123
Table V-1. Summary of the number average molecular weights determined by size exclusion chromatography and NMR spectroscopy, the polydispersity indices, average calculated degrees of polymerization, and lower critical solution temperatures as determined optically and by dynamic light scattering for the precursor PNIPAm ₅₀ homopolymer and the series of end-modified PNIPAm homopolymers.	152

LIST OF FIGURES

Figure I-1. M_n -Conversion plot for an ideal controlled/living polymerization.	3
Figure I-2. Silyl ketene acetal initiator used in GTP.....	7
Figure I-3. Structure of traditional and newly-developed nitroxides.....	16
Figure I-4. Examples of initiators used in ATRP.....	19
Figure I-5. Examples of transition-metal catalyst used in ATRP.	20
Figure I-6. Ideal kinetic plot for a RAFT polymerization and possible causes of deviations from idealized behavior.....	27
Figure I-7. Idealized M_n vs conversion plot for a RAFT polymerization and possible causes for deviations.	31
Figure I-8. General structures of RAFT CTAs and examples of the four types of CTA. .	31
Figure I-9. Most versatile CTAs for RAFT polymerization.	37
Figure I-10. Examples of functional styrenic monomers polymerized by RAFT.....	42
Figure I-11. Examples of acrylate and acrylamide monomers suitable for RAFT polymerization.	43
Figure I-12. Examples of methacrylate and methacrylamide monomers suitable for RAFT polymerization.	44
Figure I-13. Graphic illustration of several available (co)polymer architectures via RAFT.	45
Figure I-14. R group approach CTAs for the preparation of star (co)polymers via RAFT.	50
Figure I-15. Z group approach CTAs for the preparation of star (co)polymers via RAFT.	51
Figure I-16. Organotellurium mediators for TERP.	54
Figure I-17. Examples of non-ionic WSP monomers.	57
Figure I-18. Illustrative structures of the ionic polymer family.....	58
Figure I-19. Examples of cationic and anionic monomers.	59
Figure I-20. Examples of four different kinds of methacrylate-based betaines.....	60
Figure I-21. Schematic illustration of polyelectrolyte effect.	63
Figure I-22. Schematic illustration of anti-polyelectrolyte effect.....	64
Figure I-23. Reversible self-assembly of AB diblock copolymers.....	65

Figure I-24. Reversible micellization of block copolymers comprised of AMPS and AMBA in aqueous solutions upon the change of pH.....	67
Figure I-25. The normal and inverse micellizations of the NIPAm-VBZ diblock copolymer under different stimuli, e.g. pH and temperature.	68
Figure I-26. ¹ H NMR spectra of the P(NIPAm-b-VBZ) copolymer at pH 11.3 and room temperature (A), and the same AB diblock copolymer at pH 1.1 and room temperature (B).	71
Figure III-1. a/b : ¹ H and ¹³ C NMR spectra of 1,3-bis(dimethylamino)propan-2-yl methacrylate (M1) recorded in CDCl ₃ ; c/d: ¹ H and ¹³ C NMR spectra of 1-(bis(3-(dimethylamino)propyl)amino)propan-2-yl methacrylate (M2) recorded in CDCl ₃ , and e/f: ¹ H and ¹³ C NMR spectra of 2-((2-(2-(dimethylamino)ethoxy)ethyl)methylamino)ethyl methacrylate (M3) recorded in CDCl ₃	95
Figure III-2. Pseudo first order kinetic plots for the homopolymerizations of M1 at CTA:AIBN ratios of 2:1 and 5:1, under bulk conditions, at 70 °C.	97
Figure III-3. Pseudo first order kinetic plots for the homopolymerizations of M2 at CTA:AIBN ratios of 2:1 and 5:1, under bulk conditions, at 70 °C.	98
Figure III-4. Pseudo first order kinetic plots for the homopolymerizations of M3 at CTA:AIBN ratios of 2:1 and 5:1, under bulk conditions, at 70 °C.	98
Figure III-5. M _n vs conversion and polydispersity index vs conversion for the M1-M3 homopolymerizations at CTA:AIBN ratios of 2:1 and 5:1, under bulk conditions, at 70 °C.	100
Figure III-6. a. ¹ H NMR spectrum, recorded in CDCl ₃ , for a 1:1 statistical copolymer of M1 with LAMA, and b. The SEC trace (RI signal) for the same M1-stat -LAMA copolymer.	104
Figure III-7. Series of digital pictures of 1 wt % aqueous solutions of M1-M3 homopolymers demonstrating the reversible, temperature-induced phase transitions.	106
Figure III-8. Digital pictures of a 1 wt % solution of an M2 homopolymer at 23°C and pH values of 10.43 (a) and 12.68 (b) demonstrating the pH induced phase transition.	107
Figure IV-1. Chemical structures of monomers used in this study.	116
Figure IV-2. ¹ H (a) and ¹³ C (b) NMR spectra, recorded in CDCl ₃ , of <i>N,N</i> -di- <i>n</i> -propylbenzylvinylamine.	117
Figure IV-3. Aqueous size exclusion chromatogram (a) (RI signal) of a polyMPC homopolymer, and the ¹ H NMR spectrum (b) of the same homopolymer	

recorded in D ₂ O, with peak assignments.	119
Figure IV-4. Aqueous size exclusion chromatograms (RI signal) of examples of PMPC-based AB diblock copolymers. P(MPC ₅₈ - <i>b</i> - DMAPS ₄₂) (a) and P(MPC ₈₂ - <i>b</i> - DEAm ₁₈) (b) demonstrating successful block copolymer formation.	124
Figure IV-5. ¹ H NMR spectra of the P(MPC ₅₆ - <i>b</i> - DEAm ₄₄) at ambient temperature recorded in D ₂ O.	127
Figure IV-6. ¹ H NMR spectra of the P(MPC ₅₆ - <i>b</i> - DEAm ₄₄) at 50°C recorded in D ₂ O.	127
Figure IV-7. Size distributions measured by dynamic light scattering as a function of temperature highlighting the formation of aggregates.	128
Figure IV-8. ¹ H NMR spectra, recorded in D ₂ O, of the P(MPC ₅₀ - <i>b</i> - VBZ ₅₀) at ambient temperature under basic conditions.	129
Figure IV-9. ¹ H NMR spectra, recorded in D ₂ O, of the P(MPC ₅₀ - <i>b</i> - VBZ ₅₀) at ambient temperature under acidic conditions.	129
Figure IV-10. Size distributions of the P(MPC ₅₀ - <i>b</i> - VBZ ₅₀) measured by dynamic light scattering as a function of pH highlighting the formation of aggregates.	130
Figure IV-11. ¹ H NMR spectra, recorded in D ₂ O, of the P(MPC ₇₀ - <i>b</i> - DnPBVA ₃₀) at ambient temperature under acidic conditions.	130
Figure IV-12. ¹ H NMR spectra, recorded in D ₂ O, of the P(MPC ₇₀ - <i>b</i> - DnPBVA ₃₀) at ambient temperature under basic conditions.	131
Figure IV-13. Size distributions of the P(MPC ₇₀ - <i>b</i> - DnPBVA ₃₀) measured by dynamic light scattering as a function of pH highlighting the formation of aggregates.	131
Figure IV-14. Experimentally determined hydrodynamic size distributions of a 1 wt% solution of the P(MPC ₇₆ - <i>b</i> - DMAPS ₂₄) copolymer in 0.5 M NaCl and deionized water demonstrating the ability to form self-assembled aggregates.	132
Figure V-1. (A) Size exclusion chromatographic (SEC) trace of the parent poly(N-isopropylacrylamide) homopolymer and (B) ¹ H NMR spectrum, recorded in CDCl ₃ , of the parent poly(N-isopropylacrylamide) homopolymer highlighting the presence of the phenyl end-group and the calculation of the absolute degree of polymerization.	148
Figure V-2. (A) ¹ H NMR spectrum, recorded in CDCl ₃ , of the propargyl-end functionalized PNIPAm ₅₀ verifying quantitative end-group modification with the SEC trace shown inset, and (B) ¹ H NMR spectrum, recorded in CDCl ₃ , of the allyl-end functionalized PNIPAm ₅₀ verifying quantitative end-group modification with the resulting SEC trace shown inset.	151
Figure V-3. Chemical structures of the three representative, commercially available, thiols	

employed in the radical thiol-ene and radical thiol-yne end-group reactions.	154
Figure V-4. ^1H NMR spectra, recorded in CDCl_3 for (A) PNIPAm ₅₀ -S-ALMA-S-HexOH, (B) PNIPAm ₅₀ -S-PROPA-(S-HexOH) ₂	155
Figure V-5. Digital pictures demonstrating the reversible temperature-induced phase separation and chemical structures of 1 wt% solutions of (A) PNIPAm ₅₀ (B) PNIPAm ₅₀ -S-ALMA.	163
Figure V-6. Plot of Z-average hydrodynamic diameter vs. temperature for a 1 wt% aqueous solution of PNIPAm ₅₀ demonstrating the a determination of the LCST.	166

LIST OF SCHEMES

Scheme I-1. Initiation step in living anionic polymerization with <i>n</i> -BuLi as the initiating species.....	5
Scheme I-2. Propagation step of living anionic polymerization.....	6
Scheme I-3. Termination of a living polystyryl carbanion by water.....	6
Scheme I-4. Mechanism of nucleophilic GTP.....	7
Scheme I-5. Mechanism for the LCP of iso-butyl ether.....	8
Scheme I-6. Common monomers for employed in LCP.....	9
Scheme I-7. Propagation and chain transfer reaction in cationic ring-opening polymerization.....	10
Scheme I-8. Examples of monomers for cationic ring-opening polymerization.....	11
Scheme I-9. Olefin metathesis and ROMP.....	12
Scheme I-10. Generic structures of Schrock and Grubbs initiators.....	13
Scheme I-11. General mechanisms of NMP, ATRP, and RAFT.....	14
Scheme I-12. Simplified mechanism of NMP.....	15
Scheme I-13. Simplified mechanism of ATRP.....	18
Scheme I-14. Mechanism of Reverse ATRP.....	21
Scheme I-15. Generally accepted mechanism of RAFT polymerization.....	24
Scheme I-16. Canonical forms of xanthates and dithiocarbamates.....	34
Scheme I-17. Guideline for the selection of Z group of RAFT CTAs.....	35
Scheme I-18. Guideline for the selection of R group of RAFT CTAs.....	36
Scheme I-19. General synthetic route to dithioesters.....	38
Scheme I-20. Synthesis of tertiary dithioester via a radical reaction.....	38
Scheme I-21. Synthetic routes to dithiocarbamate CTAs.....	39
Scheme I-22. Synthetic route to xanthate CTAs.....	40
Scheme I-23. Synthetic route to symmetrical and unsymmetrical trithiocarbonates.....	40
Scheme I-24. Synthetic route to AB diblock copolymer via RAFT polymerization by sequential monomer addition.....	47
Scheme I-25. Synthetic route to ABA triblock copolymers via RAFT polymerization mediated by difunctional R groups or difunctional Z groups CTA.....	48

Scheme I-26. Grafting polymer prepared via RAFT polymerization to gold nanoparticles.	52
Scheme I-27. Various paths for the removal of the dithiocarbonyl end group of the polymer prepared via RAFT polymerization.	53
Scheme I-28. Two mechanisms of TERP: thermal dissociation and degenerative chain transfer.....	54
Scheme I-29. Synthetic routes to sulfobetaines.	61
Scheme I-30. Synthetic routes to carboxybetaines.	61
Scheme. I-31 Synthetic routes to ammonium alkoxydicyanoethenolates	62
Scheme I-32. Synthetic routes to phosphobetaines.....	62
Scheme I-33. Mechanism of thermally induced and photo-initiated thiol-ene reactions..	74
Scheme I-34. Thiol-Michael addition of conjugated ethylene and acetylene.....	74
Scheme I-35. General mechanism of photo-initiated thiol-ene polymerization.....	76
Scheme I-36. Radical mediated thiol-ene polymerization under the presence of oxygen.	76
Scheme I-37. Surface modification via thiol-ene <i>click</i> chemistry.	77
Scheme I-38. Synthesis of dendrimers via thiol-ene <i>click</i> chemistry.	78
Scheme I-39. Convergent synthesis of 3-arm star polymer via thiol-ene click chemistry.	79
Scheme III-1. Synthetic outline for the preparation of M1-M3	94
Scheme IV-1. Synthetic outline for the preparation of an MPC homopolymer.	118
Scheme IV-2. Idealized, reversible self-assembly, with the possible formation of either micelles or vesicles, of 'smart' AB diblock copolymers based on MPC.	126
Scheme V-1. (A) Mechanism for the radical mediated thiol-ene reaction with a terminal ene, and (b) anionic chain mechanism for the amine/phosphine mediated nucleophilic thiol-ene reaction with an acrylate.	137
Scheme V-2. Proposed mechanism for the radical mediated thiol-yne reaction with a terminal alkyne.....	139
Scheme V-3. Reversible addition-fragmentation chain transfer polymerization of N-isopropylacrylamide and subsequent end-group modifications, via a combination of nucleophilic thiol-ene/radical thiol-ene and nucleophilic thiol-ene/radical thiol-yne pathways.....	146

CHAPTER I

INTRODUCTION

1. Controlled Polymerization

Controlled polymerization enables the synthesis of (co)polymers with predictable molecular weights, narrow molecular weight distributions, and tailored structures/architectures, including block copolymers, graft copolymers, branched (co)polymers, and star (co)polymers. Furthermore, it enables the attachment of functional groups at desired locations on the polymer backbone or the side chain. These properties of controlled/living polymerization (CLP) allow for the preparation of polymeric materials with well-defined functions for a variety of practical applications, and are drawing increasing interest from researchers. Currently, there are a variety of controlled/living polymerization techniques reported based on different mechanisms: anionic/cationic living polymerization, ring-opening metathesis polymerization (ROMP), stable free-radical polymerization (SFRP), atom transfer radical polymerization (ATRP), tellurium-mediated radical polymerization (TERP), and reversible addition-fragmentation chain transfer (RAFT) polymerization.¹⁻³

1.1 The Criteria for Controlled Polymerization

According to IUPAC terminology, a living polymerization is defined as “*a chain growth polymerization that proceeds in the complete absence of termination or chain transfer reactions*”.⁴ However, this criterion is impossible to meet for most modern CLP techniques. Thus, the terms *living polymerization with reversible termination* or *living polymerization with reversible chain transfer* are more precise or suitable to describe the CLP techniques discussed herein.

Experimentally, a combination of the following criteria is used to judge whether a polymerization is living or not⁵:

(1) The number average molecular weight (M_n) is a linear function of conversion.

In a living polymerization, under ideal conditions, monomer adds evenly to each propagating chain, thus, the M_n can be expressed by Equation (1):

$$M_n = \text{grams of monomer consumed} / \text{moles of propagating chain} \quad (1)$$

This can be better illustrated by plotting M_n data versus conversion, a linear relationship should be observed as shown in Figure I-1.

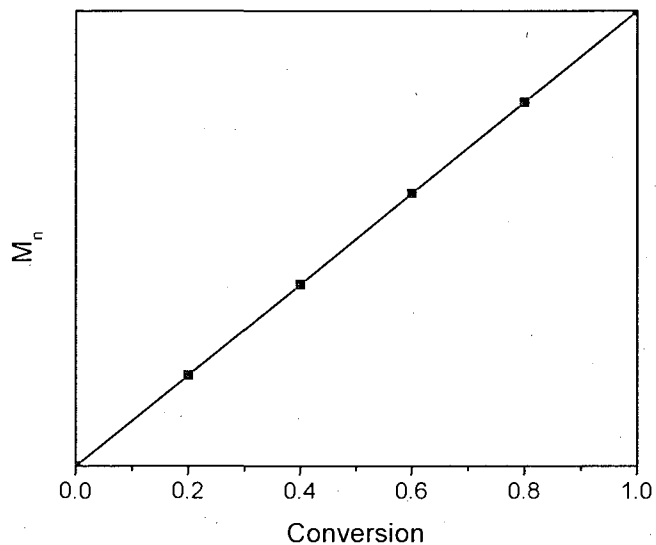


Figure I-1. M_n -Conversion plot for an ideal controlled/living polymerization.

(2) The molecular weight can be controlled by the stoichiometry of the reaction.

In Equation (1), the moles of propagating chains are determined by the initiating system employed, therefore the M_n is actually predetermined by the agents added to the system. Obviously, this criterion is sensitive to the presence of impurities which could terminate the propagating chains and consequently increase the observed molecular weight.

(3) The molecular weight distribution of the prepared polymer is narrow.

In an ideal living polymerization, all active propagating species are equally susceptible to monomer addition and the irreversible chain transfer/termination reactions do not occur, thus, the polymer product should be near monodisperse. Typical polydispersity indices (PDI) for polymers prepared via living polymerization technique

are greater than 1.0 and less than 1.3; polymers with PDI greater than 1.5 are usually considered as non-controlled.

(4) The prepared polymer is able to elongate upon further addition of monomer.

This feature of CLP technique is often used to prepare block copolymers by sequential monomer addition.

1.2 Conventional Controlled Polymerizations

Conventional CLP techniques, including living anionic polymerization and living cationic polymerization, were the only known CLP techniques before the discovery of controlled/living radical polymerization in the 1990's. Ionic polymerizations and radical polymerization differ by the nature of the propagating species. In ionic polymerizations, the propagating species is either a carbocation or carbanion, while in radical polymerizations, the propagating species is a radical. Ionic polymerization usually goes much faster than radical polymerization, but the choice of monomer is very limited. For cationic polymerization, monomers are limited to those with electron-donating substituents on carbon-carbon double bonds; for anionic polymerization, monomers are limited to those with electron-withdrawing substituents on carbon-carbon double bonds. This is due to the requirement for stabilization of the propagating species in ionic polymerization. Also, it is challenging to conduct a successful ionic polymerization in a

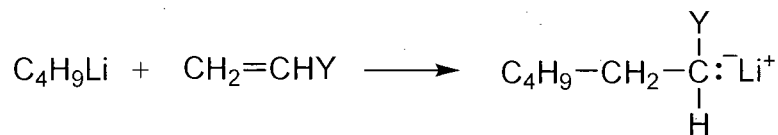
controlled fashion. Several important factors need to be carefully chosen, including solvent, temperature, initiator, and the purity of the system (ionic polymerizations do not tolerate even a trace amount of impurity).²

1.2.1 Living Anionic Polymerization (LAP)

The first example of a CLP was reported in 1956 by Szwarc, who described a living anionic polymerization of styrene at -80°C , initiated by sodium naphthalenide.^{6,7} The active carbanion is quite stable and is quenched by certain reagents such as water, alcohols, acids, and esters. The produced polymer is able to chain extend upon the addition of more monomer, and it is able to form block copolymers upon the addition of a different comonomer.

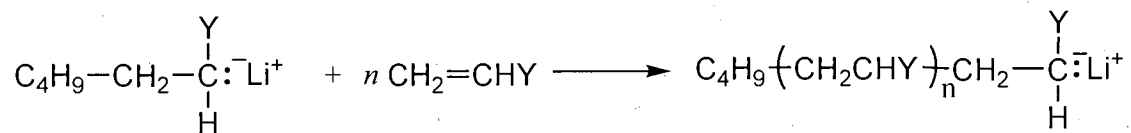
Typical initiators for anionic polymerizations include a variety of basic (nucleophilic) species.^{2,8-13} Among them, alkyllithium compounds are probably the most widely used due to their good solubility in hydrocarbon solvents (Scheme I-1).²

Initiation:



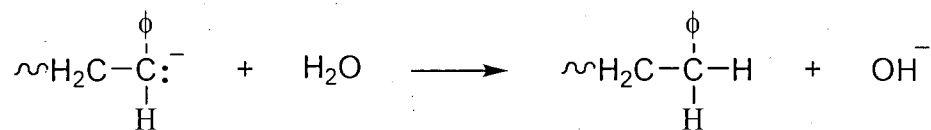
Scheme I-1. Initiation step in living anionic polymerization with *n*-BuLi as the initiating species.

Propagation:



Scheme I-2. Propagation step of living anionic polymerization.

To achieve living anionic polymerization, the temperature usually needs to be kept at ca. -78°C , in order to minimize side reactions and yield (co)polymers with low polydispersity. The choice of solvents is limited for LAP. Esters, ketones, halogenated, and protic solvents cannot be used because of their ability to react with carbanions. Polymerization should be conducted in a thoroughly clean and dry environment since trace amounts of moisture will kill the propagating carbanions (in Scheme I-3). Oxygen and carbon dioxide can also react with propagating carbanions forming peroxy and carboxy anions, which will also stop chain propagation.¹⁴



Scheme I-3. Termination of a living polystyryl carbanion by water.

Group transfer polymerization (GTP) is an alternative LAP technique, which offers the possibility of conducting LAP at moderate temperatures ($0 - 80^\circ\text{C}$).¹⁵ GTP also broadens the choice of solvents and tolerates impurities, such as water and oxygen, slightly more than traditional LAP. GTP requires the use of a silyl ketene acetal initiator

(Figure I-2). There are nucleophilic GTP and electrophilic GTP.² Electrophilic GTP proceeds via an associative or concerted mechanism, which is different to the anionic polymerization mechanism. Nucleophilic GTP proceeds via a dissociative mechanism, in which the propagating species is anionic, similar to the propagating species in anionic polymerizations (Scheme I-4). A main drawback of GTP is that it only really works for methacrylates monomer.

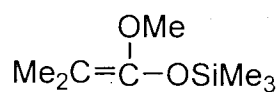
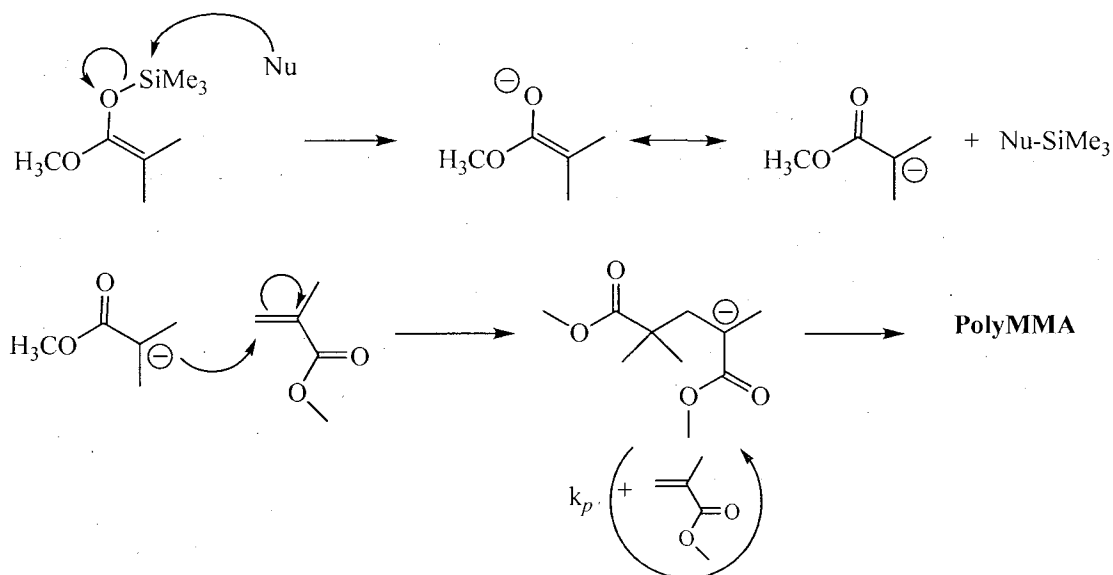


Figure I-2. Silyl ketene acetal initiator used in GTP.

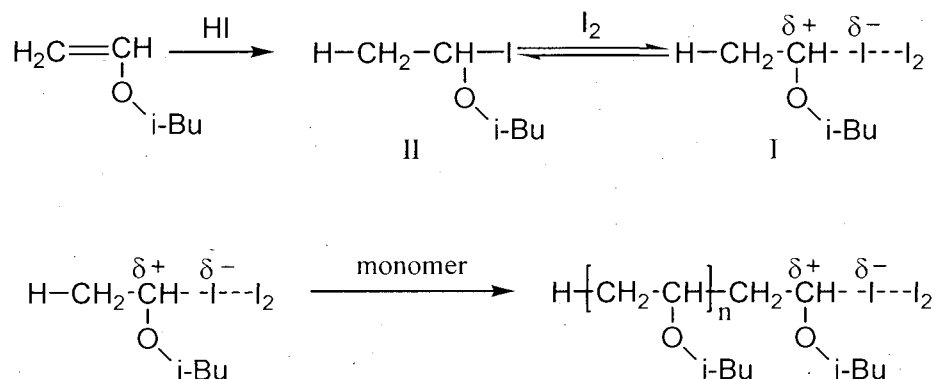


Scheme I-4. Mechanism of nucleophilic GTP.

1.2.2 Living Cationic Polymerization (LCP)

Living Cationic Polymerization of Vinyl Monomers

About 30 years after the discovery of LAP, Sawamoto et al. reported the first example of LCP in 1984, when they described the polymerization of isobutyl vinyl ether initiated by a hydrogen iodide/iodine mixture.¹⁶ The propagating species I is stabilized by a dynamic equilibrium with a dormant complex II (Scheme I-5).¹⁷ Subsequently, Faust and Kennedy reported the LCP of isobutene, which was achieved by introducing, to the polymerization process, a mixture of tertiary alcohols, esters, or ethers, with strong Lewis acids in conjunction with electron pair donors, such as tert-amyl alcohol + BCl₃ + 1-methyl-2-pyrrolidone.¹⁸

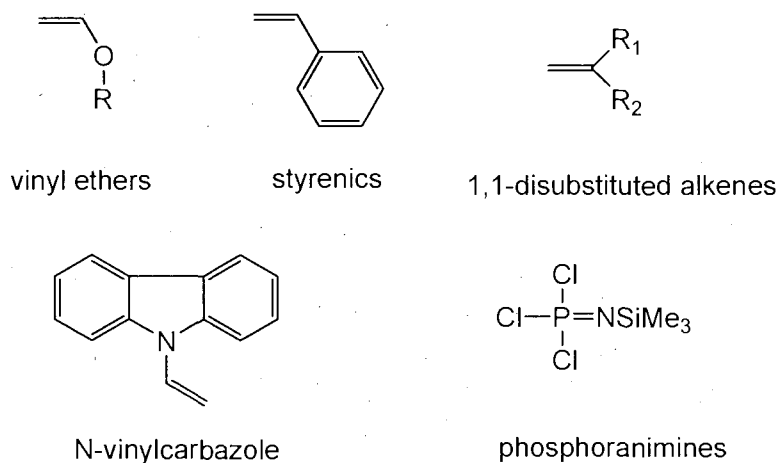


Scheme I-5. Mechanism for the LCP of iso-butyl ether.¹⁷

A truly LCP is relatively difficult to achieve compared with LAP. Even in a well-purified system every component is carefully chosen so that no nucleophile is present to terminate the cationic propagating species. Unfortunately, the polymerization

may still be poorly controlled due to a facile built-in termination reaction associated with cationic polymerization. Specifically, the transfer of β -protons to monomer, counter ion or some other basic species in the polymerization medium.² To minimize β -proton transfer, basic components also need to be avoided, but this is essentially impossible since monomer is itself a base. So, the major hurdle to achieving LCP is minimizing β -proton transfer to monomer. This can be accomplished by conducting cationic polymerization at lower temperatures to suppress transfer reactions (the activation energy for transfer is greater than that for propagation). At lower temperature, the lifetime of the propagating cationic species is extended so that significant propagation occurs prior to any undesirable β -protons transfer.

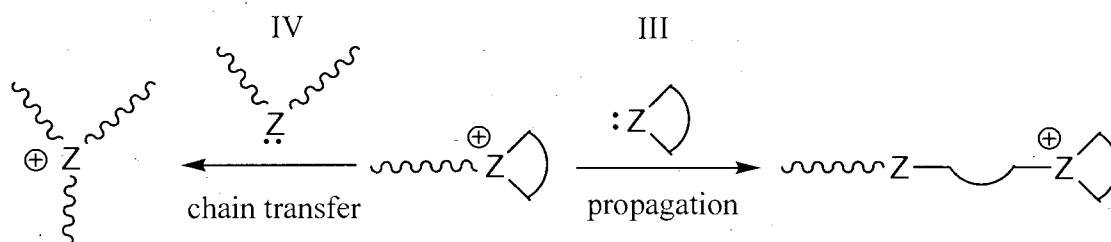
The three most important families of monomers for LCP are: vinyl ethers, 1,1-disubstituted alkenes and styrenics, due to their ability to stabilize the active carbocation centers.^{8-10,16-22} Some other vinyl monomers of less importance polymerized by LCP include N-vinylcarbazole and phosphoranimines,^{23,24} Scheme I-6.



Scheme I-6. Common monomers for employed in LCP.

Cationic Ring-Opening Polymerizations

Another important example of LCP is cationic ring-opening polymerization in which the active propagating species is an onium ion. The main driving force of ring-opening polymerization is the release of ring-strain associated with the cyclic monomer. For this reason, the ring-opening polymerization of 6-membered ring monomers is not favored due to the inherent stability of their ring structure.² A large number of heterocyclic compounds have been polymerized by cationic ring-opening mechanism, but only a few of them have been polymerized in a living fashion. This is due to the chain transfer reaction of the active onium ion to the heteroatom of a formed polymeric chain instead of that of a monomer, Scheme I-7. The formed tri-arm polymeric onium ion has less reactivity than the cyclic onium ion because of no ring-strain, and therefore leads to termination.¹

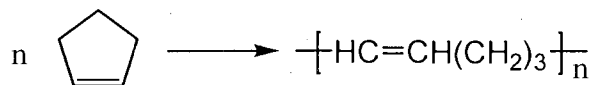


Scheme I-7. Propagation and chain transfer reaction in cationic ring-opening polymerization.

In order to minimize these transfer/termination reactions, the cyclic monomer III needs to be more nucleophilic than the linear counterpart IV, so that chain transfer is not favored. Or, during the polymerization, polymer IV isomerizes to form a new polymer species which has a lower nucleophilicity than monomer III. Another possibility to



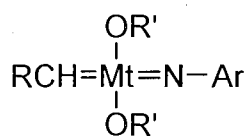
olefin metathesis



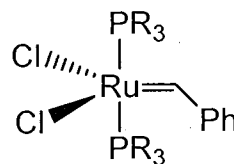
ROMP

Scheme I-9. Olefin metathesis and ROMP.

Better control of the polymerization process was achieved with the discovery and use of the Schrock and Grubbs initiators,^{25,26} Scheme I-10. Narrowly distributed polymers can be prepared via ROMP catalyzed by these two types of initiators and only modest temperatures are required. Schrock initiators are organometallic compounds based on Mo or W while Grubbs initiators are based on Ru. Schrock initiators are sensitive to air and moisture, and not tolerant to monomers with oxygen-containing functional groups (-OH, -C=O). Grubbs initiators are relatively tolerant to water and a variety of functional groups. Furthermore, the catalytic property of Grubbs initiators can be finely tuned by using different ligands attached to Ru. Currently, Grubbs' first and second generation initiators, and the Hoveyda-Grubbs initiators are probably the most important commercially available catalysts. In comparison with Grubbs's first generation initiator, the other two have better thermal stability and higher propagation rates in ROMP. However, the very fast propagation rates observed for Grubbs's second generation catalyst do not allow for living ROMP conditions.



Schrock catalyst



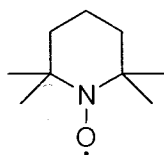
Grubbs catalyst

Scheme I-10. Generic structures of Schrock and Grubbs initiators.

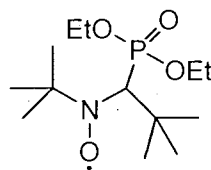
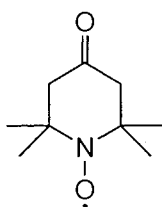
1.3 Controlled Radical Polymerizations

For about 40 years after the first example of LAP was reported, the attempt of researchers to find radical analog to LAP returned no success. In 1982, Otsu reported the radical polymerization employing *iniferter* (shorthand for **initiator-transfer agents-terminator**) which created a fast equilibrium between active free radicals and their dormant complexes.^{27,28} However, the dormant complexes still underwent slow termination leading to uncontrolled polymerizations. Although Otsu's discovery is not a living polymerization technique, it revealed a very important principle of controlled/living radical polymerization, i.e. the fast equilibrium between the propagating radical and their dormant complexes. In the 1990s, several controlled/living radical polymerization techniques were reported in succession, including: stable free radical polymerization (SFRP), best exemplified by nitroxide-mediated polymerization (NMP), atom transfer radical polymerization (ATRP), and reversible addition-fragmentation chain transfer (RAFT) polymerization, the general mechanisms of the three technique are shown in Scheme I-11. In NMP and ATRP, the equilibrium between the active

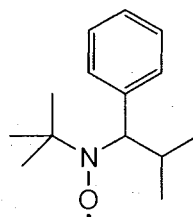
The most commonly used mediating agent for NMP, at least initially, was the commercially available 2,2,6,6-tetramethylpiperidine-1-oxyl (TEMPO).³³ The TEMPO-mediated polymerization works well for styrenic monomers but confers little control for many other common vinyl monomers. Recently, researchers developed improved nitroxides DEPN (now available under the trade name of SG1) and 2,2,5-trimethyl-4-phenyl-3-azahexane-3-oxy (Figure I-3) capable of mediating the controlled polymerization of a wider range of monomer, such as acrylates, acrylamides, 1,3-dienes, and acrylonitrile. The most significant difference between the newly-designed nitroxides and TEMPO is the presence of a hydrogen atom on one of the α -carbon to the nitrogen atom. Interestingly, the hydrogen on the α -carbon is traditionally considered a feature decreasing the stability of nitroxide radicals.³³⁻³⁵



TEMPO

N-tert-butyl-1-diethylphosphono-2,2-dimethylpropyl nitroxide
(DEPN)

4-oxo-TEMPO



2,2,5-trimethyl-4-phenyl-3-azahexane-3-oxy

Figure I-3. Structure of traditional and newly-developed nitroxides.

1.3.2 Atom Transfer Radical Polymerization (ATRP)

In 1994/95, ATRP was introduced by Matyjaszewski et al.^{36,37} and independently by Sawamoto et al.³⁸⁻⁴⁰ The general mechanism of ATRP is shown in Scheme I-13. The initiation step usually involves an alkyl halide reacting with a metal complex in a lower oxidation state. Through a redox process, active radicals capable of propagating are generated and the metal complex goes to a higher oxidation state. ATRP operates on a similar principle to NMP, i.e. via the reversible end-capping of propagating radicals to form a dormant non-propagating species. The difference is that in ATRP the reversible process is achieved via a redox reaction catalyzed by a transition metal species. The transition metal species M_t^n (oxidation state = n) acts as the activator facilitating the homolytic cleavage of the terminal C-X (X = halogen) bond to generate the active propagating species, while the oxidation state of the transition metal increases by one at the meantime, e.g. M_t^n becomes $X-M_t^{n+1}$. The complex $X-M_t^{n+1}$ acts as a radical deactivator, which readily reacts with the propagating radicals and forms the dormant polymeric chain end-capped by X group with the concomitant formation of M_t^n . The equilibrium is similar to that in NMP, so that the concentration of active propagating radicals is kept very low and therefore the probability of bimolecular termination is significantly reduced, leading to a living polymerization. ATRP, like NMP, is also a self-regulating process based on the *persistent radical effect*.^{31,32}

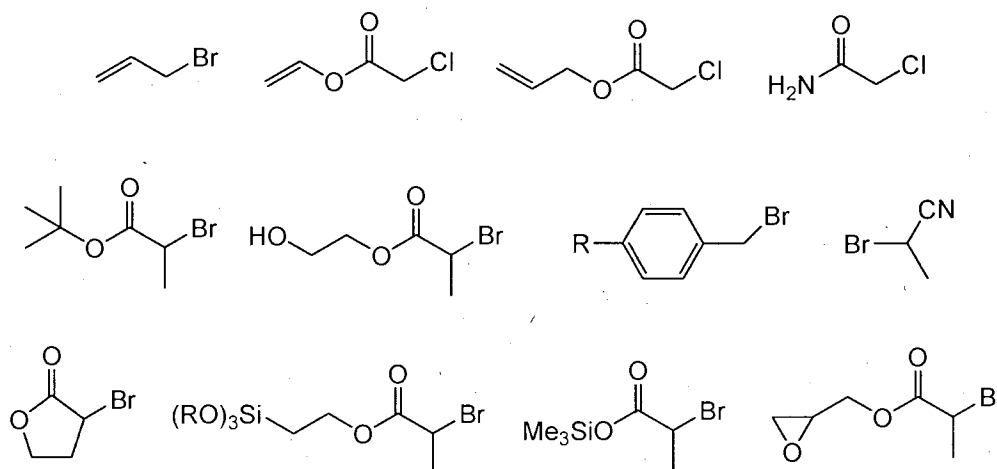


Figure I-4. Examples of initiators used in ATRP.

1.3.2.2 Transition-Metal Catalyst

In the most common ATRP system, Cu(I) is the activator and Cu(II) is the deactivator. However, the choice of the transition metal is not limited to Cu. Theoretically, a transition metal able to undergo a one electron redox reaction is suitable for ATRP. For example, other catalysts based on Ru, Fe, Pd, Ni, Rh, Mo, and Re have been reported, shown in Figure I-5. It is worth noting that the transition metal complex is usually less stable in the lower oxidation state, which requires the careful storage of the metal complex catalysts, i.e. care must be taken to avoid an oxidizing environment. In some cases, the metal complex needs to be freshly prepared prior to use for a successful ATRP. Also, the choice of other required reagents is limited to those with a limited oxidizing ability.

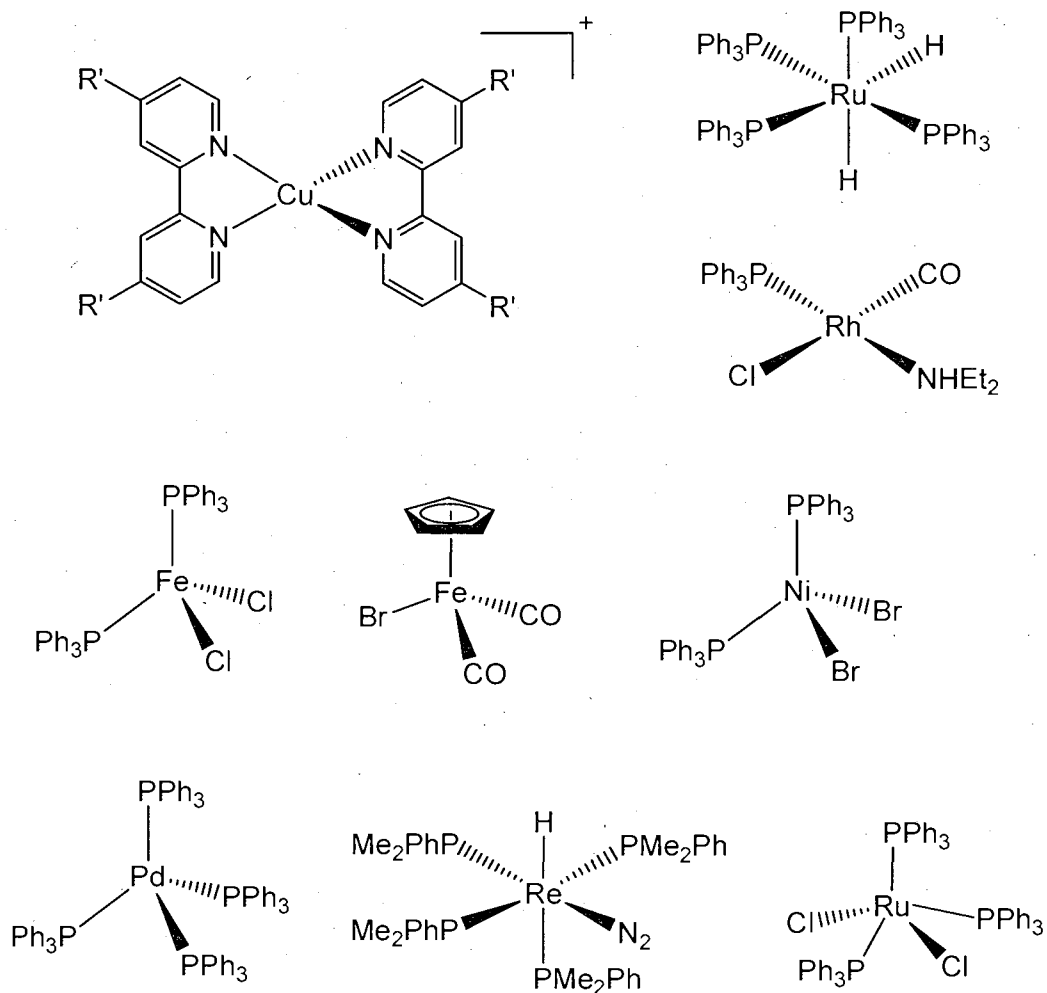


Figure I-5. Examples of transition-metal catalyst used in ATRP.³⁶⁻⁴⁵

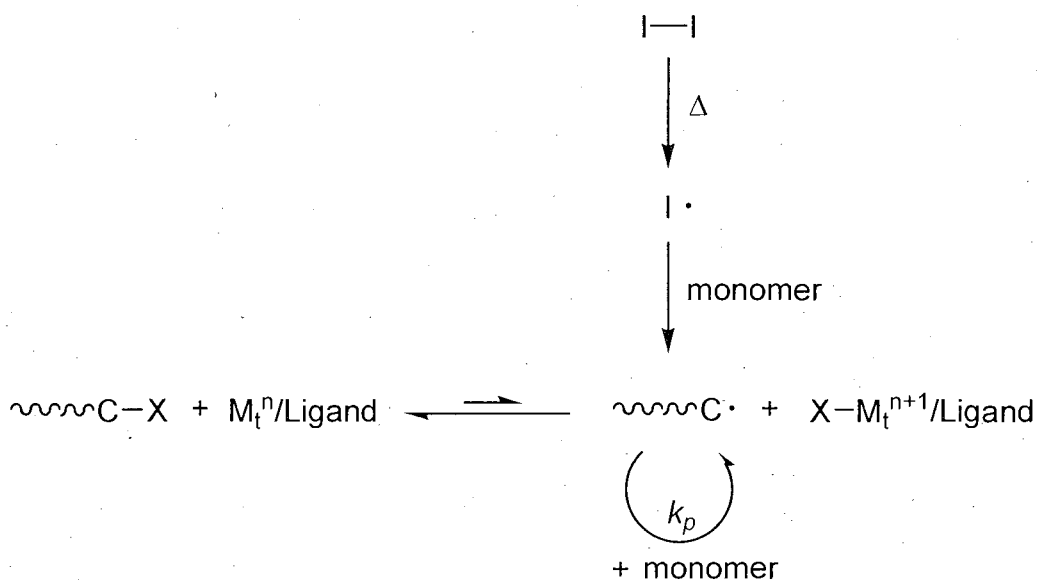
1.3.2.3 Monomer

ATRP is applicable to a wider range of monomers than NMP with nearly all commonly used vinyl monomers with activated double bonds, including acrylates, methacrylates, styrenics, acrylonitrile, acrylamides, and methacrylamides, being susceptible to polymerization.³⁶⁻⁵⁹ However, monomers with labile hydrogen atoms, such as acid-containing species, can be problematic due to their ability to competitively

complex to the transition metal and/or interact with common ligands used to solubilize Cu catalyst.

1.3.2.4 Reverse ATRP

When conventional radical initiators, such as 2,2'-azobisisobutyronitrile (AIBN), are used to initiate ATRP, this process is termed as *reverse ATRP*.^{60,61} The advantage of reverse ATRP is that the metal complex in the higher oxidative state is employed. However, this method also requires higher catalyst concentrations and elevated temperature to ensure the thermal decomposition of initiator.



Scheme 1-14. Mechanism of Reverse ATRP.

1.3.3 Reversible Addition-Fragmentation Chain Transfer (RAFT) Polymerization

1.3.3.1 Introduction

Reversible addition-fragmentation chain transfer (RAFT) polymerization was first reported in 1998 by the Commonwealth Scientific and Industrial Research Organization (CSIRO).⁶² Around the same time, Corpart et al. reported the living polymerization technique, MAcromolecular Design via Interchange of Xanthate (MADIX)^{63,64} that operates on the same principle as of RAFT, i.e. via degenerative chain transfer. Since the first report, RAFT/MADIX has drawn rapidly increasing interest of academic and industrial researchers, due to the advantages that RAFT/MADIX offers over other living polymerization techniques. Specifically: a) the versatility of monomer choice: RAFT/MADIX is applicable to a wider range of monomer types than either NMP or ATRP, b) the tolerance to a variety of functional groups, c) the moderate reaction conditions and, d) the ease of polymer end-group removal.

Mechanistically, a RAFT polymerization is very similar to a conventional free radical polymerization, but they do have some subtle differences. The living nature of RAFT polymerizations is achieved simply by employing a suitable chain transfer agent (CTA), which efficiently suppresses bimolecular termination if the CTA is chosen properly regarding the type of monomer. The match of CTA to monomer will be discussed in details in the following content.

1.3.3.2 Mechanism of RAFT polymerization

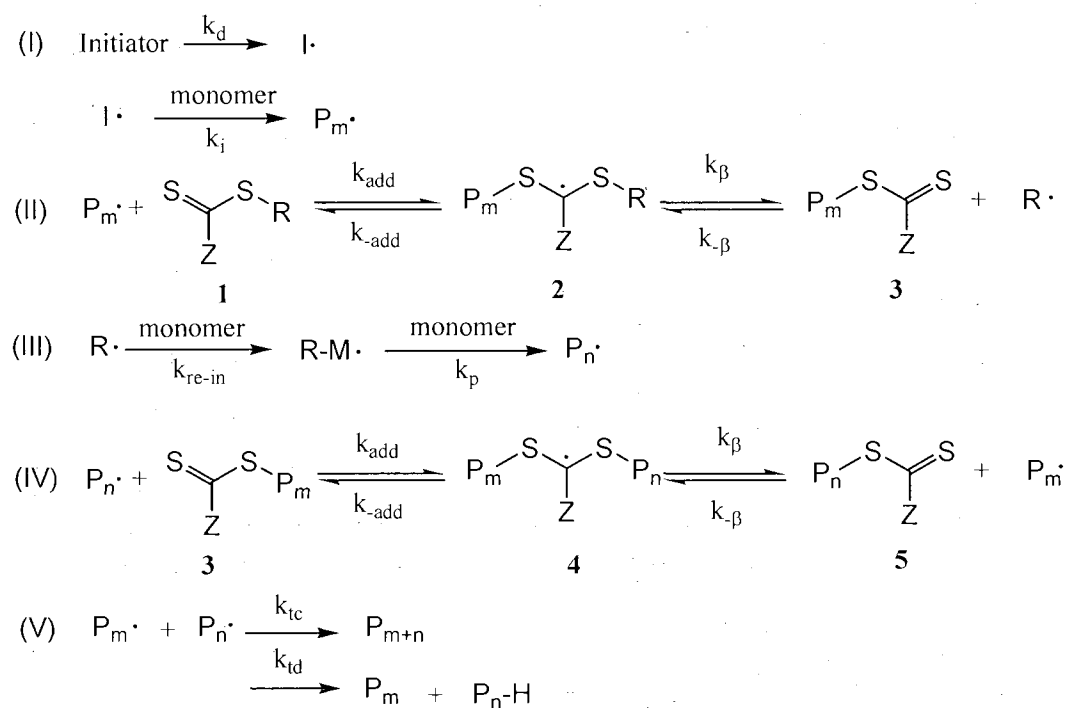
The general accepted mechanism of a RAFT polymerization is illustrated in five steps, as shown in Scheme I-15, in which CTA is shown with a general structure $ZC(=S)SR$. It involves the three main steps common to a conventional polymerization: initiation, propagation and termination.

The initiation step is the same as a conventional free radical polymerization and is typically accomplished via the thermal decomposition of an appropriate initiator generating primary radicals capable of adding to monomer.

The propagation step of RAFT polymerization includes two steps, the so-called pre-equilibrium and the main equilibrium. During the pre-equilibrium, the radical generated from initiator decomposition adds to a few monomers to form the propagating oligomeric radical, and then adds to the C=S bond of the CTA **1** to form the radical intermediate **2**, as shown in step (II). **2** may reversibly fragment either back to the initial oligomeric radical, or may fragment to generate an oligomer end-capped by CTA (moiety **3** macro-CTA) also releasing the R group of CTA in the form of a new radical, $R\cdot$. The $R\cdot$ is able to re-initiate polymerization and propagate forming an active polymeric chain, or react with **3** as in step (II). It needs to be pointed out that the radical from initiator decomposition may directly add to the CTA before adding to the monomer, following the same mechanism as step (II). Once the CTA added to the system is completely consumed and transformed to **3**, the reaction goes from the pre-equilibrium stage to the main

equilibrium stage, shown in step (IV). In the main equilibrium, where only macro-CTA is present, the propagating species reacts with the dormant species **3**, affording the thiocarbonylthio intermediate **4**. **4** may fragment either back to the initial active species P_n^\cdot and dormant species **3**, or to the new active species P_m^\cdot and dormant species **5**. By the rapid exchange between these active and dormant species, each polymer chain is conferred equal probability to grow, and therefore the molecular weight of the produced polymer is narrowly distributed.

Termination, by either combination or disproportionation, of RAFT polymerization is illustrated in step (V). Although largely suppressed due to the rapid degenerative chain transfer throughout the polymerization process, termination is unavoidable since RAFT polymerization is a radical process.



Scheme I-15. Generally accepted mechanism of RAFT polymerization.⁶⁵

Based on the mechanism discussed above, we can conclude:

- a) RAFT polymerization works on the principle of degenerative chain transfer, which differs from the reversible termination principle of NMP or ATRP. There are no long-lived radicals in RAFT; therefore control is not conferred by the *persistent radical effect*.
- b) The majority of the polymer chains are initiated by the R group of the CTA and terminated by thiocarbonylthio groups.
- c) The molecular weight increases linearly with conversion of monomer and can be predetermined by the molar ratio of monomer to CTA added.
- d) RAFT polymerization is mediated by radicals, thus the concentration of radicals determines the rate of polymerization. The higher radical concentration, the higher the rate of polymerization and the higher the probability of termination, leading to polymers with a broad molecular weight distribution.

1.3.3.3 Kinetics of RAFT polymerization

Application of the steady-state assumption, as in a conventional radical polymerization, the rate of a RAFT polymerization can be expressed according to Equation (2):

$$R_p = -d[M]/dt = k_p[R\cdot][M] \quad \text{Equation (2)}$$

where R_p is the rate of polymerization,

$[M]$ is the monomer concentration,

k_p is the rate coefficient,

$[R\bullet]$ is the radical concentration.

The radical concentration is assumed to be a constant during the RAFT polymerization, thus, we can replace $k_p[R\bullet]$ with k_{app} , defined as the apparent rate constant. Therefore, Equation (2) is transformed to:

$$R_p = -d[M]/dt = k_{app}[M] \quad \text{Equation (3)}$$

Through a few mathematical transformations (integration of rate expression), Equation (3) can be expressed as:

$$\ln \frac{[M]_0}{[M]_t} = k_{app} \cdot t \quad \text{Equation (4)}$$

Where $[M]_t$ is the monomer concentration at a given reaction time,

$[M]_0$ is the starting monomer concentration,

t is the reaction time.

Since $[M]_t = [M]_0 \cdot (1-x)$, where x is conversion of monomer, the Equation (4) can be expressed as:

$$\ln \frac{1}{1-x} = k_{app} \cdot t \quad \text{Equation (5)}$$

If plot $\ln[1/(1-x)]$ against reaction time t , a linear relationship is observed when controlled, the slope of which is equal to k_{app} (Figure I-6). In the early stage of a RAFT polymerization, if initiation is slow, there is not enough radicals to trigger the polymerization, and thus the polymerization rate would be slow at the beginning and

accelerate later due to the subsequent increase in radical concentration. Also, if termination occurs to an appreciable extent then the radical concentration decreases remarkably (usually happens in the later stage of polymerization), the polymerization rate will decrease significantly. This can be easily explained by the Equation (2), since R_p is directly related to the radical concentration. In both cases, the polymerization rate is no longer first order and a deviation from linearity would be observed in the kinetic plot, in Figure I-6.

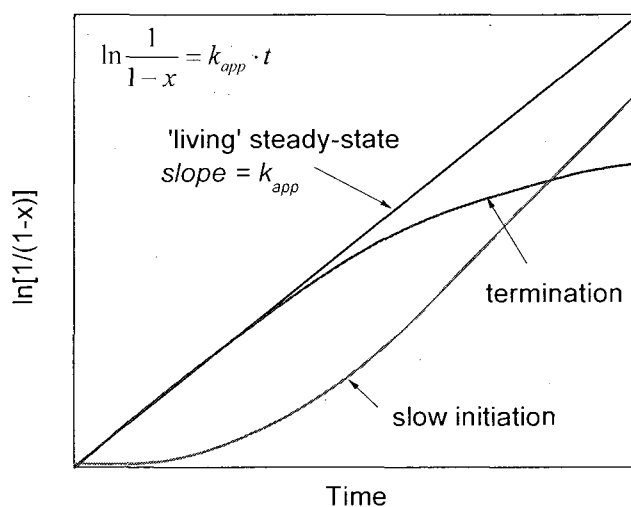


Figure I-6. Ideal kinetic plot for a RAFT polymerization and possible causes of deviations from idealized behavior.

According to the proposed RAFT mechanism, the activation-deactivation process is a degenerative chain-transfer reaction, and a new radical is generated for each radical consumed in the reversible transfer reaction. Therefore, the chain-transfer reaction does not affect the overall polymerization rate. Theoretically, the kinetics of the RAFT

polymerization should follow those of the conventional free radical polymerization and should not be dependent on the CTA concentration. However, these predictions are different from what are commonly observed in RAFT polymerizations. The rate of RAFT polymerization is often slower than that of the conventional free radical polymerization for the same monomer; also, an increase of the CTA concentration usually causes a significant decrease of the polymerization rate. The cause of this retardation is still under discussion and no convincing explanations have been accepted by all researchers. Generally, there are two main explanations put forward to explain such retardation.⁶⁶

a) Side Reactions Involving the Intermediate Radicals

The carbon-centered intermediate radicals (species **2** and **4** in Scheme I-15) may be involved in a variety of side reactions during polymerization. Monteiro et al. first proposed the termination of the intermediate radicals with a propagating polymeric chain, affording a three-armed star product.⁶⁷ Following this, other research groups reported the observation of three-armed and four-armed star products (formed by the combination of two intermediate radicals). These observations are made for the RAFT polymerization of styrene mediated by cumyl dithiobenzoate and for butyl acrylate mediated by *tert*-butyl dithiobenzoate. However, the Centre for Advanced Macromolecular Design (CAMD) group reported that they could not isolate any three- or four-armed star products in their studies. But the products from combination or disproportionation termination were successfully isolated, along with side products formed by the oxidation of the macro-CTA.

It needs to be pointed out that the formation of three- or four-armed star products is observed in model systems where the radical concentration is high. To date, there is no direct evidence of such reactions happening during a RAFT polymerization performed under more “typical” conditions.

b) Slow Fragmentation of the Intermediate Radical

The CAMD group developed a computer simulation system for the RAFT polymerization of styrene mediated by cumyl dithiobenzoate. They suggested that the carbon-centered intermediate radical has a lifetime longer than 10^{-5} s,⁶⁸⁻⁷⁰ and thus indicating a high concentration of the intermediate radicals ($\sim 10^{-4}$ M). This conflicts with the experimental Electron Spin Resonance (ESR) data, which suggest the concentration of the intermediate radicals is lower than 10^{-7} M.⁷¹ Other research groups have also reported in the computer simulation of RAFT polymerization based on a different model and they suggested the concentration of the intermediate radicals should be closer to 10^{-7} M rather than 10^{-4} M. Several recent publications reported that the intermediate radical generated from dithiobenzoate is more stable than those generated from aliphatic dithioesters and trithiocarbonates. This suggested that the retardation in the RAFT polymerization of methyl acrylate and styrene mediated by cumyl dithiobenzoate may be due to the slow fragmentation of the “stabilized” intermediate species.

1.3.3.4 MW control of RAFT polymerization

In an ideal RAFT polymerization, monomers are added equally to all the propagating chains. Considering that all chains are either initiated by the radical from initiator, $I\bullet$, or by the R group on the CTA, the $R\bullet$, and that the concentration of $I\bullet$ is negligible compared with $R\bullet$, the theoretical M_n can be simply expressed by Equation (6):

$$M_n = [M]_0 \cdot MW_{monomer} \cdot x / [CTA]_0 + MW_{CTA} \quad \text{Equation (6)}$$

Where $[M]_0$ is the initial concentration of monomer,

$MW_{monomer}$ is the molecular weight of monomer,

x is the fractional conversion of monomer,

$[CTA]_0$ is the initial concentration of CTA,

MW_{CTA} is the molecular weight of CTA.

From Equation (6), a linear relationship can be drawn if we plot M_n against conversion, in Figure I-7. In the case of slow initiation, there are fewer radicals in the system, thus more monomer adds to each propagating polymeric chain, leading to a higher M_n than predicted. When conventional chain transfer happens during a RAFT polymerization, the propagating polymer chains cease to grow before all the monomer is consumed, thus the M_n will be lower than predicted value.

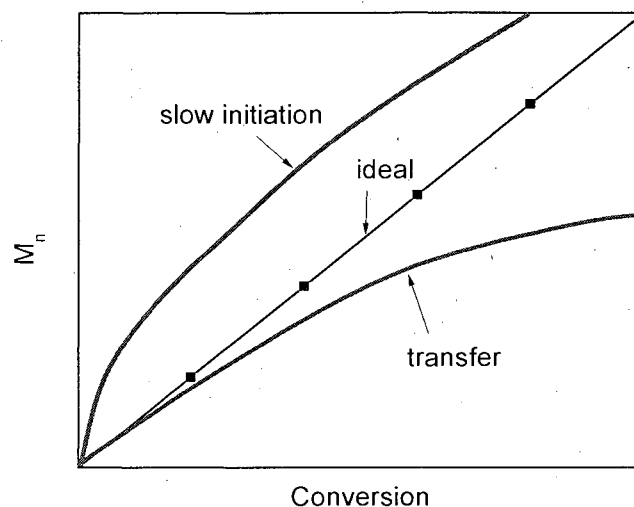


Figure I-7. Idealized M_n vs conversion plot for a RAFT polymerization and possible causes for deviations.

1.3.3.5 Chain Transfer Agent (CTA) for RAFT polymerization

The key to a successful RAFT polymerization is the introduction of a suitable CTA. All CTAs used in RAFT have the general structure $ZC(=S)SR$. Depending on the nature of the Z and R groups, RAFT CTAs can be classified into one of four common groups, dithioesters, trithiocarbonates, dithiocarbamates, and xanthates, Figure I-8.

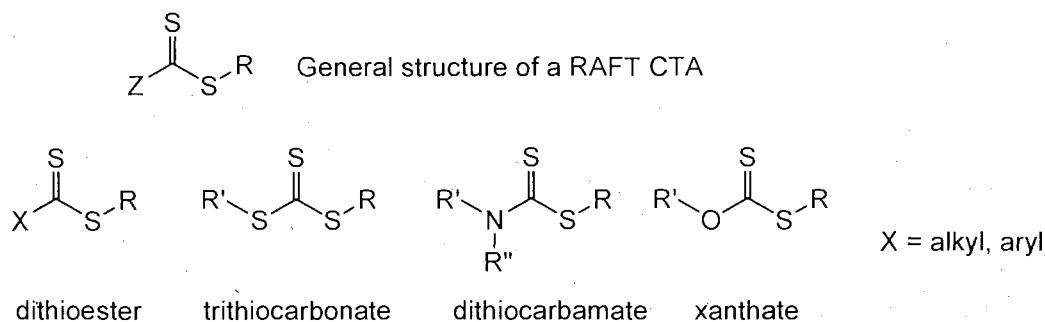


Figure I-8. General structures of RAFT CTAs and examples of the four types of CTA.

A RAFT polymerization is a combination of a series of equilibrium reactions, initiation, re-initiation, propagation, addition, and fragmentation. To achieve living characteristics, these reaction rate constants need to be well balanced. The balance is achieved by choosing a suitable CTA for a given monomer, i.e. choosing the proper Z and the R groups.

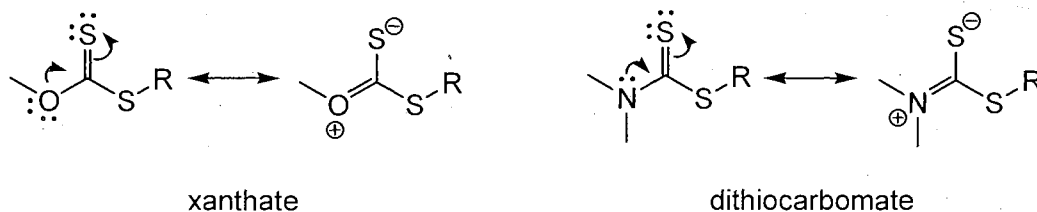
a) Effect of Z group

The Z group is the activating group of the CTA, and strongly influences the stability of the carbon-centered intermediate radical. The Z group should have a strong stabilizing influence to favor the formation of the intermediate radical thus increasing the reactivity of the C=S bond toward radical addition, i.e. a high k_{add} . On the other hand, the stability of the intermediate radical affects the fragmentation rate (k_{β}); the more stable the intermediate is, the slower it fragments. Therefore, it needs to be finely tuned so that the rates of addition and fragmentation are well balanced. There are many publications concerning the effect of different Z groups. Based on those studies, the phenyl group is considered as the most ideal activating group because it balances the stability and the reactivity towards fragmentation of the intermediate radical. However, it is common to observe rate retardation when the phenyl Z group is used since the Z group has a strong stabilizing effect on the intermediate radical.

Benzyl and alkyl Z groups have a less stabilizing effect on the intermediate radical, and the fragmentation rate is hence faster. As a result, little or no retardation in

the RAFT polymerization of styrene is observed. Faster polymerization rates are observed for more reactive monomers such as *N*-isopropylacrylamide (NIPAm) and methacrylates. However, for the bulkier and less active monomers, such as methyl methacrylate (MMA), the RAFT polymerization does not offer good control due to the less stable intermediate radical.

In the cases where *Z* is an oxygen (xanthate) or nitrogen (dithiocarbamate), the lone pair electrons on the O or N atoms are delocalized with the C=S bond, Scheme I-16.⁶³ The delocalization decreases the reactivity of the C=S bond toward radical addition, i.e. a lower k_{add} . Again, the low k_{add} results in the overall poor control of the molecular weight of polymers for bulky monomers (e.g. methacrylates). However, for the more active monomers (e.g. vinyl acetate), the lower k_{add} is required to allow the addition of the fast propagating radical onto the C=S bond and give overall control of the molecular weight of the product. Xanthates and dithiocarbamates have been reported to work best for the RAFT polymerization of vinyl acetate; other successful examples include styrene, methyl acrylate, ethyl acrylate, butyl acrylate, *t*-butyl acrylate (tBA), acrylamide, and vinyl formamide. It is noteworthy that if the lone pair electrons of the O or N are located on an aromatic ring, or conjugated with another electron-withdrawing group, the delocalization is weakened and thus the reactivity of C=S bond is increased. This type CTA can be used to mediate the RAFT polymerization of the bulkier monomers (e.g. MMA).

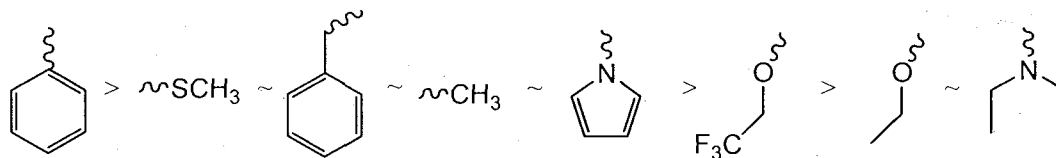


Scheme I-16. Canonical forms of xanthates and dithiocarbamates.

When the Z group is a sulfur atom, the resulting CTA is a trithiocarbonate.

Trithiocarbonates can offer good reactivity of C=S bond toward radical addition, while minimizing the retardation of the polymerization rate. A variety of monomers have been successfully polymerized under the mediation of trithiocarbonate CTAs, and include styrene, methyl acrylate, ethyl acrylate, butyl acrylate, 2-(hydroxyethyl)acrylate, acrylamide, *N,N*-dimethylacrylamide, *N-tert*-butylacrylamide, *N*-isopropylacrylamide, MMA, acrylic acid, dibutyl itaconate, and dicyclohexyl itaconate.

According to the literature, the Z groups can be arranged with regard to their versatility with common monomers as such: dithiobenzoates > trithiocarbonates ~ dithioalkaneates > dithiocarbamates (where the lone pair electrons on N atom are conjugated with other electron-withdrawing group) > xanthates > dithiocarbamates. More specifically, experimental data and *ab initio* calculations suggest the following guideline for the selection of CTA Z group:⁷²

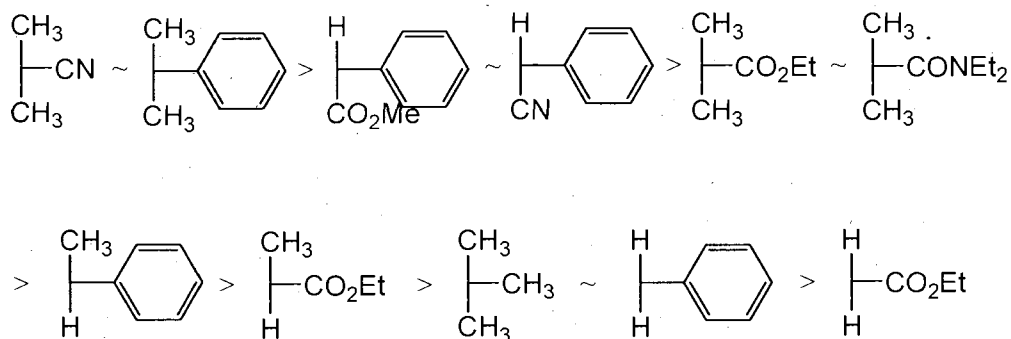


Scheme I-17. Guideline for the selection of Z group of RAFT CTAs.

b) *Effect of R group structure*

The R group affects the RAFT process mainly during the pre-equilibrium stage. There are two requirements for a suitable R group: i) it has to be a good radical leaving group in comparison with the propagating polymeric chain, otherwise there will not be enough macro-CTA in the system to give good control over the molecular weight; ii) it has to be a good re-initiating species to add to the monomer, otherwise the polymerization will cease or proceed at an extremely slow rate because the CTA acts like a radical scavenger in this case (it consumes propagating radical and generates non-propagating radicals). The R group also plays a role in stabilizing the thiocarbonylthio intermediate radical, but not as much as the Z group does. There are numerous publications evaluating the effect of different R groups. To date, the cumyl and cyanoisopropyl groups seem to be most efficient for re-initiation. There have been attempts to use R groups that mimic the propagating polymeric radical. Such a strategy has been reported to be efficient with styrene, dimethyl acrylamide, and other acrylates. In the case of using ester/amide functional R groups, which allows easy transformation to other functional groups at the end of polymeric chain, the strategy works for styrene and acrylate monomers but poorly for methacrylates. This is due to the poor leaving ability of

such R groups in comparison with the polymethacrylate radical. Again, based on the experimental and *ab initio* calculations, there is a guideline available for the selection of the R group for the RAFT CTA:⁷²



Scheme I-18. Guideline for the selection of R group of RAFT CTAs.

By combining different Z and R groups, there is, clearly, a large variety of CTAs available, with different structures and reactivity. However, we can narrow the choices to a few CTAs that work for most common monomers. The cumyl dithiobenzoate (CDB), cyanoisopropyl dithiobenzoate (CPDB), methoxycarbonylphenylmethyl dithiobenzoate, and cyanobenzyl dithiobenzoate, Figure I-9, are the most versatile CTAs and work efficiently in the RAFT polymerization of styrenics, (meth)acrylates, and (meth)acrylamides. We need to add the cyanoalkyl xanthate, which works for the RAFT polymerization of vinyl acetate and its derivatives.⁶⁶

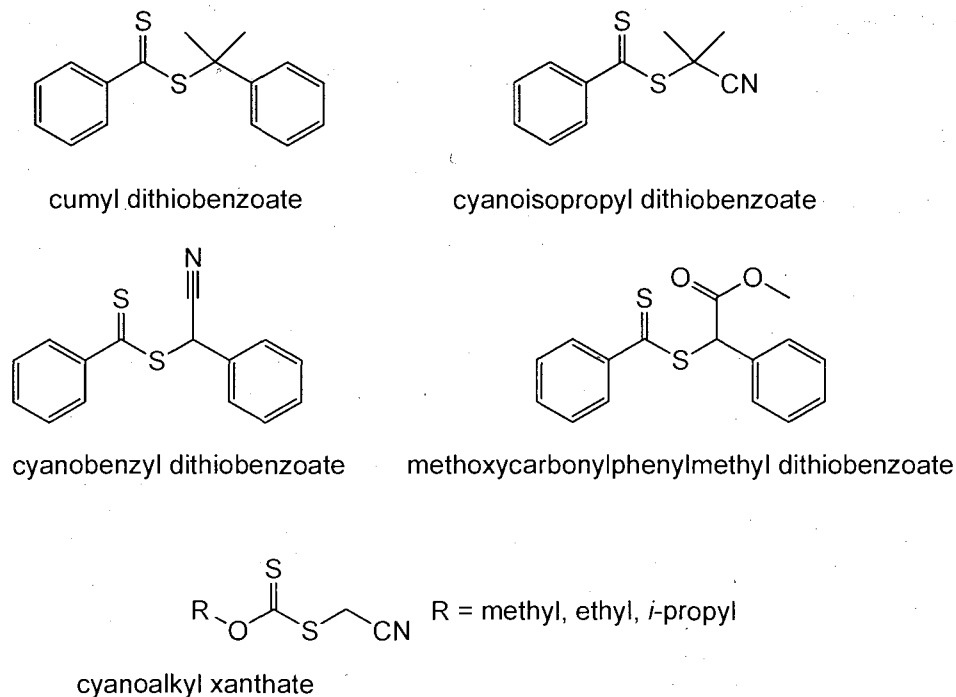


Figure I-9. Most versatile CTAs for RAFT polymerization.

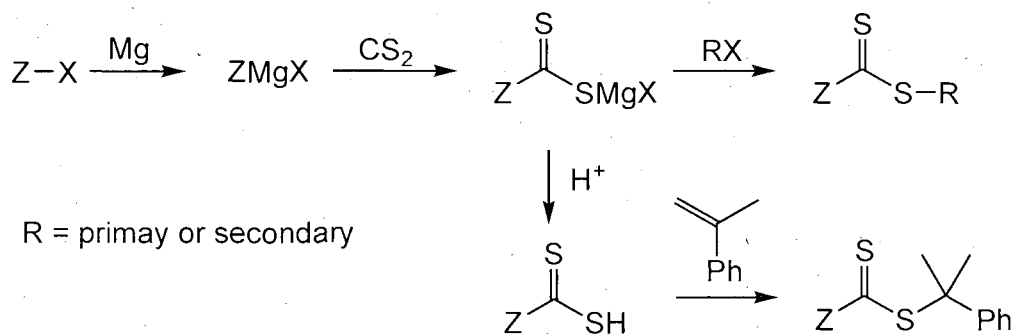
1.3.3.6 Synthetic Routes to RAFT CTAs

Currently, there are few RAFT CTAs commercially available which offer sufficient control over most of the common monomers. Therefore, typically the desired RAFT CTA has to be prepared in the laboratory. Fortunately, there are several reliable synthetic routes for the preparation of RAFT CTAs.

a) Preparation of dithioesters

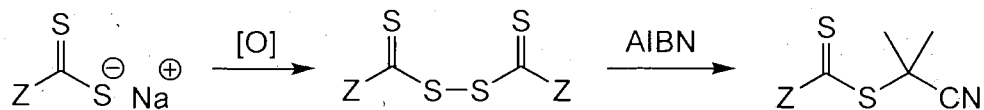
The synthesis of dithioesters generally starts from the halo derivatives of the Z group (ZX).⁶² Reaction of ZX with magnesium generates the Grignard reagent ZMgX, which is subsequently reacted with CS₂ to afford ZC(=S)SMgX via a nucleophilic

addition reaction to a C=S bond. Subsequent reaction of $ZC(=S)SMgX$ with the halo derivative of R group (RX), via an S_N2 reaction, affords the desired dithioester, Scheme I-19. This approach works well for primary and secondary R groups and generates the corresponding dithioesters with good yield. However, for tertiary R groups (e.g. cumyl group), yields are very low, and a modification is adopted, Scheme I-19. A dithiocarboxylic acid ($ZC(=S)SH$) is prepared by protonation of $ZC(=S)SMgX$ and subsequently reacted with α -methyl styrene (following Markovnikov's rules) affording the cumyl dithioester.⁷³



Scheme I-19. General synthetic route to dithioesters.

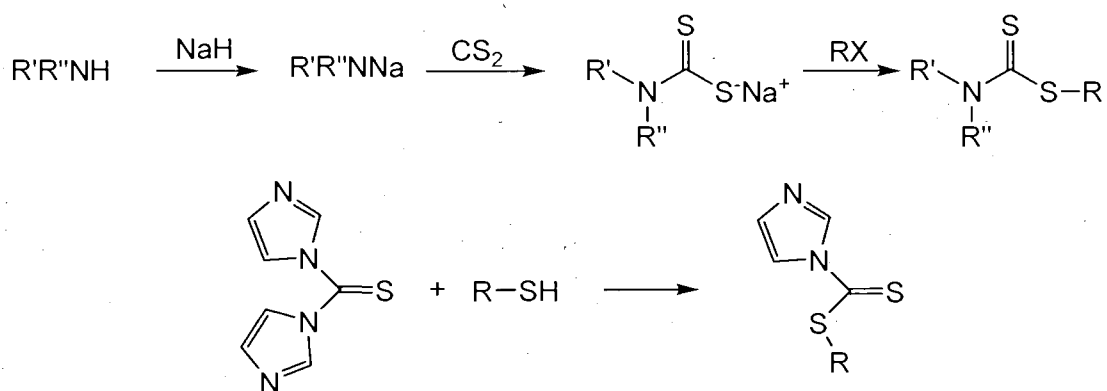
There is an alternative approach to prepare tertiary dithioesters via a radical process, Scheme I-20. A bis(thiocarbonyl) disulfide is synthesized by the oxidation of the thiocarboxylate and subsequently reacted with a free radical initiator (e.g. AIBN) via radical addition, affording the tertiary dithioester.⁷⁴⁻⁷⁶



Scheme I-20. Synthesis of tertiary dithioester via a radical reaction.

b) Preparation of Dithiocarbamates

The preparation of dithiocarbamate starts from preparing the sodium salt of the mono or disubstituted amine (Z^-Na^+) by the deprotonation of ZH with sodium hydride (NaH). The sodium salt subsequently reacts with CS_2 via a nucleophilic addition affording the sodium dithiocarbamate ($ZC(=S)S^-Na^+$), which can directly react with the halide derivative of the R group (RX) via an S_N2 reaction generating the desired dithiocarbamate CTA, Scheme I-21. However, such a strategy does not work well for an imidazole Z group. To prepare imidazole-based CTAs the reaction of a thiocarbonyl diimidazole (commercially available) with an alkyl mercapto derivative through a nucleophilic exchange reaction, Scheme I-21, is more efficient. The synthesis of dithiocarbamates with a tertiary R structure can be accomplished via the radical process highlighted in Scheme I-20.^{77,78}

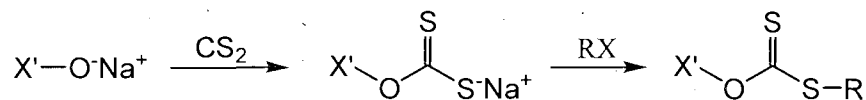


Scheme I-21. Synthetic routes to dithiocarbamate CTAs.

c) Preparation of xanthates

The synthesis of xanthates is accomplished via the same general routes as

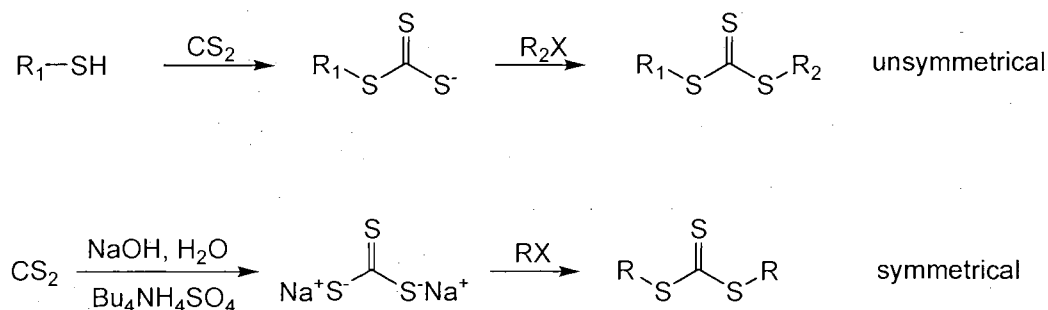
employed for dithiocarbamates. An alkoxide salt with the desired Z group structure ($X'-O^-Na^+$) is reacted with CS_2 to generate the $X'OC(=S)S^-$ salt which can be directly alkylated by RX to form the desired xanthate CTA, Scheme I-22.⁶³



Scheme I-22. Synthetic route to xanthate CTAs.

d) *Preparation of trithiocarbonates*

The synthesis of trithiocarbonates is probably the most straightforward for all the RAFT CTAs, due to the relatively easy purification. It is noteworthy that the trithiocarbonate CTAs can be symmetric or unsymmetric. For the unsymmetric species, a thiol reacted with CS_2 affording a trithiocarbonate anion, which is then alkylated, via an S_N2 reaction, yielding the target CTA. For the symmetrical version, a di-anion of the trithiocarbonate is generated first followed by alkylation.⁷⁹



Scheme I-23. Synthetic route to symmetrical and unsymmetrical trithiocarbonates.

1.3.3.7 Monomers suitable for RAFT

RAFT is easily the most versatile toward the monomer types and functionality among the controlled/living radical polymerization techniques. To date, there have been a very large number of monomers reported that successfully polymerize under RAFT conditions, including essentially all the commonly employed monomers with activated vinyl groups, such as (meth)acrylates and (meth)acrylamides, as well as styrenics, monomers with non-activated vinyl groups such as vinyl esters and vinyl amides and finally monomers such as the diallylammoniums.

The RAFT polymerization of styrene has been thoroughly studied by researchers under various conditions. It has been successfully polymerized in a controlled fashion by the mediation of dithioesters, trithiocarbonates and dithiocarbamates. The RAFT polymerization of styrene mediated by xanthates usually produces polymers with broad molecular weight distributions. Styrenic monomers with different functional groups have also been polymerized via RAFT, Figure I-10.⁸⁰⁻⁹⁶

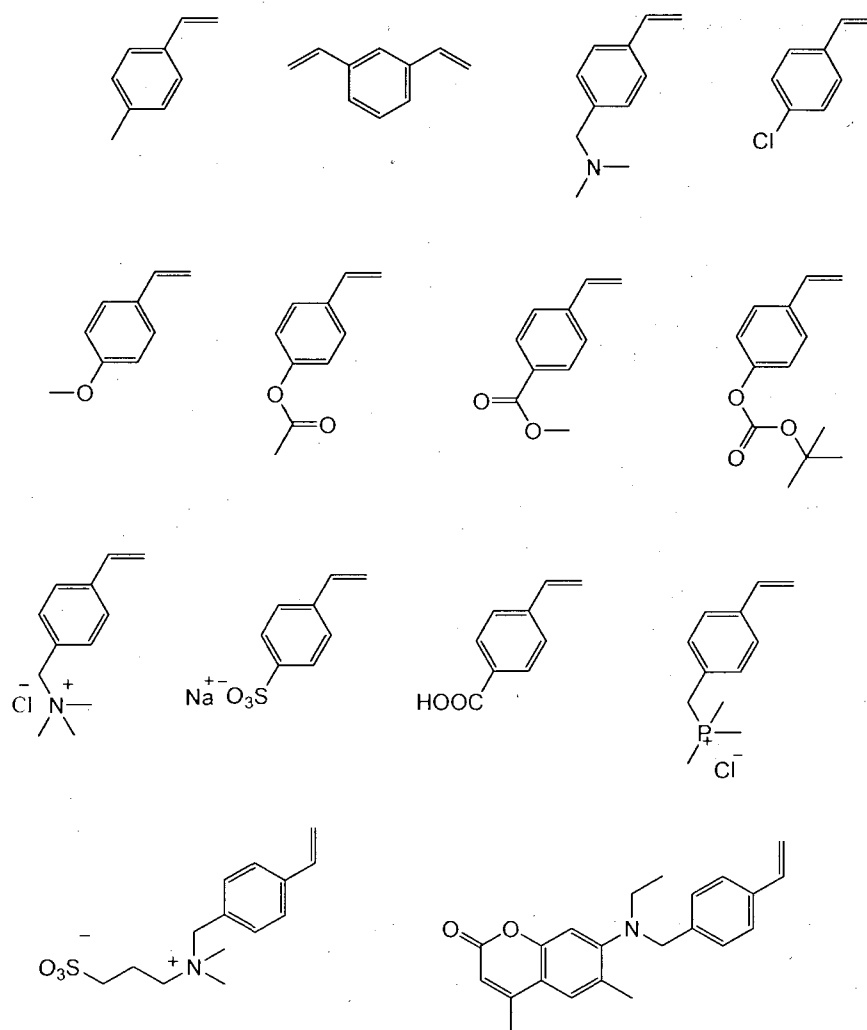


Figure I-10. Examples of functional styrenic monomers polymerized by RAFT.

Acrylates and acrylamides are both fast propagating monomers. The controlled RAFT polymerization of these monomers can be accomplished with dithioesters or trithiocarbonates. In the case of xanthates or dithiocarbomates, the polymerizations usually produce broadly distributed products. Examples of acrylates and acrylamides successfully polymerized by RAFT in a controlled fashion are shown in Figure I-11.⁹⁷⁻¹¹⁷

have been proved to be very efficient for methacrylates and methacrylamides. Examples of methacrylates and methacrylamides successfully polymerized by RAFT with various functionality are shown in Figure I-12.^{68,71,81,97,113,118-135}

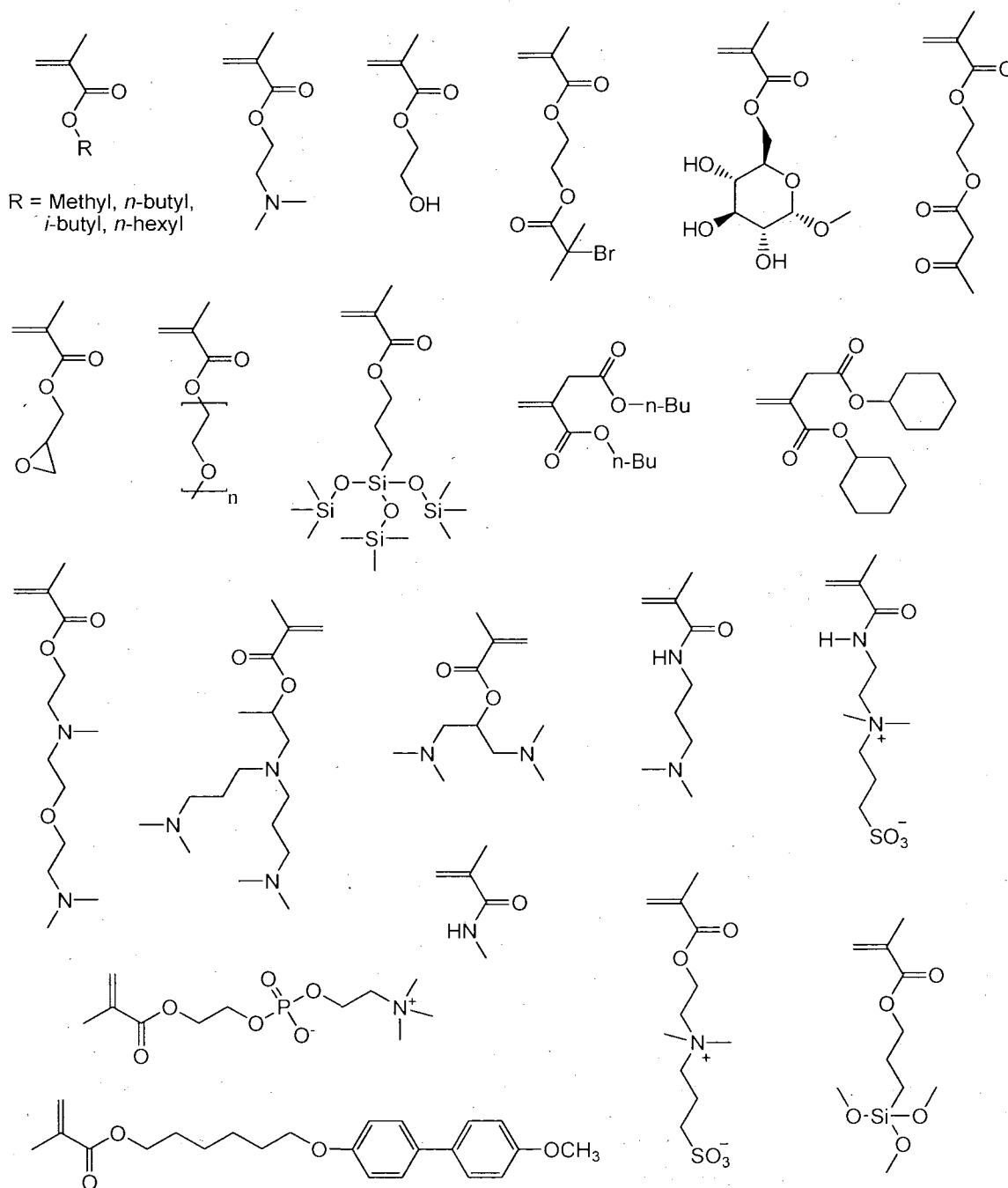


Figure I-12. Examples of methacrylate and methacrylamide monomers suitable for RAFT polymerization.

Vinyl acetate and its derivatives are monomers with extremely high reactivity. The RAFT polymerization of such monomers is only successfully accomplished under the mediation of xanthates. Other monomers that have been polymerized via RAFT, include 2-vinylpyridine, 4-vinylpyridine, acenaphthylene, 1,1-dichloroethene, 1-hexene, acrylonitrile, 1-octene, and 1-decene.^{136,137}

1.3.3.8 Advanced macromolecular architecture via RAFT polymerization

An important feature of RAFT polymerization is the ability to prepare the (co)polymer with advanced macromolecular architectures such as block, star, and graft (co)polymers (Figure I-13).

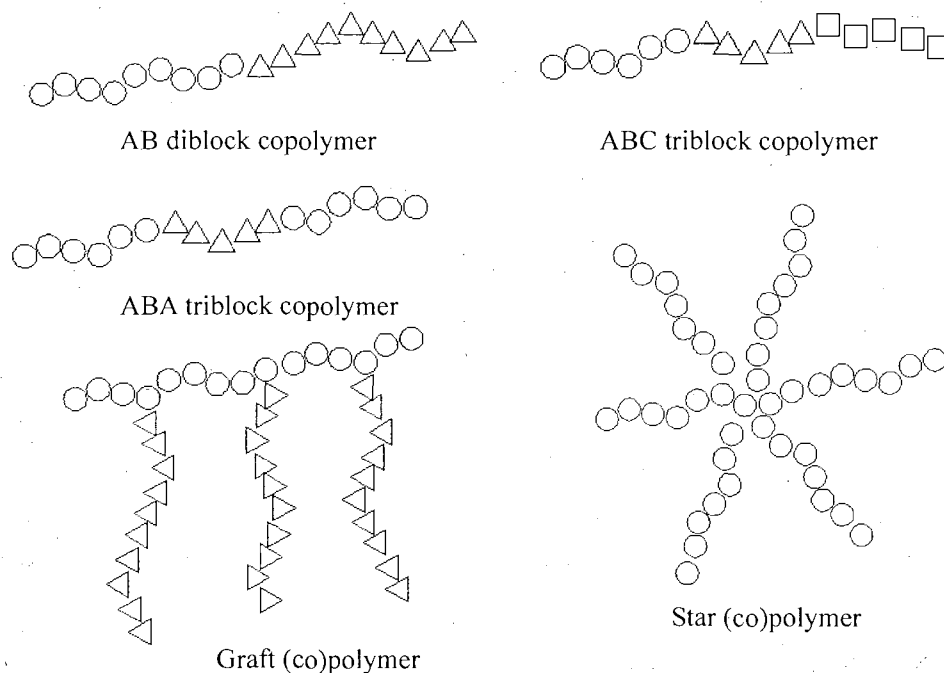
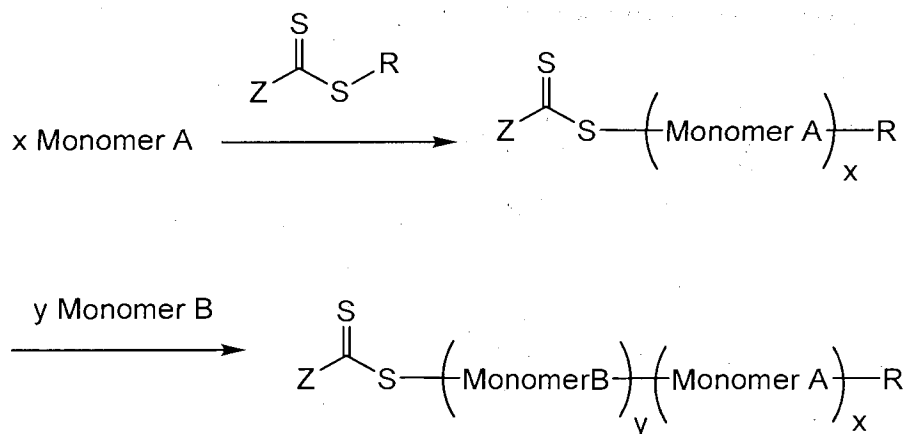


Figure I-13. Graphic illustration of several available (co)polymer architectures via RAFT.

a) *AB diblock copolymer*

The synthesis of AB diblock copolymers is straightforward via RAFT polymerization since, ideally, each polymer chain is capped by a ZC(=S)S- group at one end and R group at the other. Such a polymer can be used as a macro-CTA to mediate a RAFT polymerization of a second monomer to generate an AB diblock copolymer (Scheme I-24). In this approach, monomer A is initially polymerized to less than quantitative conversion, and the second monomer B can be either added directly to the polymerization system or after the homopolymerization of A, the polyA, is isolated from residual monomer. If B is added directly into the reaction system, there will be some tapering of the A block to the B block. If homopolymer A is purified prior to be used as a macro-CTA, tapering is not an issue. Following the same general strategy, ABC triblock copolymers can also be prepared. It needs to be pointed out that the sequence of monomer addition needs careful consideration in such an approach. The first polymer block needs to have a greater or comparable leaving ability, with regards to the leaving ability of the next block under the reaction conditions. For example, to prepare a diblock copolymer consisted of MMA and methyl acrylate (MA), the MMA needs to be polymerized first. The reverse sequence will lead to the production of a mixture of two homopolymers.

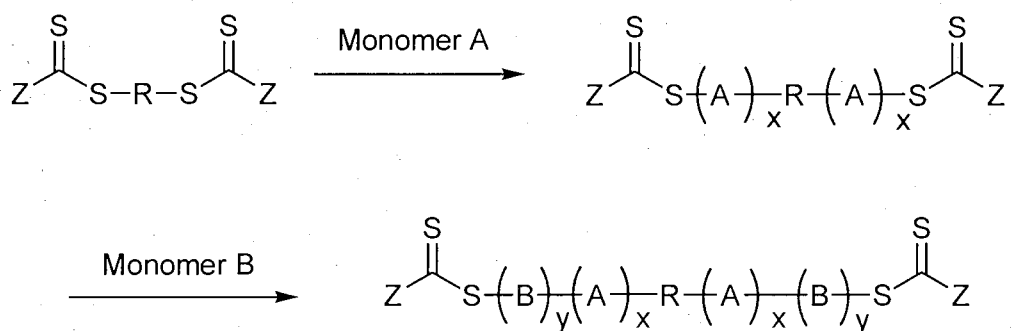


Scheme I-24. Synthetic route to AB diblock copolymer via RAFT polymerization by sequential monomer addition.

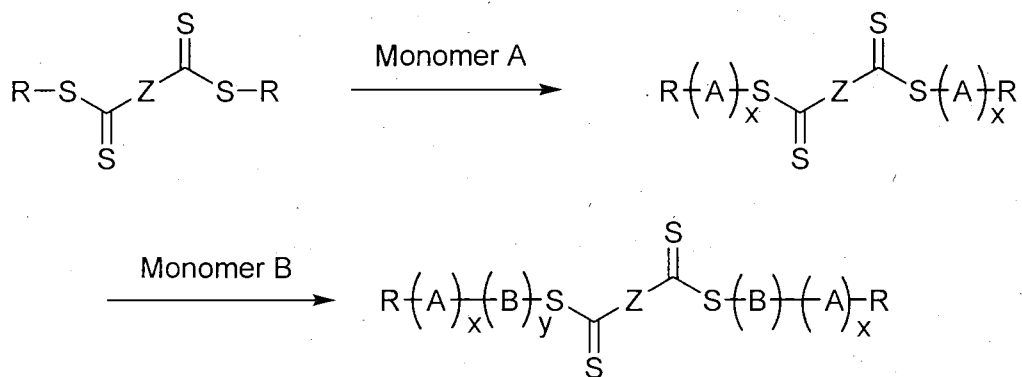
b) *ABA triblock copolymer*

There are two possible approaches to prepare ABA triblock copolymers via RAFT polymerization based on the use of difunctional CTAs: difunctional R group CTAs and difunctional Z group CTAs. For the difunctional R group approach, chain propagation occurs at both ends of the chain therefore the sequential addition of monomer A followed by monomer B generates a BAB triblock copolymer with the dithiocarbonyl moiety on each end and the R group at the center (Scheme I-25). For the difunctional Z group approach, chain propagation happens at the center of chain therefore the sequential addition of monomer A followed by monomer B generates an ABA triblock copolymer with the dithiocarbonyl group at the center and R group at each end. It is noteworthy that the symmetrical trithiocarbonate CTA works in the same manner as the difunctional Z group CTA for preparing ABA triblock copolymers.

Difunctional R groups approach



Difunctional Z groups approach



Scheme I-25. Synthetic route to ABA triblock copolymers via RAFT polymerization mediated by difunctional R groups or difunctional Z groups CTA.

c) *Star (co)polymers*

Star (co)polymers can be prepared via RAFT polymerization using multifunctional CTAs. The mechanism is similar to the synthesis of ABA triblock copolymers. In fact, the first step of the synthesis of an ABA triblock can be viewed as the synthesis of a two-armed star polymer. Again, there are R group and Z group approaches. For the R group approach, the polymerization is mediated by a CTA with a

multi-functional R group core which has multiple Z group branches attached. In the polymerization, the star arms grow away from the core. For the Z approach, the structure of the CTA is reverse, i.e. Z group as the core and R group as the branches. Examples of such CTAs are shown in Figure I-14 and I-15.^{79,138-141} In the R group approach, since the polymeric radicals are attached to the star core, the conversion needs to be kept relatively low to avoid the combination termination reaction between two star radicals. Such a situation does not exist in the Z group approach, thus the conversion does not need to be kept low. In the Z group approach, the polymeric arms are detached from the core while they propagate and attach back to the core while they are dormant. Therefore, the combination termination only happened between arms but not stars, which affords star (co)polymers with polydispersity as low as 1.1.

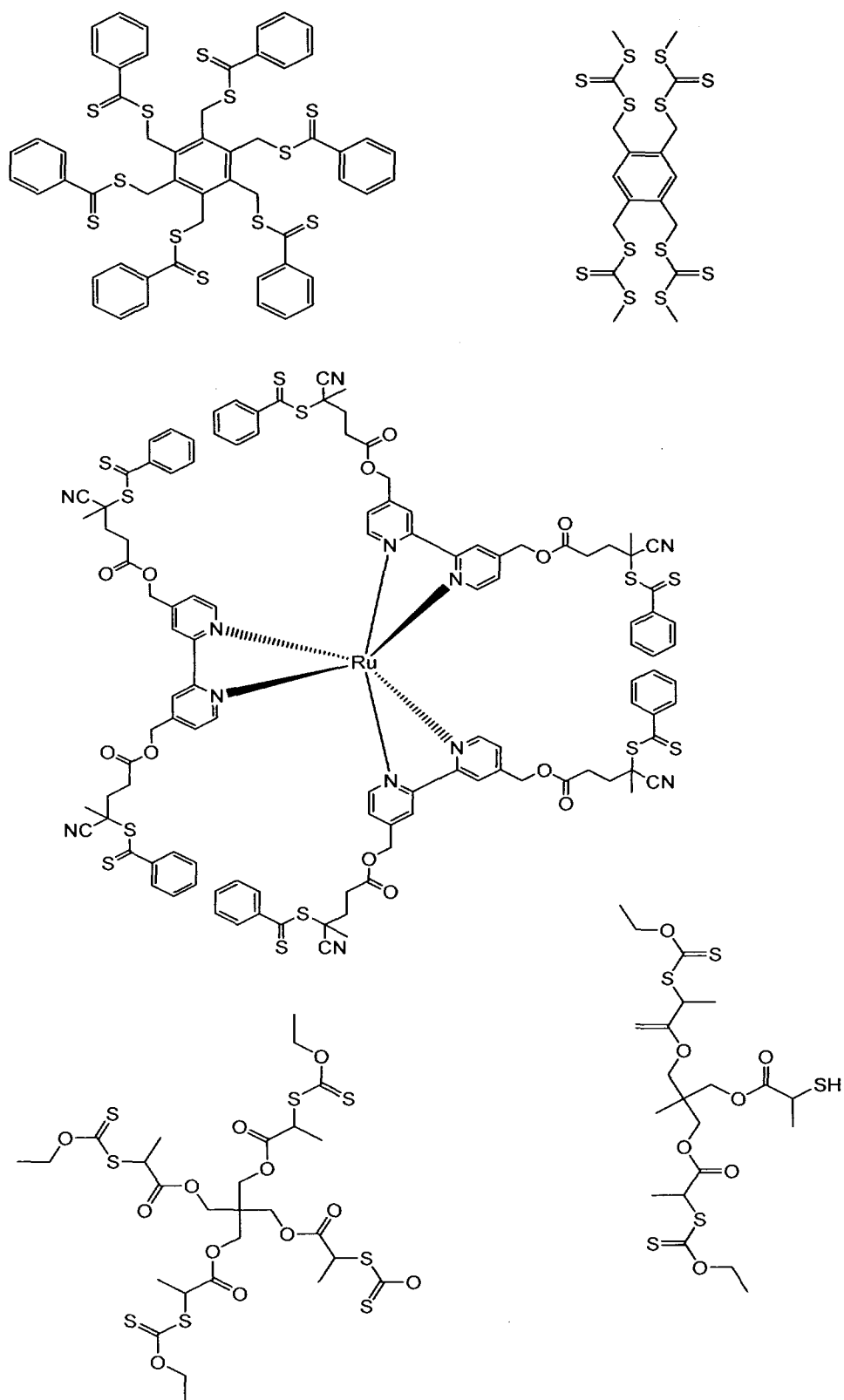


Figure I-14. R group approach CTAs for the preparation of star (co)polymers via RAFT.

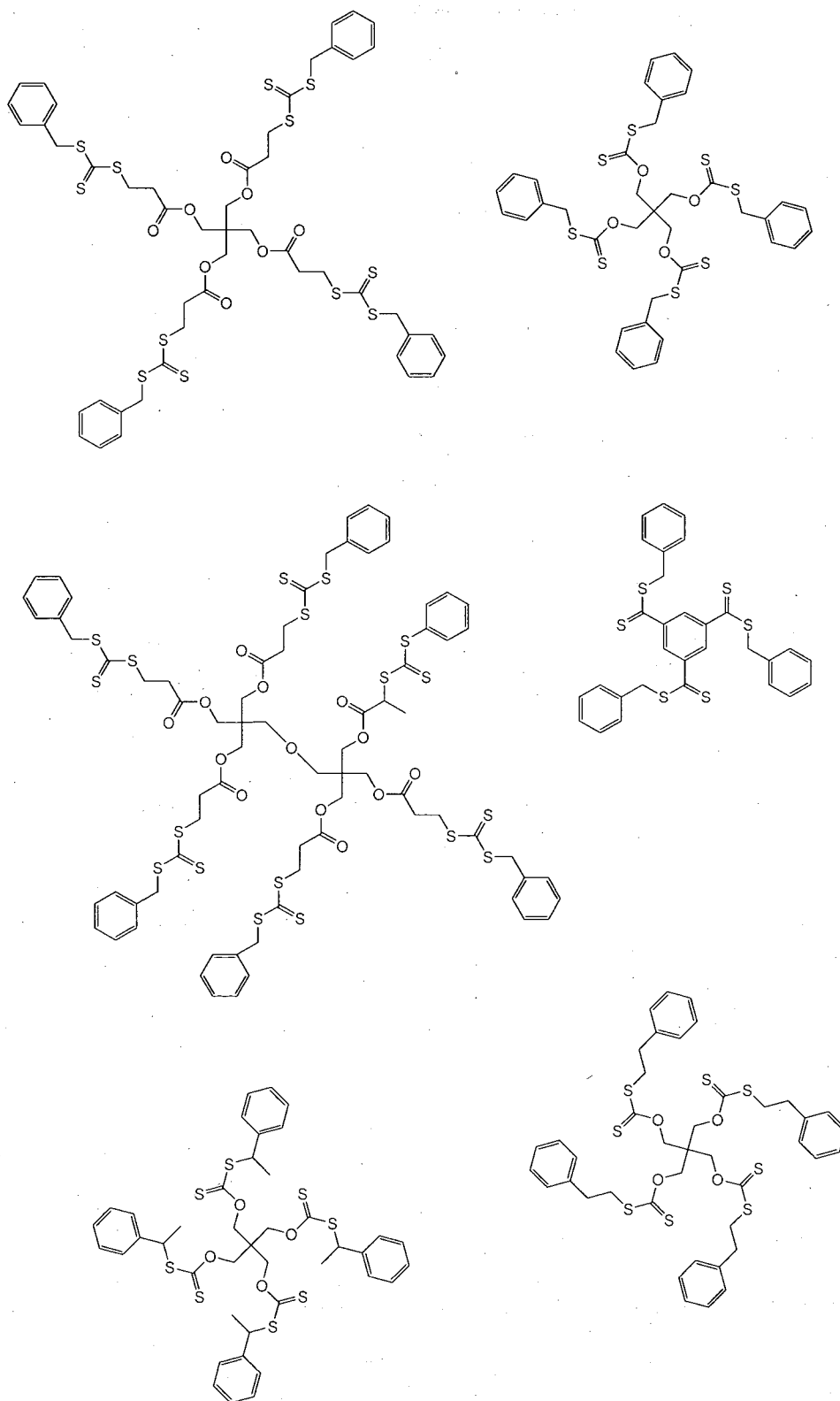
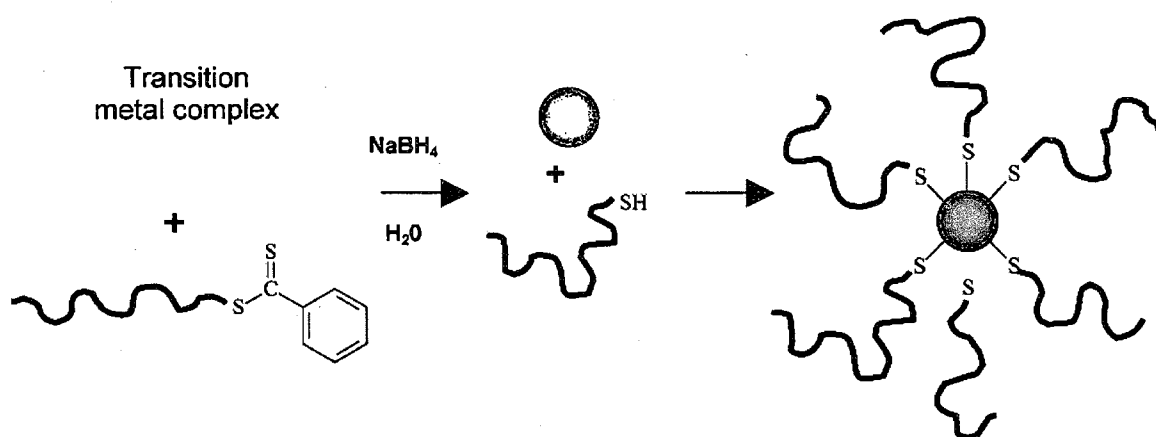


Figure I-15. Z group approach CTAs for the preparation of star (co)polymers via RAFT.

d) Surface-grafted (co)polymers

The synthesis of surface-grafted (co)polymers starts from the immobilization of a RAFT CTA to the surface either through its R group or Z group. An alternative approach is the immobilization of the initiator on the surface. Several research groups have used this method, with polypropylene which generates radicals under γ -irradiation, or with silica, using an immobilized free radical initiator.

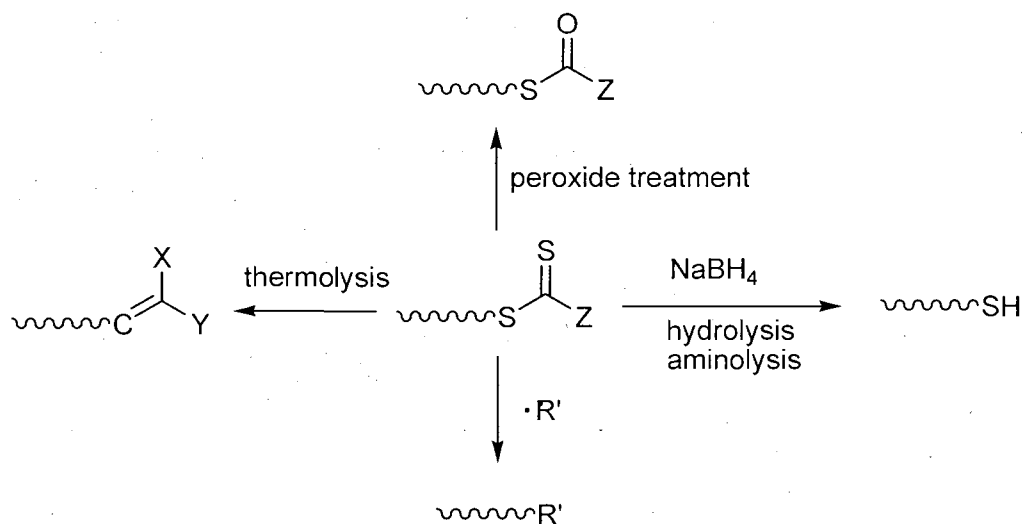
Lowe et al. first reported the grafting of RAFT polymers onto gold nano-particles. A series of water-soluble polymers, including anionic, cationic, and zwitterionic examples, were prepared via RAFT polymerization. Treatment of the polymer with NaBH_4 in the presence of gold nanoparticles resulted in the sequential hydride reduction of the thiocarbonylthio end group followed by chemical bonding of the thiolate to the gold nanoparticle surface, Scheme I-26. More recently, Hotchkiss et al. reported the surface modification of gold nanorods with polymers prepared via RAFT polymerization employing a similar procedure.¹⁴²



Scheme I-26. Grafting polymer prepared via RAFT polymerization to gold nanoparticles.

1.3.3.9 Removal of the end group of RAFT polymer

(Co)polymers prepared via RAFT polymerization usually inherit the color of the CTA, especially for dithioesters. The removal of such end groups may be important for potential industrial applications. Fortunately, there are a number of ways of cleaving the thiocarbonylthio end-groups. For example, Lowe et al. reported the use of NaBH_4 as reducing agent, under ambient temperature, to form thiolate end-functionalized polymers. Primary and secondary amines can also be used to reduce the dithiocarbonyl group to a thiol functional group. Other methods include hydrolysis, thermolysis, peroxide treatment, and radical exchange (Scheme I-27).^{127,138,142-148}



Scheme I-27. Various paths for the removal of the dithiocarbonyl end group of the polymer prepared via RAFT polymerization.

1.3.4 Tellurium-Mediated Radical Polymerization (TERP)

The Tellurium-mediated radical polymerization is one the newest examples of

the controlled/living radical polymerization and was first reported by Yamago et al. in 2002.³ TERP requires the use of an organotellurium compound as the mediator for the polymerization. Examples of such compounds are shown in Figure I-16.^{3,149,150}

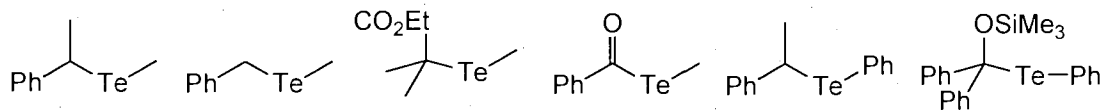
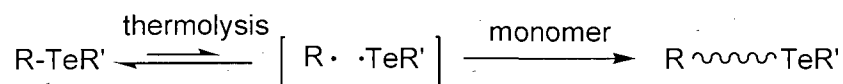


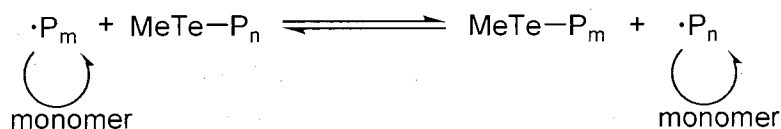
Figure I-16. Organotellurium mediators for TERP.

The organotellurium compounds readily undergo homolytic cleavage, upon thermolysis or photolysis, generating a carbon-centered radical and a stable tellurium-centered radical, similar to the process observed in NMP. However, kinetic studies reveal another mechanism, that is degenerative in nature, similar to the RAFT process (Scheme I-28). The thermal dissociation (typically at around 100 °C) serves to provide a radical source in the system; once a carbon-centered radical is generated by thermolysis, the polymerization predominantly proceeds under the control of the degenerative chain transfer mechanism.¹⁵⁰

thermal dissociation



degenerative chain transfer



Scheme I-28. Two mechanisms of TERP: thermal dissociation and degenerative chain transfer.

Conventional free radical initiators, such as AIBN, can be used to assist TERP.

In this case, the temperature of the polymerization can take place at reduced temperatures (around 60 °C), since the radical source shifts from thermolysis of organotellurium compound to the thermolysis of the AIBN. In this case, the chain transfer mechanism becomes exclusive in the polymerization.

To date, a variety of monomers have been successfully polymerized by TERP under controlled conditions, including styrene, *p*-chloro-styrene, *p*-methoxy-styrene, methyl acrylate, tBA, *n*-butyl acrylate (nBA), *N,N*-dimethyl acrylamide (DMAm), NIPAm, 2-(dimethylamino)ethyl acrylate (DMAEA), 2-hydroxyethyl methacrylate (HEMA), acrylonitrile, and MMA.^{3,149,150}

The living nature of TERP is proved with regards to the control of molecular weight, the linear increase of M_n with conversion, and the preparation of block copolymers. It is noteworthy that, unlike the other controlled/living free radical polymerization techniques, TERP exhibits tolerance to the sequence of monomer addition while preparing block copolymers. More specifically, the synthesis of AB diblock copolymers consisted of any two monomers from tBA, MMA, and styrene can be accomplished by starting with any of the chosen monomers.

More recently, Yamago et al. reported the organostibine-mediated radical polymerization (SBRP), which is analogous to the TERP. Good control over the polymerizations of styrene, nBA, MMA, NIPAm, acrylonitrile, 1-vinyl-2-pyrrolidinone and vinyl acetate were observed.¹⁵⁰

2. Stimuli-Responsive Water-Soluble (Co)Polymers

Water-soluble polymers (WSP) are macromolecular species which can dissolve in an aqueous environment. During the last several decades, WSP have drawn increasing interest from researchers due to the demand for water-based applications, such as pharmaceuticals, viscosity modifiers, dispersants and emulsifiers. Among them, stimuli-responsive WSP are of great importance since the solubility features of such WSP changes upon the change of certain conditions, such as pH, temperature, ion strength, or pressure.

2.1 Water-Soluble Polymers

2.1.1 Non-Ionic Water-Soluble Polymers

WSP are generally divided into two groups, ionic and non-ionic. Non-ionic WSP are generally derived from monomers with functional groups able to form hydrogen bonds or functional groups with high polarity. Examples of such monomer include acrylamide, acrylic acid, ethylene oxide, vinyl acetate, *N,N*-diethylacrylamide (DEAm), methyl vinyl ether, *N*-vinylpyrrolidinone, *N*-(2-methyl-4-oxopentan-2-yl)acrylamide, NIPAm, DMAm, and DMAEA (Figure I-17).¹⁵¹⁻¹⁵⁵

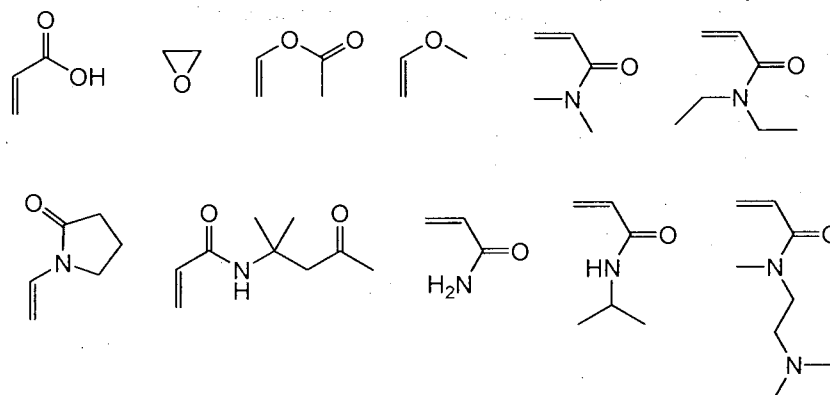


Figure I-17. Examples of non-ionic WSP monomers.

2.1.2 Ionic Water-Soluble Polymers

Ionic WSP can be further divided into two groups, polyelectrolytes and polyzwitterions. Polyelectrolytes are polymers containing anionic or cationic groups while polyzwitterions are polymers containing both anionic and cationic functional groups. Polyzwitterions can also be divided into two subgroups, polyampholytes and polybetaines, depending on the location of the anionic and cationic groups on the polymeric chain. The anionic and cationic groups are on the different repeating units in polyampholytes, while in polyzwitterions, they are located on the same repeating units (Figure I-18).

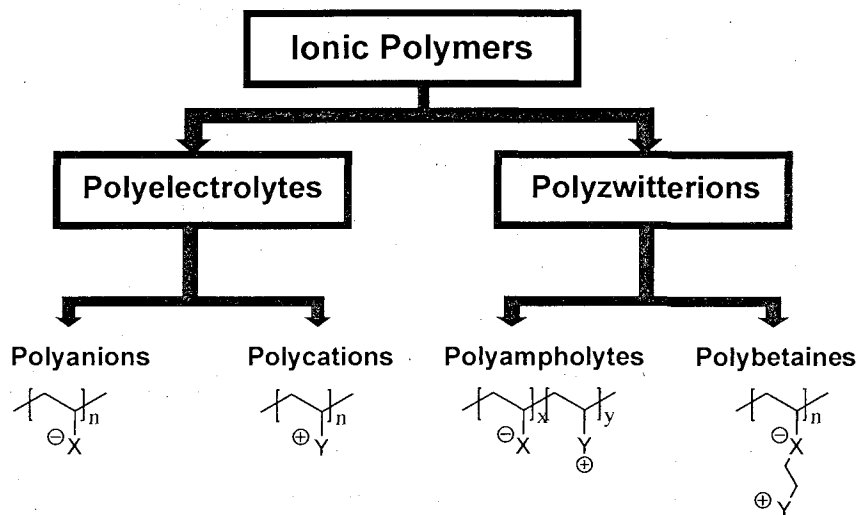


Figure I-18. Illustrative structures of the ionic polymer family.

Polyelectrolytes

Polyelectrolytes are generally prepared by the direct (co)polymerization of monomers with a cationic or anionic group. Generally, the cationic group in polyelectrolytes is an amine or ammonium group; the anionic groups include carboxylate, phosphate, and sulfonate species. Examples of such monomers are shown in Figure I-19.^{84,151,156,156-180} It is notable that there are monomers that are sensitive to pH, and others that are insensitive to the solution pH. For example, among those cationic groups, the positive charge of amine group may be neutralized when pH increased to certain degree while the quaternary ammonium salts remain positively charged negating pH change. As for common anionic groups, the carboxylate group is sensitive to changes in pH while the sulfonate group is not.

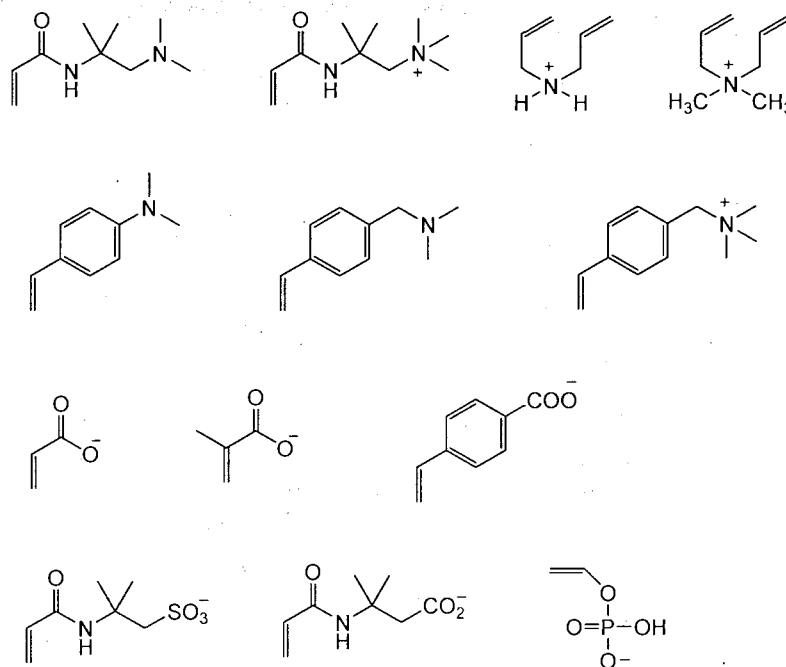


Figure I-19. Examples of cationic and anionic monomers.

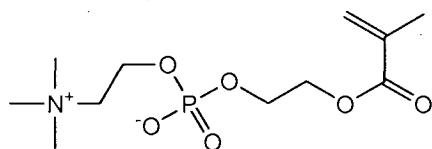
Polyampholytes

Polyampholytes are typically prepared by the direct (co)polymerization of the anionic and cationic monomers. The first reported examples of polyampholytes were statistical copolymers synthesized via conventional free radical polymerization. Before the invention of controlled free radical polymerization techniques, controlled anionic polymerization is the main technique for preparing block polyampholytes. However, anionic polymerization can not be used to directly polymerize monomers with labile protons, and therefore acid groups need to be protected prior to polymerization. Due to the recent development of controlled/living free radical polymerization techniques, namely ATRP, NMP and RAFT, researchers are now able to prepare block

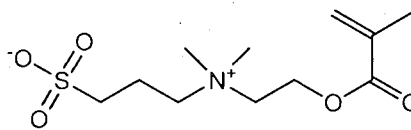
polyampholytes without having to protect the acid group.

Polybetaines

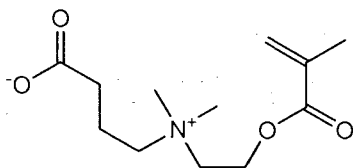
To date, there are four known betaine species that are distinguished based on the nature of the zwitterionic group: sulfobetaines,^{181,182} carboxybetaines,¹⁸³⁻¹⁸⁶ phosphobetaines,^{122,187-193} and ammonium alkoxydicyanoethenolates¹⁹⁴⁻¹⁹⁸ (a representative methacrylate derivative of each is shown in Figure I-20).



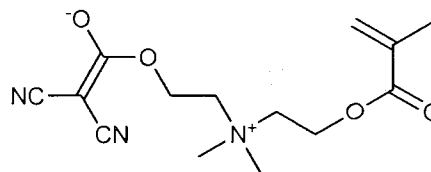
A phosphobetaine



A sulfobetaine



A carboxybetaine



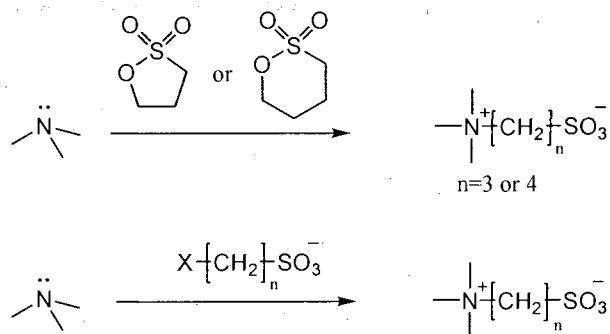
An ammonium alkoxydicyanoethenolate

Figure I-20. Examples of four different kinds of methacrylate-based betaines.

The positively charged group of all known is a quaternary ammonium species.

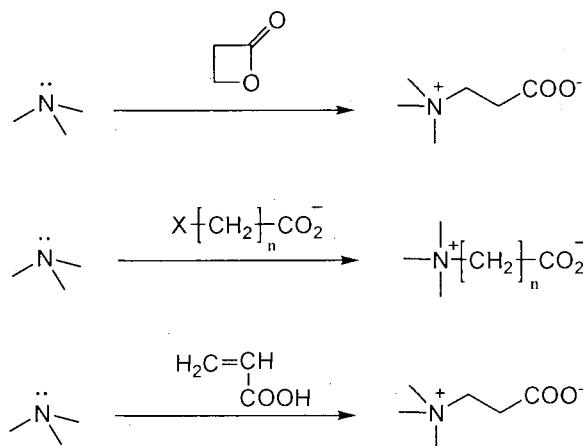
Thus, the synthesis of betaine species usually starts from a tertiary amine group.

Sulfobetaines are typically prepared from the reaction of a tertiary amine with a sulfone, or from the reaction of a tertiary amine with haloalkylsulfonate, shown in Scheme I-29.¹⁹⁹



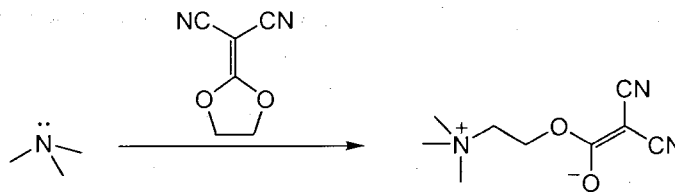
Scheme I-29. Synthetic routes to sulfobetaines.

Carboxybetaines can be prepared following similar synthetic routes to sulfobetaines by using analogous betainizing agents, lactones or haloalkylcarboxylates. Haloalkylcarboxylic esters can also be used as carboxylating agent to react with the tertiary amine and the product can be easily converted to carboxybetaines by hydrolysis of the ester group, Scheme I-30.¹⁹⁹



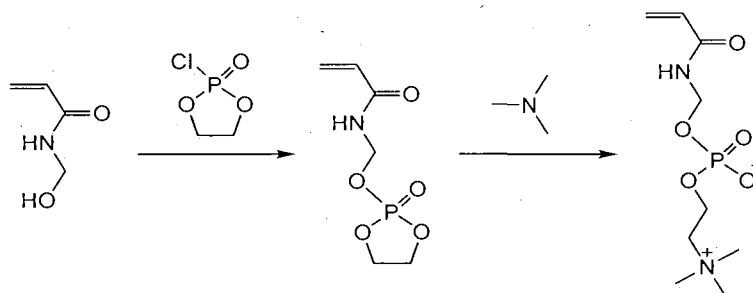
Scheme I-30. Synthetic routes to carboxybetaines.

Ammonium alkoxydicyanoethenolates are prepared by the reaction of a tertiary amine with cyclic dicyanoethylene acetal, Scheme I-31.¹⁹⁹



Scheme. I-31 Synthetic routes to ammonium alkoxydicyanoethenolates

To date, the phosphobetaine species are probably the most studied among the betaine family due to their excellent biocompatibility. Typically, such phosphobetaines are synthesized from the reaction of 2-chloro-2-oxo-1,3,2-dioxaphospholane with an alcoholic group, followed by a ring-opening reaction with trimethylamine, Scheme I-32.^{199,200}



Scheme I-32. Synthetic routes to phosphobetaines.

The first example of polybetaines prepared via controlled polymerization was reported in 1996 by Lowe et al. A homopolymer of 2-(dimethylamino)ethyl methacrylate was prepared via GTP with low polydispersity.^{29,201} The dimethylamino functional group in the polymer was subsequently betainized by using 1,3-propanesultone and nearly quantitative betainization was achieved. To date, there are examples describing the direct

polymerization of betaine monomers in aqueous media via CLP techniques, and specifically via ATRP and RAFT.

Solution Behavior of Ionic Polymers

Ionic polymers exhibit interesting aqueous solution behavior. For example, polyelectrolytes undergo chain extension in deionized water at low concentration due to the coulombic repulsions between charged groups in the polymer chains; the expanded polymer coils will shrink if low molecular weight electrolyte is added to the solution or the solution pH changes which screen such coulombic repulsions, making the polyelectrolytes adopt a more collapsed, entropically favored conformation. Such behavior is known as the *polyelectrolyte effect* (Figure I-21).¹⁹⁹

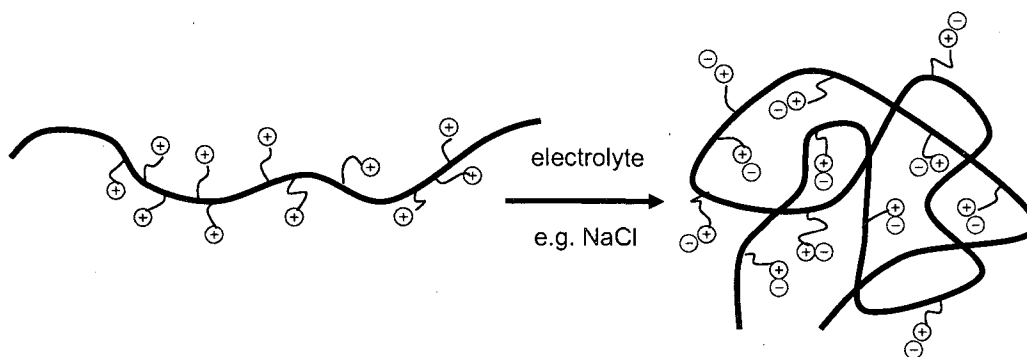


Figure I-21. Schematic illustration of polyelectrolyte effect.

The solution behavior of polyzwitterions is opposite to that of polyelectrolytes. In this case, polymer chains expand when low molecular weight electrolyte is added to the solution. Poly-zwitterions usually exhibit poor solubility in pure water, and the

solubility increases when low molecular weight electrolyte is added to the solution. This can be explained by the positive and negative charges that polyelectrolytes bear. While they are electrically neutral, there exist net attractive ionic interactions, which cause intra- and intermolecular ionic bonding, reflected in the formation of an insoluble ionically cross-linked network structure. The addition of low molecular electrolyte will penetrate the ionic network, screen the intra-/inter-molecular ionic interactions, and hence increase solubility. Such behavior is named the *anti-polyelectrolyte effect*, as it is opposite to the *polyelectrolyte effect* (Figure I-22).¹⁹⁹

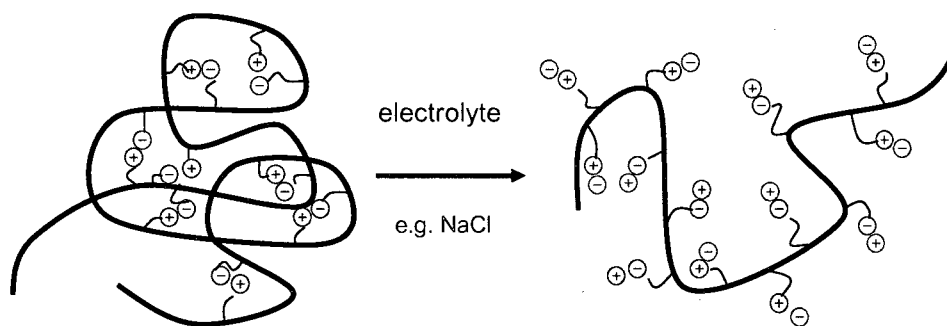


Figure I-22. Schematic illustration of anti-polyelectrolyte effect.

2.2 Polymeric Micelles

Block copolymers comprised of two or more blocks with different solubility are known to be capable of forming polymeric micelles in selective solvents. Generally, the micellization process occurs when the block copolymer is dissolved in a solvent that is a good solvent for one block and a precipitant for another. The insoluble block forms the core of the micelle and the soluble block forms the flexible outer corona of the micelle

(Figure I-23). Such micelles are usually spherical with a narrow size distribution but the shape and size distribution may change under different conditions.

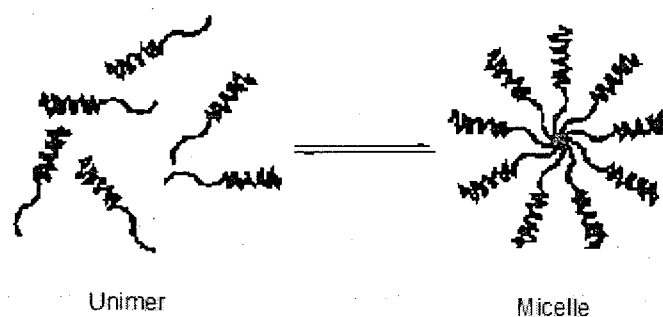


Figure I-23. Reversible self-assembly of AB diblock copolymers

It is noteworthy that the micellization of block copolymers happens only above a critical micelle concentration (CMC), below which only unimers are present in the solution. Above the CMC, the unimers are in equilibrium with the multi-molecular micelles. Such a micellar system is usually characterized by the following parameters:²⁰²

- CMC: the critical micelle concentration
- CMT: the critical micelle temperature
- M^m : the molecular weight of micelle
- Z: the aggregation number, e.g. the average number of polymer chains in a micelle
- R_g : the radius of gyration of the micelle
- R_h : the total hydrodynamic radius of the micelle
- R_c : the radius of the micellar core

- L: the thickness of the shell (corona) formed by the soluble block
- K: the equilibrium constant between the unimers and micelles

2.3 Self-Assembly of Stimuli-Responsive Copolymers

Diblock copolymers able to form micelles usually contain a hydrophilic and a hydrophobic block. In an aqueous environment, under certain conditions such amphiphilic block copolymers will self-assemble with, the hydrophobic block forming the micellar core and the hydrophilic block forming the stabilizing micellar shell. In the case of hydrophilic-hydrophilic diblock copolymers, they exist as unimers in an aqueous environment. However, the solubility of one, or both, of hydrophilic blocks may be changed by an external stimulus. Thus the hydrophilic-hydrophilic diblock copolymer is turned into hydrophobic-hydrophilic species and is able to form micelles. Such polymers are generally described as stimuli-responsive polymers, which include thermo- or temperature-responsive, pH-responsive, and salt-responsive polymers, depending on the nature of the stimulus that they respond to.

For example, Sumerlin et al. reported the synthesis of diblock copolymers of sodium 2-acrylamido-2-methylpropanesulfonate (AMPS) and sodium 3-acrylamido-3-methylbutanoate (AMBA) in aqueous solution by RAFT polymerization.¹⁵⁶ Both the AMPS and AMBA monomers are soluble in aqueous solution at higher pH (above the pK_a of the carboxylic group of AMBA). When the pH is lowered to below the pK_a of the

carboxylic group, the AMBA block becomes protonated and hydrophobic while the AMPS block remains hydrophilic. As a result, the copolymers self-assemble into polymeric micelles. It is noteworthy that the process is completely reversible; the polymeric micelles dissociate when the pH is increased to above the pKa of the AMBA block (Figure I-24).

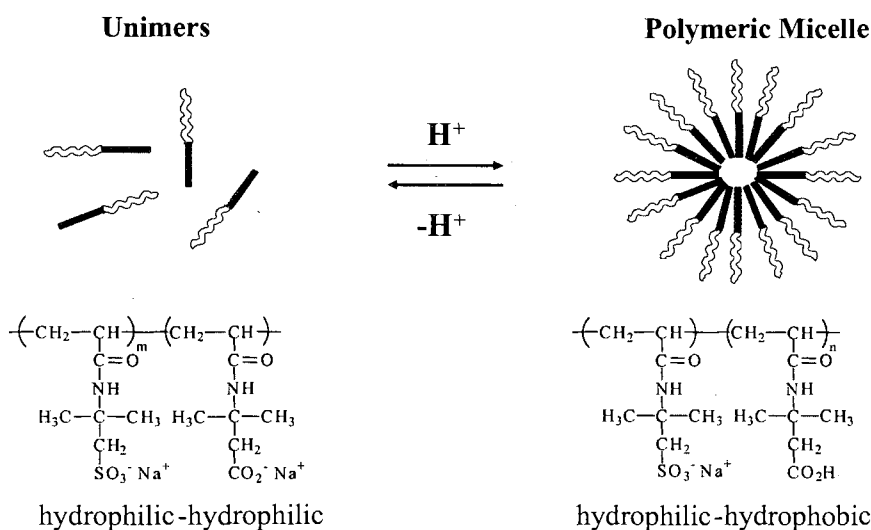


Figure I-24. Reversible micellization of block copolymers comprised of AMPS and AMBA in aqueous solutions upon the change of pH.

In such AMPS-AMBA diblock copolymers, the AMBA block is the only component responsive to an external stimulus. In the case where both blocks are stimuli-responsive, the polymers are termed as doubly responsive block copolymers or Schizophrenic block copolymers. For example, Lowe et al. reported the synthesis of a doubly responsive copolymer comprised of *N*-isopropylacrylamide (NIPAm) and 4-vinylbenzoic acid (VBZ) prepared via RAFT polymerization.⁸⁷ The NIPAm block is thermo-responsive, and has a lower critical solution temperature of 32 °C. In contrast, the

VBZ block is pH-responsive, similar to AMBA. At ambient temperature and high pH, the copolymer exists as unimers in aqueous solution. If the temperature is raised to above the LCST of NIPAm while the pH remains elevated, the NIPAm block becomes hydrophobic and forms the insoluble micellar core which is stabilized by the soluble VBZ shell.

Conversely, if the pH is lowered while the temperature remains below 32 °C, the VBZ block becomes hydrophobic and forms the insoluble micellar core which is stabilized by the soluble NIPAm shell (Figure I-25).

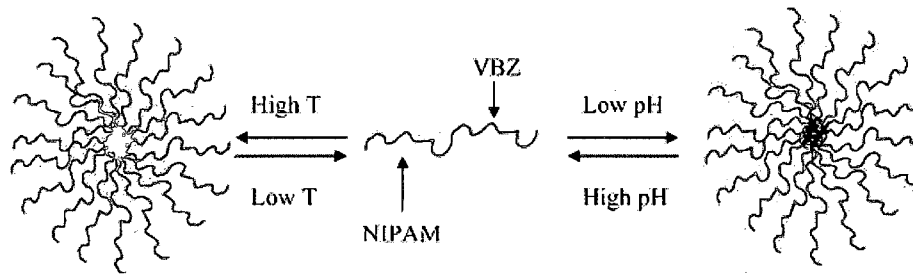


Figure I-25. The normal and inverse micellizations of the NIPAm-VBZ diblock copolymer under different stimuli, e.g. pH and temperature.⁸⁷

2.4 Experimental Technique to Study Self-Assembly

Experimental techniques employed to study polymeric micelles generally include nuclear magnetic resonance (NMR) spectroscopy, transmission electron microscopy (TEM), size exclusion chromatography (SEC), static light scattering (SLS), dynamic light scattering (DLS), small angle neutron scattering (SANS) and small angle X-ray scattering (SAXS), fluorescence spectroscopy, viscometry, ultracentrifugation, and stop flow techniques. The characteristic information that these techniques can offer is

listed in Table I-1.²⁰²

Table I-1. Experimental techniques for micelle characterization.

TEM	visual images of the polymeric aggregates, size, shape
NMR spectroscopy	chain dynamics
SLS	weight-average molecular weight (M_w)
DLS	hydrodynamic volume, i.e. R_h
SEC	R_h , M^m , dynamics of the equilibrium between unimers and micelles
SANS and SAXS	M_w , R_g , R_c
Fluorescence spectroscopy	Chain dynamics, CMC, hybridization of micelles
Viscomety	R_h , intrinsic viscosity
Ultracentrifuge	Micelle density, Z average molecular weight
Stop flow technique	Kinetics of micelle formation and dissociation

Among these techniques, NMR, DLS, SLS, and fluorescence spectroscopy are probably most used for the characterization of micelles. Thus, they are discussed in more detail in the following subsections.

2.4.1 *NMR Spectroscopy*

NMR spectroscopy is a quick and convenient method for monitoring the chain dynamics of block copolymers by examination of the solvation of individual polymeric blocks. In general, the block soluble in the solvent used for NMR spectroscopy gives resonance signals while the block insoluble does not give signals. For example, the aqueous stimuli-responsive properties of NIPAm-VBZ AB diblock copolymers can be studied by the ^1H NMR spectroscopy. At ambient temperature and basic pH, both NIPAm and VBZ blocks are soluble in the aqueous solution; and the ^1H NMR spectrum of this copolymer recorded under such condition showed signals for both blocks. However, the signals associated with VBZ block disappear in the ^1H NMR spectrum at ambient temperature and acidic condition, when the VBZ block becomes protonated and insoluble in water (Figure I-26). Such observations indicate the formation of polymeric micelles and the VBZ micellar core is shielded from the aqueous environment which causes the disappearance of its corresponding signals.

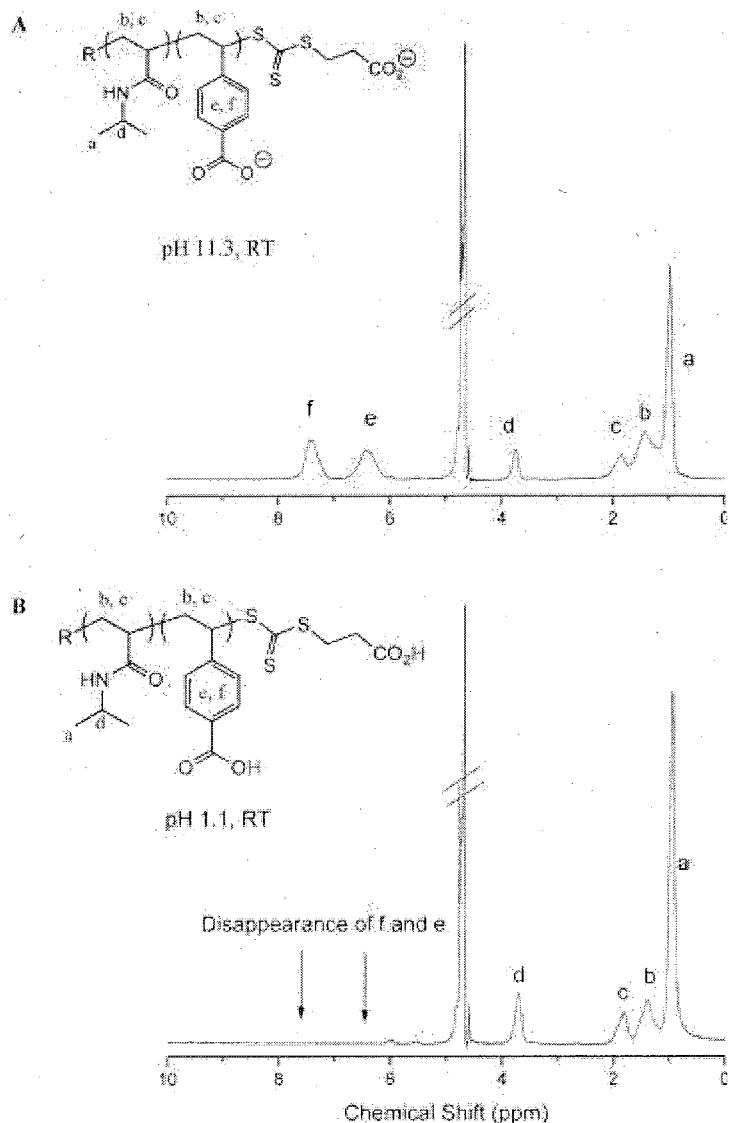


Figure I-26. ^1H NMR spectra of the P(NIPAm-b-VBZ) copolymer at pH 11.3 and room temperature (A), and the same AB diblock copolymer at pH 1.1 and room temperature (B).⁸⁷

2.4.2 DLS and SLS

Both DLS and SLS work by shining a laser beam onto a solution and measure the scattered light generated by hitting the particles in the solution. The DLS technique measures the time-dependent fluctuations in the intensity of scattered light which occurs

because the particles are undergoing random, Brownian motion. Analysis of these intensity fluctuations enables the determination of the distribution of diffusion coefficients of the particles, which are converted into a size distribution using the Stokes-Einstein Equation.

$$R_h = k_B T / 6\pi\eta D_0 \quad \text{Equation (7)}$$

where k_B is the Boltzmann constant

T is the absolute temperature in Kelvin degrees

η is the viscosity of the solvent

D_0 is the diffusion coefficient

DLS is able to detect the size change of block copolymers caused by forming aggregates. More specifically, when all blocks of a block copolymer are soluble in a solution, the R_h measured by DLS approximately equals to the unimer size; when polymeric micelles form under certain condition, the R_h shall significantly increase.

SLS measures total scattered intensity of light as a function of angle and concentration. This is commonly summarized in a Zimm plot. Scattered light intensities are measured at several angles for each solution concentration and a pure solvent. Then, it is possible to determine M_w and R_g of the species under investigation.

2.4.3 *Fluorescence Spectroscopy*

To study the micellization of polymers by fluorescence spectroscopy, a probe

molecule is added in the solution with the polymer. Under certain condition that the polymer forms micelles, the probe molecule will preferentially partition into the hydrophobic micellar core, and the intensity of the probe molecule observed by fluorescence spectroscopy decreases significantly in comparison with the intensity when the polymer exists in the unimer form.

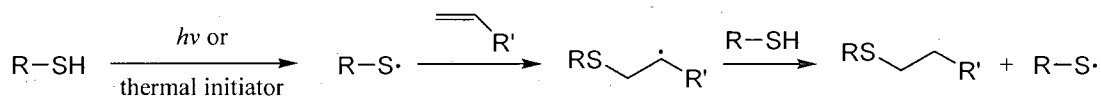
3. Thiol-Ene Chemistry

The thiol-ene coupling reaction, which was discovered over a century ago,²⁰³ is the hydrothiolation of a C=C bond. To date, the thiol-ene reaction has been extensively studied under a wide range of conditions. Due to its broad applicability (addition is possible virtually any ene) and excellent regioselectivity, the thiol-ene coupling reaction has been used as a powerful tool for the formation of C-S bonds. Recently, the thiol-ene coupling reaction has attracted renewed interest given the recognition of its “click” characteristics, including its rapid rates of reaction, its tolerance towards protic species and oxygen, and its ease of execution.^{204,205}

3.1 Conventional Thiol-Ene Chemistry

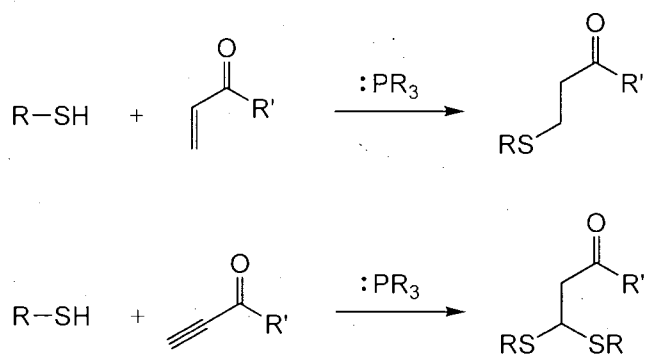
The thiol-ene coupling reaction can be conducted under a variety of conditions such as thermally-initiated, photochemical initiation,^{204,206,207} nucleophilic catalysis,²⁰⁸

amino acid catalyzed,²⁰⁹ Lewis acid catalysis,²¹⁰ and organometallic compound catalyzed.²¹¹ The thermal-initiated and photo-initiated thiol-ene reactions proceed via a radical mechanism and give anti-Markovnikov products (Scheme I-33). Such radical thiol-ene reactions are highly versatile toward ene substrate, being applicable to virtually any ene.



Scheme I-33. Mechanism of thermally induced and photo-initiated thiol-ene reactions.²⁰⁷

Phosphines are well-known catalysts for conventional Michael additions to activated C=C bonds and, can be used to catalyze the thiol-ene reaction, also known as thiol-Michael addition, for activated enes.²¹² Such reaction conditions are also applicable to activated yne yielding the double addition product.²¹³⁻²¹⁷ Amines have also been reported as efficient catalysts for the thiol-ene reaction, Scheme I-34.



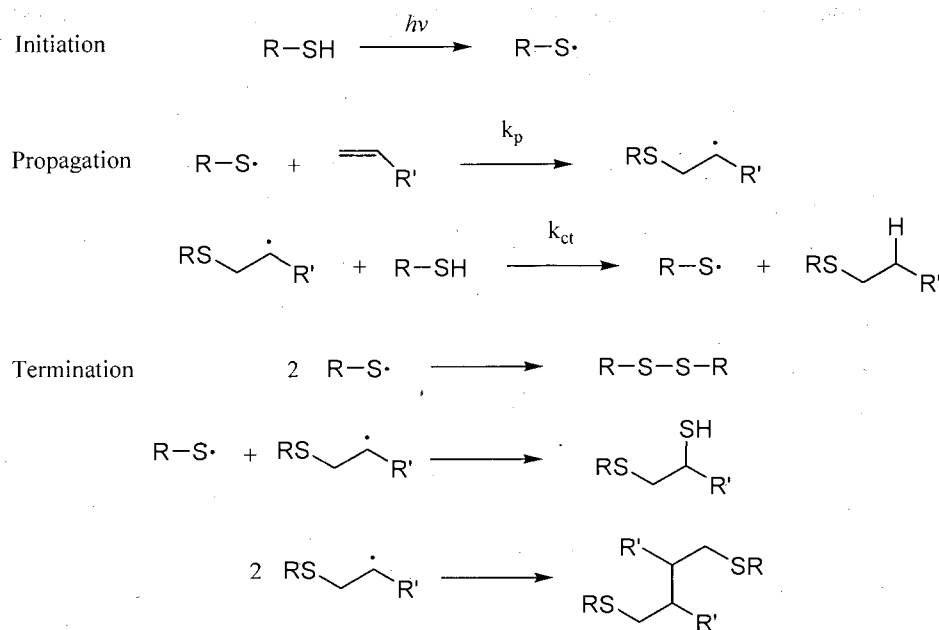
Scheme I-34. Thiol-Michael addition of conjugated ethylene and acetylene

The hydrothiolation of acetylenes with aryl and alkyl thiols catalyzed by

organometallic compounds has been extensively studied and gives exclusively Markovnikov or anti-Markovnikov products. Suitable catalysts include those based on nickel, palladium, rhodium, platinum, cesium, indium, thorium, uranium and selenium.^{214,216-221} Among these catalysts, the InBr_3 -catalyzed hydrothiolation of alkylacetylenes with aryl or alkyl thiols gives double addition products;²¹⁷ other catalysts can only afford mono addition products under specific conditions.

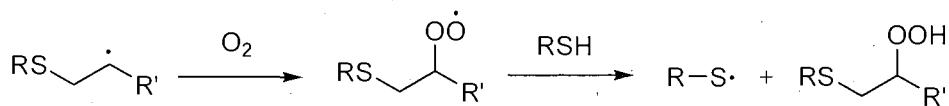
3.2 Applications of Thiol-Ene Reaction in Polymer Synthesis

The radical-mediated thiol-ene reaction (Scheme I-35) is widely used in polymer synthesis for the preparation of perfect networks by exposing a mixture of a multifunctional thiol and a multifunctional ene to UV light. The prepared polymeric network is highly cross-linked and has a narrow glass transition region. The UV-induced thiol-ene polymerization is currently employed in surface-coating with several important advantages including tolerance toward oxygen and water, rapid curing, and low toxicity. Furthermore, the thiol-ene polymerization technique is used to produce optical elements^{222,223} and dental restorative materials.²²⁴



Scheme I-35. General mechanism of photo-initiated thiol-ene polymerization.²⁰⁴

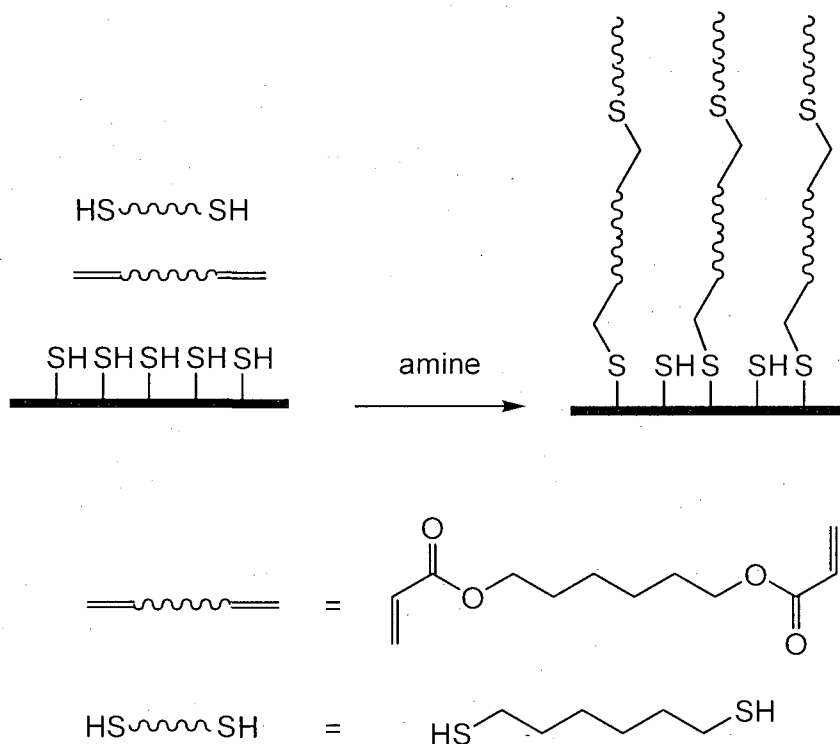
A unique feature of photo-initiated thiol-ene polymerization is the radical step growth mechanism. Importantly, unlike typical radical polymerization where the presence of oxygen kills propagation, the thiol-ene polymerization process is insensitive to the presence of oxygen. This can be explained by the ease of chain transfer from a peroxy radical, formed from molecular oxygen, with thiols readily forming a hydroperoxide species and a new, highly reactive thiyl radical, Scheme I-36.²⁰⁴



Scheme I-36. Radical mediated thiol-ene polymerization under the presence of oxygen.

Recently, the click character of the thiol-ene reaction has attracted increasing interest of researchers. For example, Khire et al. reported the surface modification of a

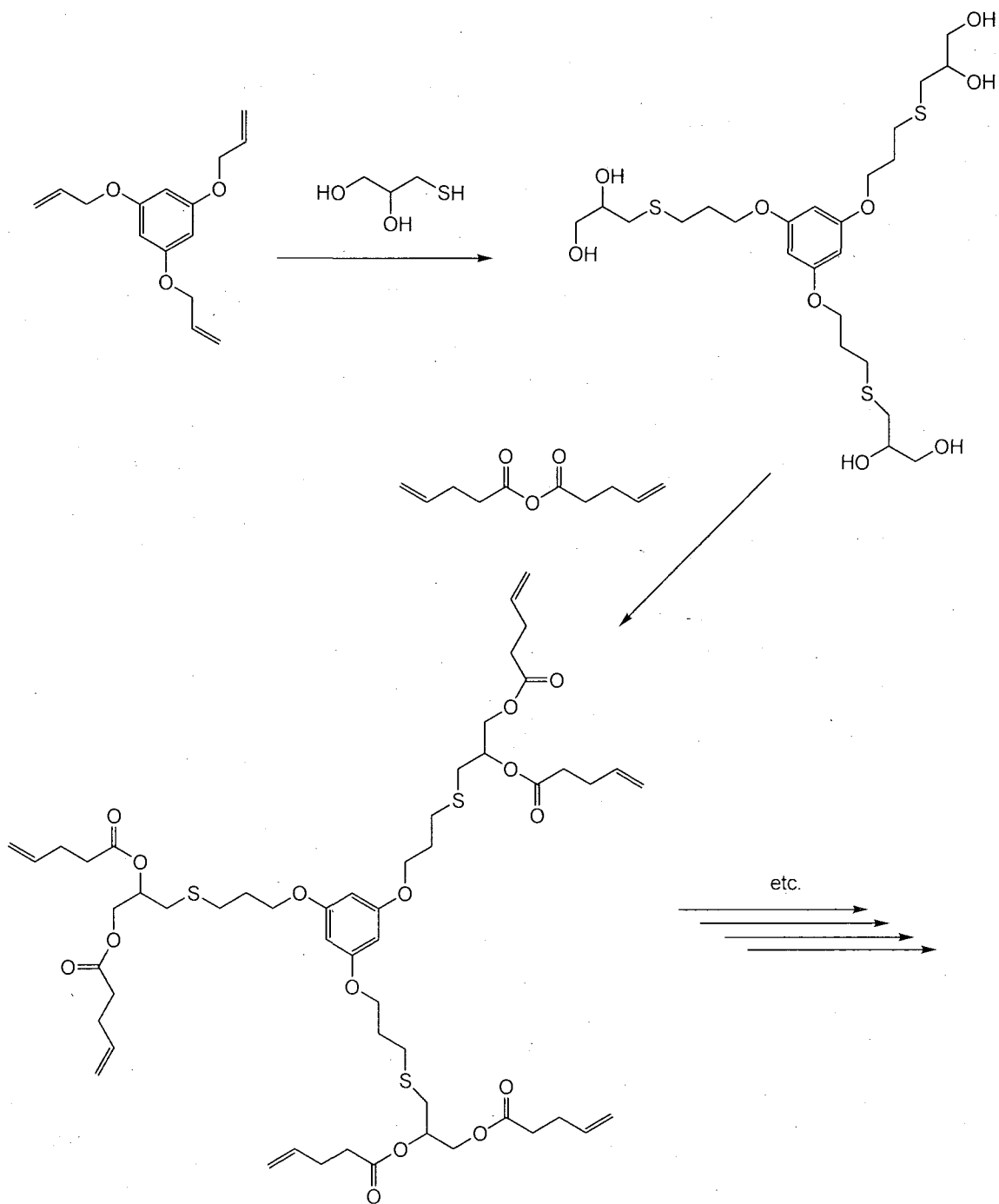
self-assembled monolayer using thiol-acrylate conjugate addition.²²⁵ On a surface modified with a thiol-terminated monolayer, the conjugate addition of a dithiol and a diacrylate proceeds in the presence of an amine catalyst. The thickness of the film is controlled by the thiol-acrylate ratio and the extent of reaction (Scheme I-37).



Scheme I-37. Surface modification via thiol-ene *click* chemistry.

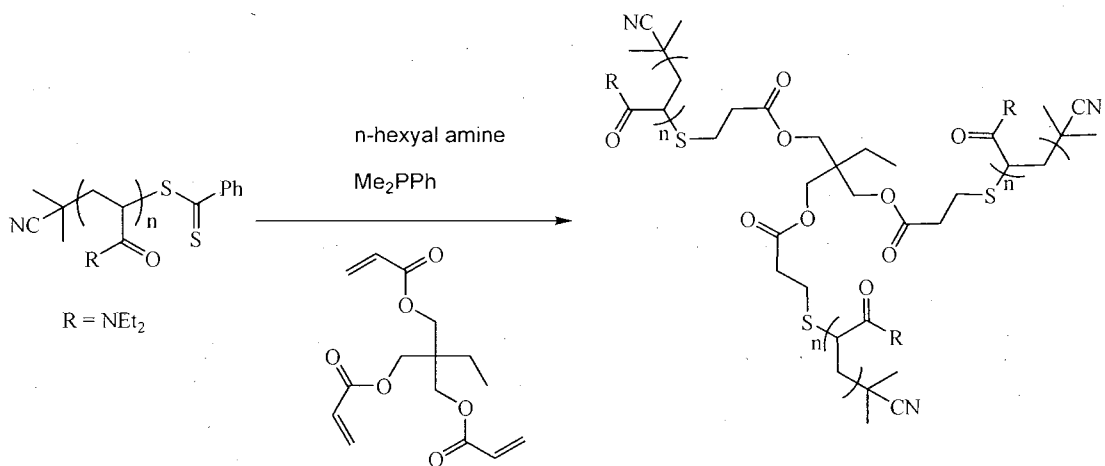
Killops et al. reported the synthesis of dendrimers in which the thiol-ene click reaction is used to build the dendritic backbone and functionalize the chain ends.²²⁶ The tri-alkene, 1,3,5-tris(allyloxy)benzene, serves as the dendrimer core and reacts with 3-mercaptopropane-1,2-diol under photo-initiated conditions to afford the first-generation hexa-hydroxy dendrimer [G1]-OH₆. [G1]-OH₆ further reacts with 4-pentenoic anhydride to esterify the hydroxyl group at the end of each chain converting each OH group to ene

group, affording [G1]-ene₆. Higher generation dendrimers are synthesized by repeating the thiol-ene and esterification reactions (Scheme I-38).



Scheme I-38. Synthesis of dendrimers via thiol-ene *click* chemistry.

More recently, Chan et al. reported the convergent synthesis of 3-arm star polymer from poly(DEAm) prepared via RAFT polymerization, using the thiol-ene coupling reaction. In the presence of hexylamine and dimethylphenylphosphine, the dithioester end group of the RAFT polymer cleaved to a thiol functionality which subsequently adds to tri-acrylate *in situ* via a thiol-Michael addition and affords a 3-arm star polymer (Scheme I-39). It should be pointed out that the phosphine serves more than a catalyst for the thiol-Michael addition; it also prevents the formation of the polymeric disulfide species than can form after end-group reduction.



Scheme I-39. Convergent synthesis of 3-arm star polymer via thiol-ene click chemistry.

CHAPTER II

OBJECTIVES OF RESEARCH

Water-soluble polymers (WSP) have drawn increasing interest from researchers due to the increasing development of aqueous-based commercial polymeric products. Among them, stimuli-responsive WSP are particularly interesting since the solubility of such materials changes upon the application of certain conditions, such as a change in pH, temperature, ionic strength, or pressure. AB diblock stimuli-responsive WSP are of special importance due to their ability to reversibly self-assemble into polymeric aggregates such as micelles and vesicles, which is induced by the application or removal of a specific stimulus. To synthesize WSP with well-defined molecular characteristics, including predetermined molecular weights, narrow molecular weight distributions, and advanced macromolecular architectures, the recently developed controlled/living radical polymerization techniques are widely employed, i.e., Nitroxide mediated polymerization (NMP), atom transfer radical polymerization (ATRP), and reversible addition-fragmentation chain transfer (RAFT) radical polymerization. Among them, RAFT polymerization is arguably the most suitable technique for preparing well-defined WSP due to its versatility with respect to monomer types, tolerance toward a wide range of functionality, and ease of conducting the polymerization.

The objective of this research is to prepare a variety of novel water-soluble, stimuli-responsive (co)polymers with well-defined macromolecular characteristics via

RAFT polymerization. More specifically, this project includes three parts:

1. Design and synthesis of novel stimuli-responsive WSP containing multiple tertiary amine functional groups.
2. Synthesis of novel water-soluble, stimuli-responsive AB diblock copolymers based on the biocompatible monomer, 2-(methacryloyloxy)ethyl phosphorylcholine (MPC).
3. Synthesis of a series of water-soluble N-isopropylacrylamide (NIPAm) polymers with well-defined mono and bis-functional end groups by using a combination of nucleophilic and radical thiol-ene/thiol-yne reactions.

Chain Transfer Agent (CTA) Synthesis

The key to a successful RAFT polymerization is the choice of a suitable RAFT CTA. In this project, 1-cyano-1-methylethyl dithiobenzoate (CPDB) is chosen to mediate RAFT polymerizations in organic media, due to its wide applicability to (meth)acrylate, (meth)acrylamide, and styrenic monomers. In the case of polymerization in aqueous environment, 4-cyanopentanoic acid dithiobenzoate (CTP) is chosen due to its versatility and solubility in water.

Synthesis of Novel WSP Containing Tertiary Amine Groups

An important group of WSP consists of polymers containing amine groups. Herein, three novel methacrylic monomers containing di- and tri- tertiary amine functional groups are firstly prepared. Subsequently, kinetic studies of the three

monomers will be conducted to examine their ability to polymerize under RAFT conditions. A combination of pseudo-first order kinetic plots and molecular weight data will be used to determine whether the controlled/living criteria are met.

Synthesis of Novel MPC-based AB Diblock Copolymers

MPC is one of the most thoroughly studied betaine monomers due to its excellent biocompatibility and anti-adherent properties. Herein, an MPC homopolymer is synthesized and subsequently used as a macro-CTA to mediate RAFT polymerizations of several stimuli-responsive comonomers, i.e. *N,N*-diethylacrylamide (**DEAm**), *N*-(3-sulfopropyl)-*N*-methacryloxyethyl-*N,N*-dimethylammonium betaine (**DMAPS**), 4-vinylbenzoic acid (**VBZ**), and *N,N*-di-*n*-propylbenzylvinylamine (**DnPVBA**), affording the target AB diblock copolymers. These stimuli-responsive copolymers are able to self-assemble into polymeric aggregates upon the application of particular stimuli. Such self-assembly behavior will be studied using a combination of ¹H NMR spectroscopy and DLS.

Synthesis of Mono and Bis End-Functionalized Poly(NIPAm)

A homopolymer of NIPAm is prepared via RAFT polymerization mediated by CPDB. The characteristic dithiobenzoate end group of such RAFT-synthesized polymer is reduced to thiol function and immediately adds to the activated ene of allyl methacrylate and propargyl acrylate, affording ene- and yne- end-functionalized

poly(NIPAm), respectively. The end- and yne- end functionalized poly(NIPAm) is further reacted with several different thiol compounds via radical thiol-ene and thiol-yne reaction to produce the mono- and bis- end-functionalized poly(NIPAm).

CHAPTER III

SYNTHESIS OF DI- AND TRI- TERTIARY AMINE CONTAINING METHACRYLIC MONOMERS AND THEIR (CO)POLYMERIZATION VIA RAFT

1. Introduction

(Co)Polymers that are able to undergo a conformational change or phase transition in aqueous media in response to an applied stimulus are interesting for numerous reasons including the ability to form higher ordered structures, often reversibly, such as micelles or vesicles. The applied stimulus can be as simple as a change in solution temperature, pH, electrolyte concentration, or a combination of such environmental changes. Of all the established stimulus-responsive, or “smart”, (co)polymers those containing tertiary amine methacrylates have been shown to exhibit a rich and varied aqueous solution behavior. In particular, copolymers containing 2-(dimethylamino)ethyl methacrylate (DMAEMA), 2-(diethylamino)ethyl methacrylate (DEAEMA), 2-(di-*iso*-propylamino)ethyl methacrylate (DiPAEMA), and morpholinoethyl methacrylate (MEMA) as building blocks are known to possess extremely interesting aqueous solution properties. The usefulness of these monomers as building blocks for the preparation of smart materials lies in the fact that the corresponding homopolymers possess very different properties in water. For example,

homopolymers of DMAEMA, while soluble over the useful pH range, do possess a lower critical solution temperature (LCST) between ~47 and 32 °C depending on its degree of polymerization,¹⁶¹ and as such are temperature responsive. In contrast, homopolymers of DEAEMA and DiPAEMA possess pH-responsive properties. DEAEMA and DiPAEMA homopolymers are soluble in water at low pH when the tertiary amine residues are protonated but become hydrophobic at intermediate-to-high pH when the amine functionalities are deprotonated. Homopolymers of MEMA, in a similar fashion to polyDMAEMA, possess an LCST between ca. 34 and 53 °C, again, depending on its degree of polymerization. Additionally, polyMEMA can also be readily salted out of solution with Na₂SO₄ and is thus both temperature and electrolyte responsive. Such differing aqueous solution characteristics have been exploited by Armes and co-workers who have conducted extensive studies of AB diblock and ABC triblock copolymers, prepared by either group transfer polymerization (GTP)^{161,163,164,227,228} or atom transfer radical polymerization (ATRP),²²⁹ derived from combinations of these monomers, as well as with other hydrophilic building blocks. For example, Bütün et al.²²⁸ described the GTP synthesis of a series of near-monodisperse AB diblock copolymers of DEAEMA and MEMA with DEAEMA contents ranging from 27-50 mol %. Given the different responses to environmental changes of these two building blocks, as noted above, the authors demonstrated, via a combination of NMR spectroscopy, dynamic light scattering, and small angle neutron scattering, that it is possible to form both normal and inverse micelles in the same solution simply by controlling the solution conditions. Dissolution

of the AB diblock copolymers in acidic media, where the copolymers exist as unimers, followed by the addition of KOH resulted in the formation of polymeric micelles with the DEAEMA block in the core stabilized by a MEMA corona. Under these conditions the DEAEMA residues are largely deprotonated and thus hydrophobic whereas the MEMA residues remain hydrophilic. In the case of the symmetric AB diblock, the formation of inverse micelles, i.e. with MEMA in the core and DEAEMA in the corona, could be achieved at pH 6.7 in the presence of 1.0 M Na₂SO₄. It should also be noted that polyamines are interesting from a biological perspective given that such (co)polymers are known to serve as delivery/transfer vehicles for biomolecules such as DNA and RNA.²³⁰⁻²³³

Reversible addition-fragmentation chain transfer (RAFT)^{66,94,234-238} radical polymerization is a controlled radical polymerization (CRP) process mediated by thiocarbonylthio compounds most commonly derived from the dithioester²³⁹⁻²⁴³ or trithiocarbonate^{82,87,244-249} families of functional species. As a synthetic technique, RAFT has proven to be an extremely versatile tool with respect to substrate choice, functional group tolerance, and general reaction conditions. For example, (co)polymers derived from the common monomer families such as styrenics,^{82,87,250-255} (meth)acrylamidos,^{247,256-258} and (meth)acrylics^{97,241,259,260} can be readily prepared²³⁵ under a range of experimental conditions. Additionally, monomers that have proven to be more difficult to polymerize in a controlled fashion via other CRP techniques, such as diallylammonium²⁶¹ substrates and non-activated vinyl esters and vinyl

amides,^{137,138,174,262} have been successfully polymerized via RAFT with appropriate choice of RAFT chain transfer agent (CTA). Additionally, given the presence of the readily reducible thiocarbonylthio end-groups, RAFT-prepared (co)polymers serve as convenient masked macromolecular thiols suitable for post-polymerization reaction.^{142,147,208,249,263}

Given the impressive and varied aqueous solution behavior of (co)polymers prepared from commercially available methacrylic monomers²⁶⁴ we decided to explore the synthesis and RAFT (co)polymerization of new tertiary amine-containing methacrylates. Monomers were prepared via a straightforward acylation of the corresponding multi-aminoalcohol with methacryloyl chloride, and their homo-/co-polymerization behaviors evaluated under typical RAFT conditions mediated by the RAFT chain transfer agent 1-cyano-1-methylethyl dithiobenzoate. Finally the aqueous phase behavior of the new multiamine-containing homopolymers was determined.

2. Experimental

All reagents were purchased from the Aldrich Chemical Company at the highest available purity and used as received unless stated otherwise. All aminoalcohols were purified by fractional distillation under reduced pressure prior to use in syntheses.

1-Cyano-1-methylethyl dithiobenzoate (CPDB) was prepared according to a literature

procedure.¹¹ Hexyl and lauryl methacrylates were purified by passage through a column of basic alumina. 2,2-Azobis(2-methylpropionitrile) (AIBN) was recrystallized from methanol, and stored in a freezer at -20 °C until needed.

Synthesis of 1,3-bis(dimethylamino)propan-2-yl methacrylate (M1)

To a 1-L, three-necked round bottom flask equipped with N₂ inlet/outlet and magnetic stir bar was added 1,3-bis-dimethylaminopropan-2-ol (24.2, g, 0.165 mol), triethylamine (TEA) (21.8 g, 0.215 mol), and anhydrous diethyl ether (250 mL). The flask was placed in an ice/water bath and purged with N₂ for 30 min. Methacryloyl chloride (22.5 g, 0.215 mol, in 50 mL anhydrous diethyl ether) was added drop-wise over 1 h under vigorous stirring. The stirring was continued for an additional 12 h at room temperature. Subsequently, the NEt₃·HCl precipitate was filtered and washed with diethyl ether (3 x 100 mL). Inhibitor (2,2-diphenyl-1-picrylhydrazyl (DPPH)) was then added to the solution to prevent polymerization. The diethyl ether was removed in vacuo, followed by a fractional distillation under reduced pressure to separate unreacted starting material and the product. The target compound was obtained in a ca. 65 % yield (note: **M1** has a boiling point (bp) of ~30 °C at ~1 mBar). ¹H NMR, CDCl₃: δ (ppm) = 6.03 (m, 1H, =CH₂), 5.48 (m, 1H, =CH₂), 5.10 (m, 1H, CH), 2.43 (d, 4H, 2 x CH₂), 2.20 (s, 12H, 4 x CH₃), 1.87 (m, 3H, CH₃). IR: ν (cm⁻¹) = 2970-2770 (aliphatic C-H), 1712 (C=O), 1634 (C=C), 1160 (C-O).

Synthesis of 1-(bis(3-(dimethylamino)propyl)amino)propan-2-yl methacrylate (M2)

To a 1-L three-necked round bottom flask equipped with N₂ inlet/outlet and magnetic stir-bar was added 1-(bis(3-(dimethylamino)propyl)amino)propan-2-ol (40.5 g, 0.165 mol), TEA (21.8 g, 0.215 mol), and anhydrous diethyl ether (250 mL). The flask was placed in an ice/water bath and purged with N₂ for 30 min. Methacryloyl chloride (22.5 g, 0.215 mol, in 50 mL anhydrous diethyl ether) was added drop-wise over 1 h under vigorous stirring. The reaction was allowed to continue stirring for an additional 12 h at room temperature. Subsequently, the NEt₃·HCl precipitate was filtered and washed with diethyl ether (3 x 100 mL). DPPH was then added to the solution to prevent polymerization. The ether was removed in vacuo, followed by a fractional distillation under reduced pressure to separate the unreacted starting material and the product. The target compound was obtained in a ~50 % yield. (note, **M2** has a bp of ~85 °C at ~1 mBar). ¹H NMR, CDCl₃: δ (ppm) = 5.95 (m, 1H, =CH₂), 5.40 (m, 1H, =CH₂), 4.92 (m, 1H, CH), 2.48-2.14 (m, 10H, 5 x CH₂), 2.08 (s, 12H, 4 x CH₃), 1.81 (m, 3H, CH₃), 1.45 (m, 4H, 2 x CH₂), 1.11 (d, 3H, CH₃). IR: ν (cm⁻¹) = 2966-2758 (aliphatic C-H), 1712 (C=O), 1634 (C=C), 1164 (C-O).

Synthesis of 2-((2-(2-(dimethylamino)ethoxy)ethyl)methylamino)ethyl methacrylate (M3)

M3 was prepared using two different methods. Firstly, it was prepared using the same general procedure as described above for both **M1** and **M2**, and successfully yielded the target compound in ca. 50% yield (note **M3** has a bp of ~72 °C at ~1 mBar).

Additionally, we briefly examined the enzyme (Novozyme-435) catalyzed esterification of vinyl methacrylate with the diamino alcohol following a method reported previously for preparing sugar (meth)acrylate monomers.²⁶⁵

To a 50 mL round-bottomed flask equipped with a magnetic stir bar was added 2-((2-(2-(dimethylamino)ethoxy)ethyl)methylamino)ethanol (3.88 g, 0.02 mol), vinyl methacrylate (2.0 g, 0.02 mol), Novozyme-435 (300 mg), and acetonitrile (15 mL). The flask was heated at 50°C for 5 days. After removal of the Novozyme 435 by filtration, and the acetonitrile by rotary evaporation, ¹H NMR of the crude product indicated >95% conversion. **M3** was isolated by vacuum distillation to give a recovered yield of ca. 50%. ¹H NMR, CDCl₃: δ (ppm) = 6.09 (m, 1H, =CH₂), 5.54 (m, 1H, =CH₂), 4.24 (t, 2H, CH₂), 3.52 (m, 4H, 2 x CH₂), 2.75 (t, 2H, CH₂), 2.66 (t, 2H, CH₂), 2.48 (t, 2H, CH₂), 2.34 (s, 3H, CH₃), 2.24 (s, 6H, 2 x CH₃), 1.92 (m, 3H, CH₃). IR: ν (cm⁻¹) = 2938-2766 (aliphatic C-H), 1704 (C=O), 1630 (C=C), 1156 (C-O).

Homopolymerization of M1

General procedure:

All polymerizations are targeted at $M_n = 30,000$. A mixture of **M1** (2.17 g, 10.1 mmol), CPDB (16 mg, 7.2×10^{-2} mmol), and AIBN (6 mg, 3.7×10^{-2} mmol) were added to a scintillation vial (20.0 mL capacity) equipped with a magnetic stir bar. The mixture was stirred for at least 30 min to ensure complete dissolution of CPDB and AIBN in the monomer. Aliquots (1.0 mL each) were transferred to 10 different vials (10.0 mL

capacity), which were then sealed with rubber septa. Each vial was purged with nitrogen for 30 min. The vials were then immersed in a preheated oil bath at 70 °C. Vials were removed at various time intervals, and polymerization was terminated by rapid freezing with liquid nitrogen. The samples were analyzed using a combination of size exclusion chromatography (SEC) and NMR spectroscopy. Conversions were determined by ^1H NMR spectroscopy.

Homopolymerizations of M2 and M3

The homopolymerizations of **M2** and **M3** were performed following the same procedure as detailed for **M1**. Two homopolymerizations were performed for each monomer at different CTA:AIBN ratios to evaluate the kinetic behavior.

Statistical copolymerization of M1 and lauryl methacrylate

Below is detailed a typical procedure for a statistical copolymerization of **M1** with lauryl methacrylate. The same general method was followed for all copolymer syntheses:

All copolymerizations are targeted with an M_n of 30,000 at quantitative conversion. A mixture of **M1** and LMA (0.8 g total), at a pre-determined molar ratio, CPDB (5.9 mg, 2.7×10^{-2} mmol), and AIBN (0.9 mg, 0.55×10^{-2} mmol) were added to a scintillation vial (10.0 mL capacity) equipped with a magnetic stir bar. The vial was sealed with a rubber septum and purged with nitrogen for 30 min. The vial was then

immersed in a preheated oil bath at 60 °C for ~10 hours. Polymerization was terminated by rapid freezing with liquid nitrogen and exposure to air. The highly viscous material was then diluted with THF. The copolymer was isolated by precipitation into a large excess of methanol (for **M1**- and **M3**-LMA copolymers with < 60 mol% **M1/M3** and **M3**-HexMA copolymers with < 40 mol% **M1/M3**) or hexane (for **M1**- and **M3**-LMA copolymers with ≥ 60 mol% **M1/M3** and **M3**-HexMA copolymers with ≥ 40 mol% **M1/M3**). The samples were analyzed using a combination of size exclusion chromatography (SEC) and NMR spectroscopy.

General Instrumentation

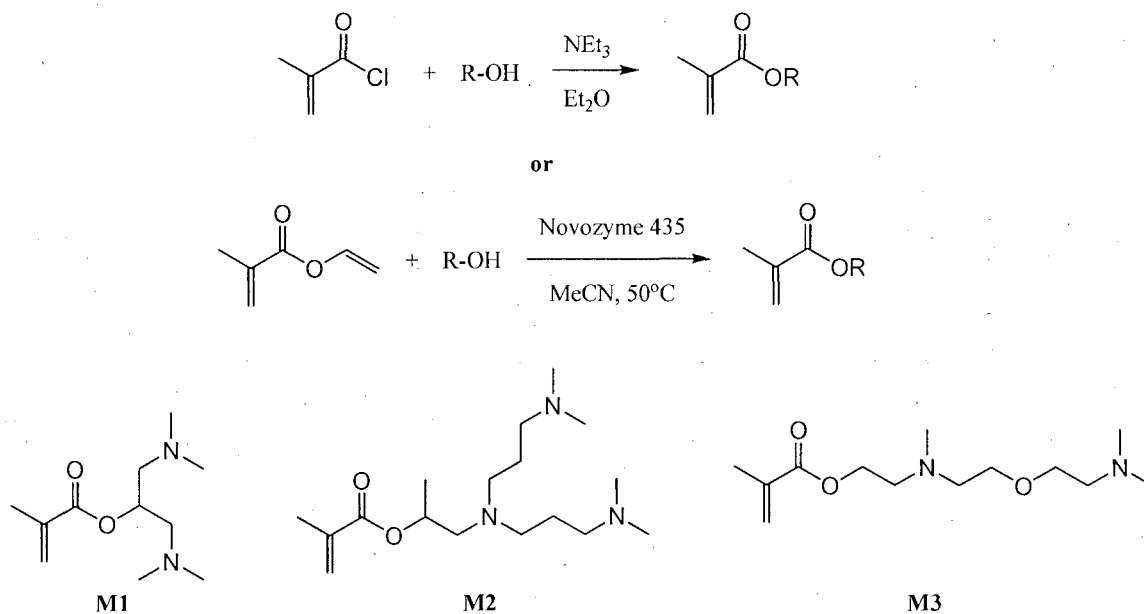
¹H and ¹³C NMR spectra were recorded on a Bruker 300 53 mm spectrometer in appropriate deuterated solvents. Size exclusion chromatographic analysis was performed on a Waters system comprised of a Waters 515 HPLC pump, Waters 2487 Dual λ absorbance detector, and Waters 2410 RI detector equipped with a PolymerLabs PLgel 5μm guard column and a PolymerLabs PLgel 5μm MIXED-C column (molecular weight range: 200-2,000,000 g/mol), in THF stabilized with 281 ppm BHT at a flow rate of 1.0 mL/min. The column was calibrated with a series of narrow molar mass distribution poly(methyl methacrylate) standards. The digital thermometer used in solution studies was a Traceable[®] expanded range thermometer. pH measurements was performed on a Accumet[®] AR15 pH meter calibrated with three pH buffers (pH = 4.00, 7.00, and 10.00).

3. Results and Discussion

The extremely interesting and varied aqueous solution properties exhibited by (co)polymers derived from commercially available tertiary amine containing methacrylates prompted us to examine the synthesis of multi tertiary amine containing monomers with the expectation that (co)polymers derived from these substrates would likewise possess certain stimulus-responsive characteristics in water. The emphasis herein is on a demonstration of the kinetic features of the homopolymerizations, a demonstration of the ability to prepare statistical copolymers, and a basic evaluation of the stimulus responsive characteristics of the homopolymers with an emphasis on the effect of changes in solution temperature and pH.

The methacrylic monomers containing two or three tertiary amine functional groups were prepared via an acylation reaction between methacryloyl chloride and the corresponding multi-aminoalcohol in the presence of triethylamine (TEA) in diethylether, Scheme III-1. In the case of **M3** its synthesis was also examined via the enzyme catalyzed reaction between the aminoalcohol and vinyl methacrylate, following a procedure that has been previously reported for the synthesis of sugar (meth)acrylate monomers.⁴⁷ While this procedure requires extended reaction times, compared to the methacryloyl chloride route, an advantage of this route is the easy removal, via filtration, of the enzyme catalyst. Analysis of the crude product mixture from the Novozyme-435

catalyzed reaction indicated a yield of ca. 95%.



Scheme III-1. Synthetic outline for the preparation of **M1-M3**.

In all instances, the target monomers **M1-M3** were obtained in ca. 50-60% yield after purification. The structure of the new monomers was confirmed using a combination of ^1H and ^{13}C NMR spectroscopy. Figure III-1 shows the ^1H and ^{13}C spectra, recorded in CDCl_3 , for all three monomers with peak assignments, verifying structure and purity.

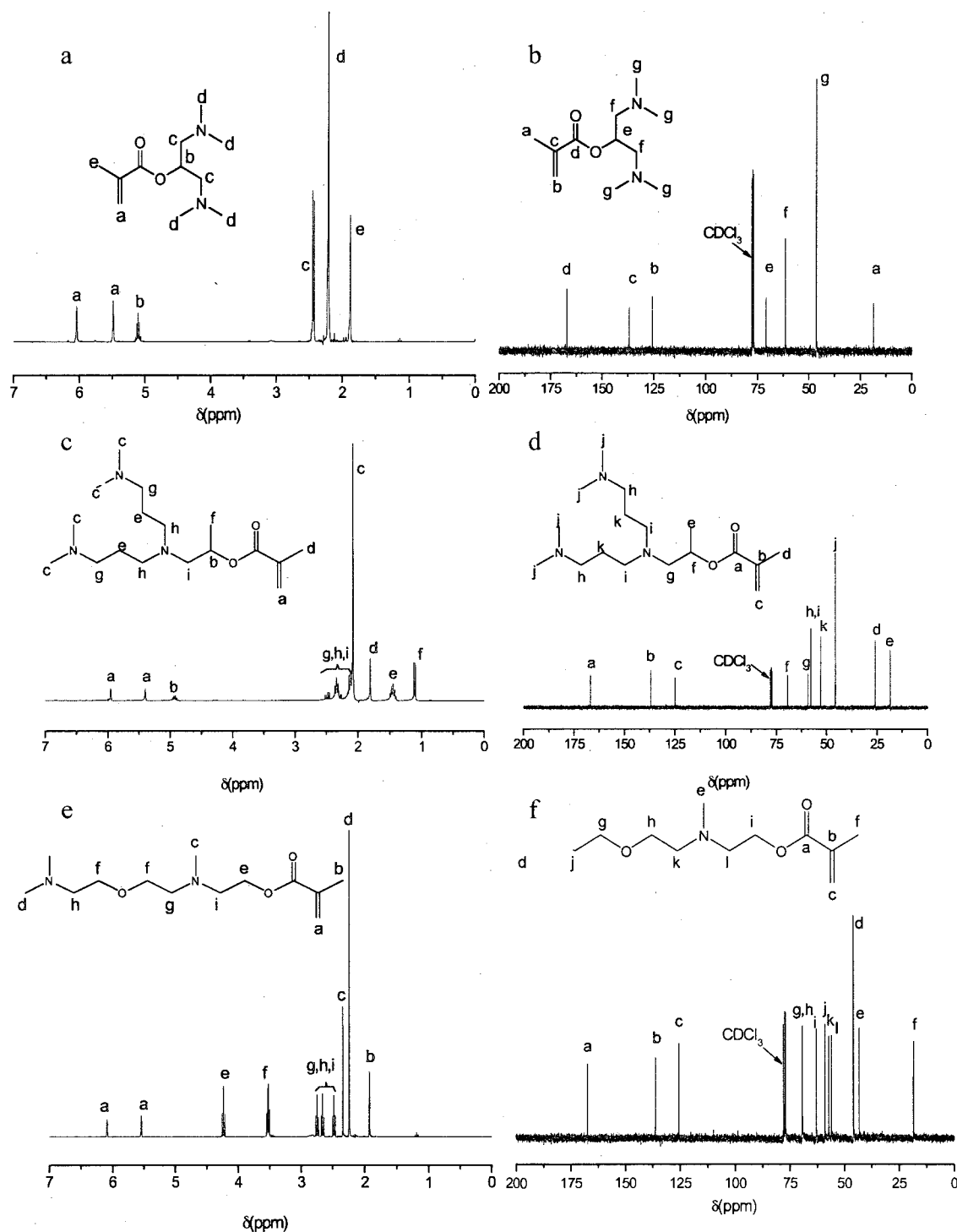


Figure III-1. a/b : ^1H and ^{13}C NMR spectra of 1,3-bis(dimethylamino)propan-2-yl methacrylate (**M1**) recorded in CDCl_3 ; c/d: ^1H and ^{13}C NMR spectra of 1-bis(3-(dimethylamino)propyl)amino)propan-2-yl methacrylate (**M2**) recorded in CDCl_3 , and e/f: ^1H and ^{13}C NMR spectra of 2-((2-(2-(dimethylamino)ethoxy)ethyl)methylamino)ethyl methacrylate (**M3**) recorded in CDCl_3 .

While **M1** has been reported previously²⁶⁶ it has never, to the best of our knowledge, been polymerized via a controlled polymerization technique. Both **M2** and **M3** are new methacrylic monomers. With monomers in-hand their RAFT homopolymerization employing the 1-cyano-1-methylethyl dithiobenzoate (CPDB)/AIBN RAFT chain transfer agent (CTA)/initiator combination was examined. Homopolymerizations of **M1-M3** were performed under bulk conditions, at 70°C, under a nitrogen atmosphere, at two different CPDB:AIBN ratios to evaluate the kinetics. Figure III-2, III-3 and III-4 shows the experimentally determined pseudo first order kinetic plots for the homopolymerizations of **M1-M3** at CPDB:AIBN ratios of 2:1 and 5:1. Several points are worth noting. In all instances the kinetic plots are linear indicating a constant number of active species (assuming k_p is essentially chain length independent). This is entirely consistent with previous observations of RAFT (co)polymerizations employing a wide range of CTAs. For **M1-M3** we observe that homopolymerizations conducted at the lower, 2:1, ratio of CPDB:AIBN proceed at a faster rate than those performed at the higher ratio of 5:1. This is entirely consistent with established effects of the CTA:I ratio on the kinetics of RAFT (co)polymerizations. In the case of the homopolymerizations conducted at a CPDB:AIBN of 2:1 the apparent rate constants, $k_{app} = k_p[P^*]$, lie in the range of ~0.0086-0.0139 min⁻¹. In the case of the 5:1, CPDB:AIBN, homopolymerizations the corresponding k_{app} values are 0.0041-0.0073 min⁻¹. In all instances induction periods are observed, with those at the lower CPDB:AIBN ratios being shorter. The occurrence of such induction periods is not uncommon in

dithioester-mediated RAFT (co)polymerizations and can be especially pronounced in the case of cumyl dithiobenzoate-mediated polymerizations. The fundamental cause of such induction periods is still not entirely clear although several explanations have been proposed. For example, such induction periods have been ascribed to slow fragmentation of the intermediate, carbon-centered radicals, slow reinitiation, a process termed initialization, the presence of impurities in the CTA, the occurrence of as yet un-verified undesirable side-reactions, and also the possibility of hybrid features, i.e. two or more of the above noted issues occurring.¹⁴ Regardless of the exact cause of such induction periods, which we have not attempted to elucidate, the homopolymerization characteristics of all three monomers are entirely consistent with dithiobenzoate-mediated RAFT polymerizations.

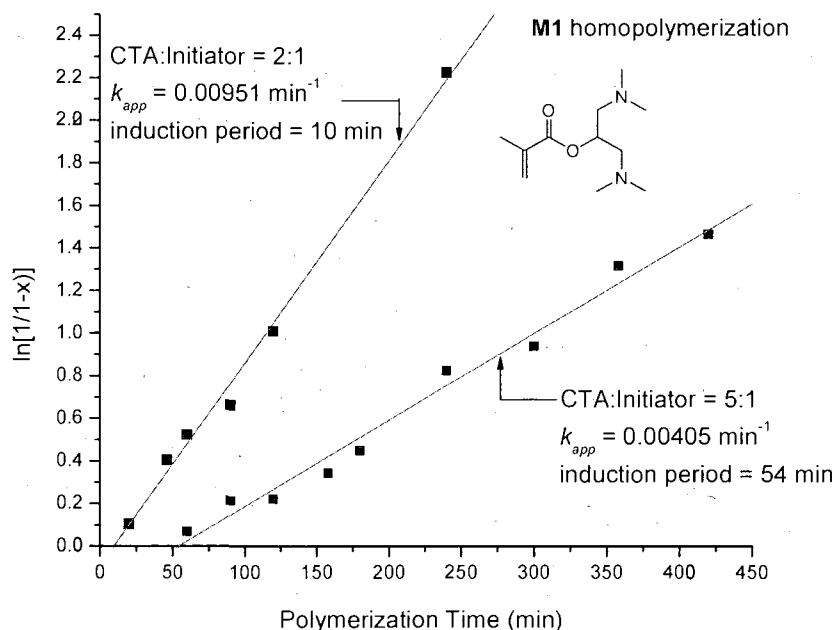


Figure III-2. Pseudo first order kinetic plots for the homopolymerizations of **M1** at CTA:AIBN ratios of 2:1 and 5:1, under bulk conditions, at 70 °C.

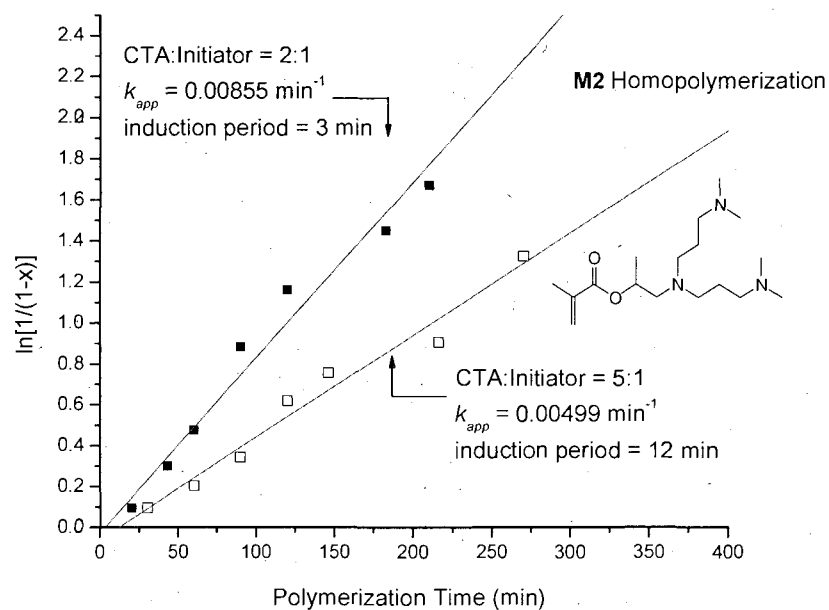


Figure III-3. Pseudo first order kinetic plots for the homopolymerizations of **M2** at CTA:AIBN ratios of 2:1 and 5:1, under bulk conditions, at 70 °C.

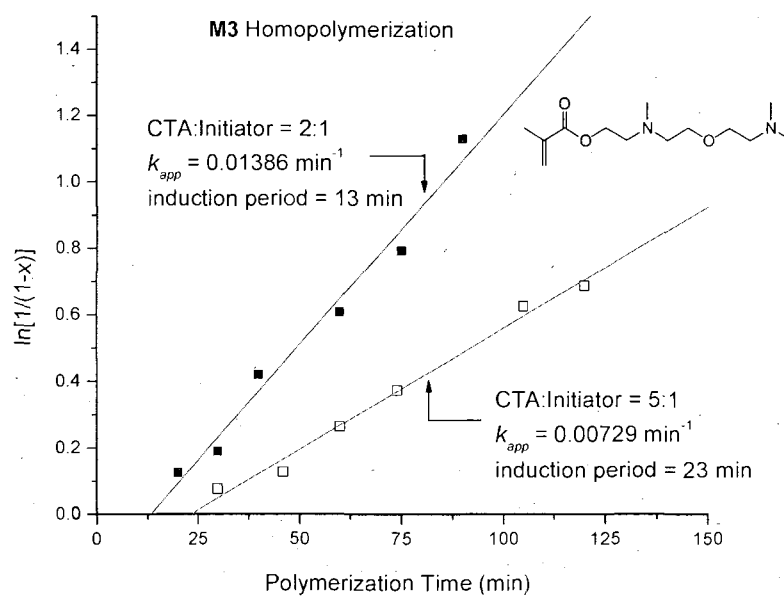


Figure III-4. Pseudo first order kinetic plots for the homopolymerizations of **M3** at CTA:AIBN ratios of 2:1 and 5:1, under bulk conditions, at 70 °C.

The kinetic results clearly confirm that **M1-M3** can be readily homopolymerized under typical RAFT conditions. While the kinetic results are encouraging, evidence of the controlled nature of these homopolymerizations is found in the M_n vs conversion plots, Figure III-5 a-f. In all instances the experimentally determined M_n s increase in a linear fashion with conversion indicating the controlled nature of the homopolymerizations. However, the measured values do not agree with the theoretical values and is likely due to the fact that the SEC instrument was calibrated with standards and as such the measured values are not absolute. The final, measured polydispersity indices (M_w/M_n) are as low as ~ 1.15 , but more typically in the range 1.20-1.25.

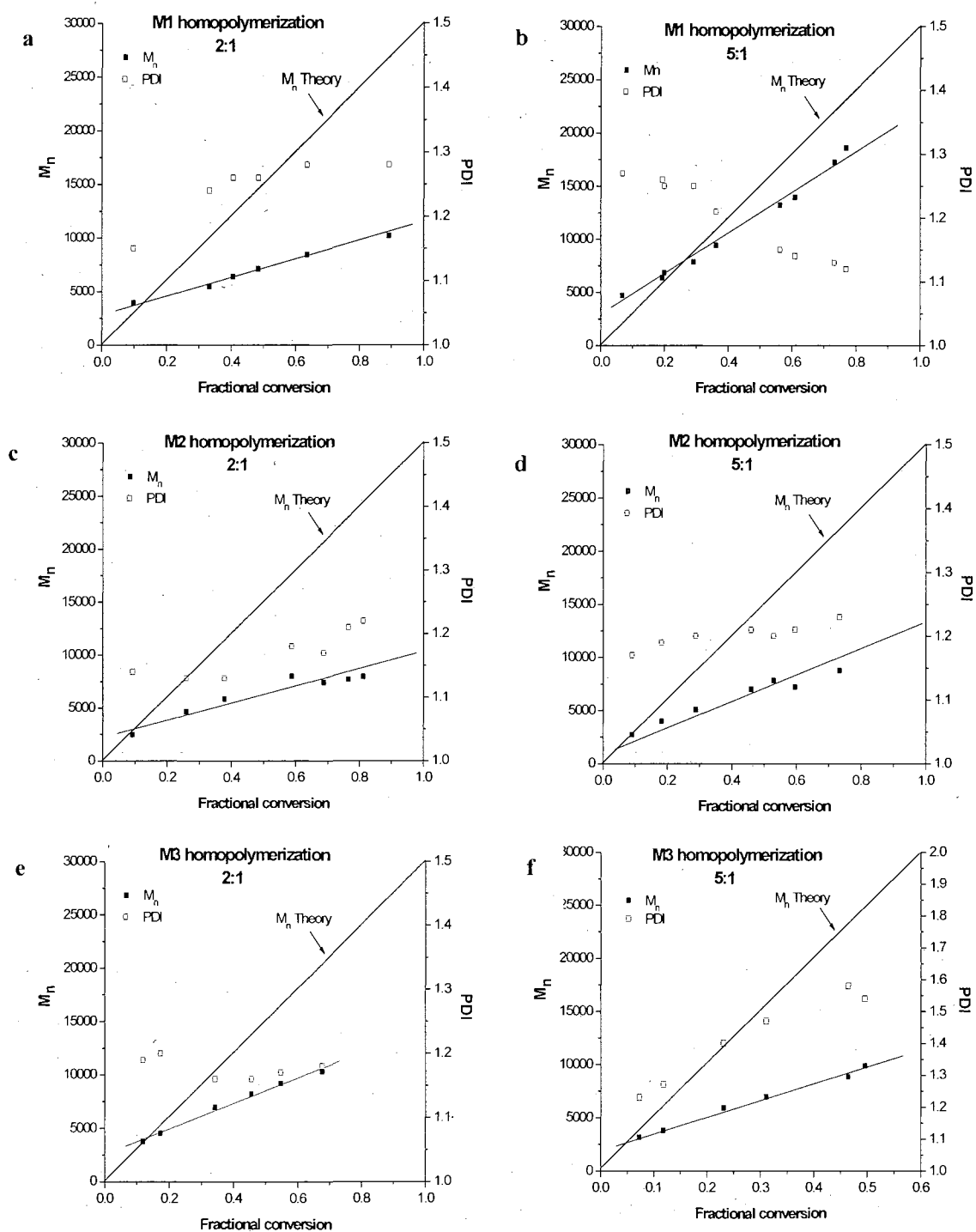


Figure III-5. M_n vs conversion and polydispersity index vs conversion for the M1-M3 homopolymerizations at CTA:AIBN ratios of 2:1 and 5:1, under bulk conditions, at 70 °C.

Having confirmed that **M1-M3** can be readily homopolymerized under typical RAFT conditions, we briefly examined the ability to prepare AB statistical copolymers with both hexyl methacrylate (HexMA) and lauryl methacrylate (LAMA) to demonstrate the ability to prepare materials with more advanced architectures. These two monomers were chosen as typical representatives of hydrophobic methacrylates, and because we have previously shown that LAMA, as well as other common hydrophobic methacrylates, readily copolymerize with DMAEMA in a statistical fashion via both conventional free radical polymerization²⁶⁷ and in a controlled manner via group transfer polymerization.²⁶⁸ Since the main focus of the paper is not a detailed evaluation of the copolymerization characteristics of **M1-M3**, copolymers were prepared only from **M1** and **M3**. Statistical copolymers of **M1** or **M3** with HexMA and LAMA were prepared at varying molar ratios ranging from 10:90 to 90:10. **M1**-based statistical copolymers were prepared at 60°C with the CPDB/AIBN RAFT CTA/initiator combination at a molar ratio of 5:1 and **M3**-based copolymers were prepared at 70 °C with the CPDB/AIBN molar ratio of 5:1. Table III-1 summarizes the theoretical and measured molar compositions, the conversions, experimentally determined M_n 's, and the polydispersity indices for the **M1**-based copolymers while Table III-2 shows the copolymers prepared from **M3**.

Table III-1. Summary of composition, conversion, M_n theory, M_n experimental and polydispersity index for a series of **M1**-lauryl methacrylate statistical copolymers.

Comonomer	Composition (theory) ^a	Composition (measured) ^b	Conversion (%) ^c	M_n (theory)	M_n expt. ^d	M_w/M_n ^d
LAMA	10:90	10:90	83	25,000	22,000	1.12
LAMA	20:80	20:80	86	26,000	22,000	1.11
LAMA	30:70	37:63	88	26,000	25,000	1.16
LAMA	40:60	26:74	95	29,000	28,000	1.17
LAMA	50:50	43:57	78	23,000	20,000	1.15
LAMA	60:40	57:43	69	21,000	16,000	1.15
LAMA	70:30	70:30	88	26,000	22,000	1.09
LAMA	80:20	79:21	85	26,000	22,000	1.11
LAMA	90:10	90:10	84	25,000	28,000	1.12

- a. Molar composition, **M1**:LAMA.
- b. Determined by ^1H NMR spectroscopy in CDCl_3 .
- c. Determined by ^1H NMR spectroscopy.
- d. Determined by size exclusion chromatography in THF. System was calibrated with narrow molecular weight poly(methyl methacrylate) standards.

Table III-2. Summary of composition, conversion, M_n theory, M_n experimental and polydispersity index for a series of **M3**-hexyl methacrylate and **M3**-lauryl methacrylate statistical copolymers.

Comonomer	Composition (theory) ^a	Composition (measured) ^b	Conversion (%) ^c	M_n (theory)	M_n expt. ^d	M_w/M_n ^d
HexMA	10:90	11:89	88	26,000	19,000	1.11
HexMA	20:80	19:81	81	24,000	15,000	1.12
HexMA	30:70	36:64	92	28,000	16,000	1.16
HexMA	40:60	35:65	76	23,000	11,000	1.14
HexMA	50:50	50:50	95	29,000	13,000	1.23
HexMA	60:40	60:40	92	28,000	11,000	1.23
HexMA	70:30	71:29	90	27,000	10,000	1.28
HexMA	80:20	77:23	88	26,000	6,400	1.26
HexMA	90:10	84:25	79	24,000	4,800	1.23
LAMA	10:90	-	86	26,000	19,000	1.09
LAMA	20:80	19:81	85	26,000	19,000	1.11
LAMA	30:70	30:70	85	26,000	17,000	1.12
LAMA	40:60	35:65	88	26,000	15,000	1.15
LAMA	50:50	51:49	89	27,000	21,000	1.24
LAMA	60:40	57:43	86	26,000	12,000	1.21
LAMA	70:30	71:29	71	21,000	7,800	1.24
LAMA	80:20	77:23	87	26,000	11,000	1.23
LAMA	90:10	88:12	56	17,000	6,000	1.18

a. Molar composition, **M3**:HexMA and **M3**:LAMA.

b. Determined by ¹H NMR spectroscopy in CDCl₃.

c. Determined by ¹H NMR spectroscopy.

d. Determined by size exclusion chromatography in THF. System was calibrated with narrow molecular weight poly(methyl methacrylate) standards.

It is clear from the data in Tables II-1 and II-2 that both **M1** and **M3** can be readily copolymerized in a statistical fashion with both HexMA and LAMA. Several points are worth highlighting. Firstly, copolymers with varying molar compositions can be easily prepared simply by controlling the initial molar ratio of monomers. Secondly, the copolymers can be prepared with narrow molecular mass distributions. In all instances the polydispersity indices are < 1.28 , and more typically 1.10-1.15. As a representative example, Figure III-6 shows the ^1H NMR spectrum and SEC trace (RI signal) of the **M1**₅₀/LAMA₅₀ copolymer. The agreement between the theoretical and measured M_n values is generally good. However, some discrepancies are observed for copolymers rich in the amine comonomer. This is not surprising given that the same behavior was observed for the **M1** or **M3** homopolymers, and is a further verification that the narrow molecular mass poly(methyl methacrylate) standards are poor equivalents for the multi-amine containing (co)polymers.

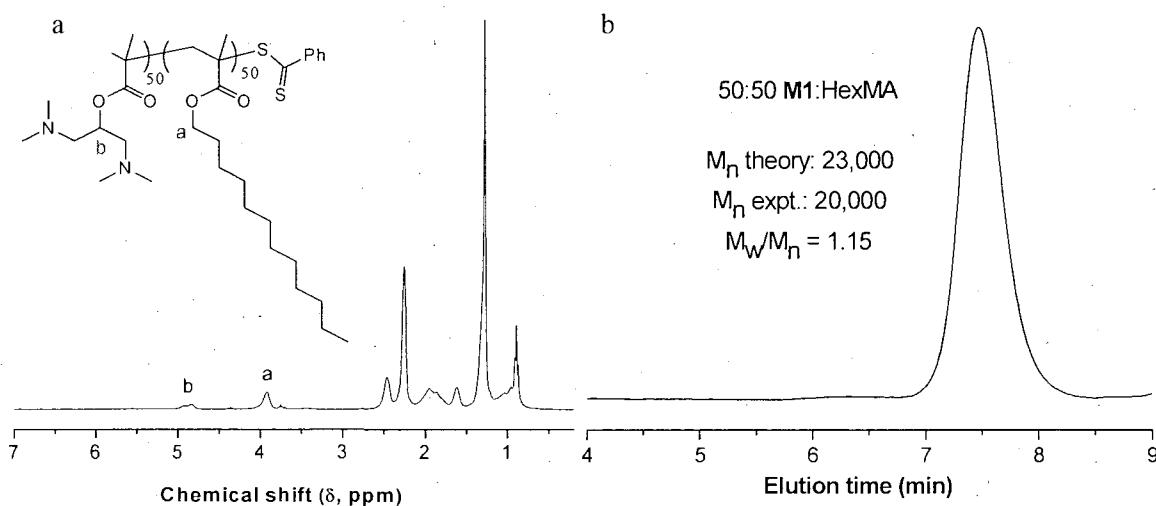


Figure III-6. a. ^1H NMR spectrum, recorded in CDCl_3 , for a 1:1 statistical copolymer of **M1** with LAMA, and b. The SEC trace (RI signal) for the same **M1**-*stat*-LAMA copolymer.

Aqueous solution behavior of polyM1, polyM2, and polyM3 homopolymers

Given the varied aqueous solution properties exhibited by (co)polymers derived from commercially available tertiary amine methacrylates including DMAEMA, DEAEMA and MEMA, the **M1-M3** homopolymers were examined with respect to their individual aqueous solution phase behavior. Specifically, their response, if any, towards changes in temperature and solution pH was examined. **M1-M3** homopolymers were dissolved in deionized water at a concentration of 1 wt%, the subsequent solution pH measured, and first evaluated with respect to their LCST characteristics. Figure III-7 shows a series of digital pictures of the 1 wt% poly**M1** solution, with a measured pH of 9.19, at 22 °C (**a**), 25 °C (**b**), and after cooling back down to 22 °C (**c**), the poly**M2** homopolymer, with a measured aqueous solution pH of 10.50, at 23 °C (**d**), 33 °C (**e**), and after cooling to 23 °C (**f**), and finally the poly**M3** solution, with a measured pH of 9.69, at 23 °C (**g**) and 62 °C (**h**) and at 61 °C (**i**). It is evident that at 22 °C (Figure III-7, **a**) the poly**M1** homopolymer is dissolved yielding a “water-white” solution. However, just a few degrees higher, at 25 °C (Figure III-7, **b**), the solution turns turbid, indicative of a hydrophilic-to-hydrophobic phase transition. This phase transition is completely reversible and cooling back down to ca. 22 °C results in re-dissolution, Figure III-7, **c**. Similar observations were made in the case of the **M2** and **M3** homopolymers. Both dissolve directly at ambient temperature in water at the specified concentration of 1 wt%. In the case of poly**M2**, the hydrophilic-to-hydrophobic phase transition occurs at ca. 33

°C, indicating that it is somewhat more hydrophilic than polyM1, whereas polyM3 has an observed LCST of ca. 63 °C and is clearly the most hydrophilic of the three homopolymers. Consistent with polyM1, cooling these solutions below these critical temperatures results in redissolution.

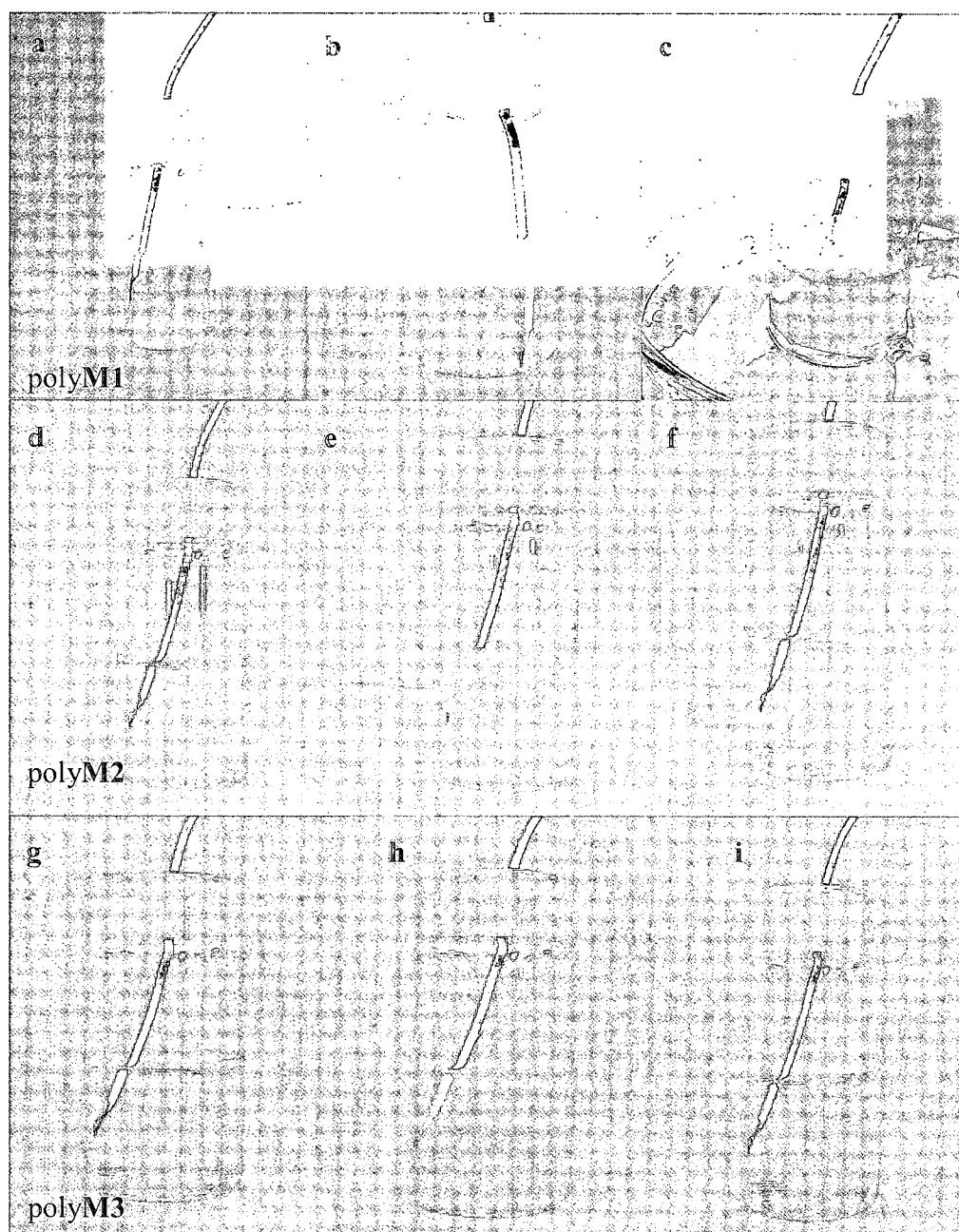


Figure III-7. Series of digital pictures of 1 wt % aqueous solutions of M1-M3 homopolymers demonstrating the reversible, temperature-induced phase transitions.

Interestingly, the **M1-M3** homopolymers are also sensitive to changes in aqueous solution pH with all homopolymers undergoing a clear phase transition at elevated pH, although the transitions did not present themselves until relatively high pH values were reached. The drop wise addition of 6.0 M NaOH to the 1 wt % solutions used above for the thermal study, under rapid stirring, results in a phase transition at high solution pH. For example, Figure III-8 shows digital pictures of the 1 wt % aqueous solution of poly**M2** at pH values of 10.43 and 12.68. The solution is clearly turbid at the higher of these pH values, while at pH 10.42 the solution appears 'water-white'. This behavior, as with the temperature induced phase separation, is completely reversible and lowering of the pH leads to re-dissolution of the **M2** homopolymer. Near identical observations were made for the **M1** and **M3** homopolymers with the pH-induced phase transitions not occurring until high values were attained.

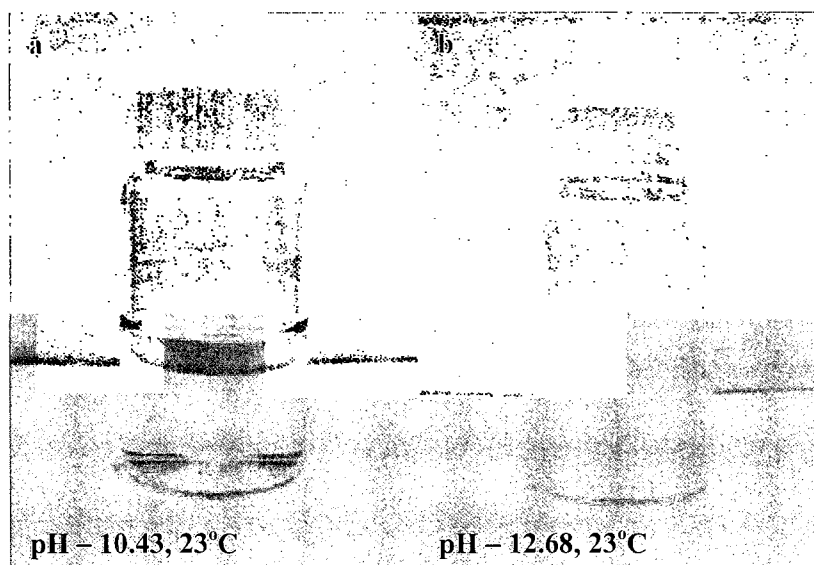


Figure III-8. Digital pictures of a 1 wt % solution of an **M2** homopolymer at 23°C and pH values of 10.43 (a) and 12.68 (b) demonstrating the pH induced phase transition.

4. Summary and Conclusions

The synthesis of multi tertiary-amine containing methacrylic monomers was described via a straightforward acylation reaction between multi-aminoalcohols and methacryloyl chloride. While 1,3-bis(dimethylamino)propan-2-yl methacrylate (**M1**) has been reported previously it had never been polymerized under controlled conditions. Both 1-(bis(3-(dimethylamino)propyl)amino)propan-2-yl methacrylate (**M2**) and 2-((2-(2-(dimethylamino)ethoxy)ethyl)methylamino)ethyl acrylate (**M3**) are new examples of amine-containing methacrylates. The homopolymerizations of **M1-M3** were shown to proceed in a controlled manner under standard RAFT conditions with 1-cyano-1-methylethyl dithiobenzoate as the RAFT agent. Subsequently, both **M1** and **M3** were shown to readily undergo statistical copolymerization with both hexyl and lauryl methacrylates to yield well-defined copolymers with narrow molecular mass distributions and composition easily tuned via the comonomer feed ratio. Finally, well-defined homopolymers of **M1-M3** were demonstrated to possess both temperature and pH-responsive properties in water. LCSTs in the range of ~25-63 °C were determined respectively while all materials phase separated from aqueous media at elevated pH values, thus making poly**M1**, poly**M2**, and poly**M3** examples of new stimuli-responsive building blocks.

CHAPTER IV

RAFT SYNTHESIS AND STIMULUS-INDUCED SELF-ASSEMBLY IN WATER OF
COPOLYMERS BASED ON THE BIOCOMPATIBLE MONOMER
2-(METHACRYLOYLOXY)ETHYL PHOSPHORYLCHOLINE

1. Introduction

Polymeric betaines (polybetaines) are zwitterionic materials in which the cationic and anionic functional groups are located on the same monomer/repeat unit.^{199,269} Such materials may be further differentiated based on the chemical nature of the negatively charged group and include the sulfo- (sulfonate),^{181,182} carboxy- (carboxylate),^{183-186,270} and phospho- (phosphonate)^{122,187-193,270} betaines as well as the less well known dicyanoetheneolates.¹⁹⁴⁻¹⁹⁸ Polybetaines were first reported in the 1950's,^{271,272} and since then have almost exclusively been prepared via the direct homogeneous aqueous radical solution polymerization of the corresponding betaine monomer. The preparation of well-defined polybetaines, as well as materials with more advanced architectures, has only been accomplished relatively recently. Lowe et al.^{29,162,201,268,273} reported the group transfer polymerization synthesis of poly(2-(dimethylamino)ethyl methacrylate) (PDMAEMA) homopolymers as well as copolymers with various methacrylic comonomers of controlled molecular weight and low polydispersity that were modified post-polymerization by reaction of the tertiary amine residues in the DMAEMA residues with 1,3-propanesultone yielding the

corresponding well-defined polysulfopropylbetaines. Such polymer analogous reactions are facile, selective, and essentially quantitative. The advent of controlled radical polymerization techniques has facilitated the direct (co)polymerization of sulfo-, carboxy-, and phosphobetaine monomers. For example, atom transfer radical polymerization has been employed extensively by Armes and co-workers in the preparation of a wide-range of materials based on the methacrylic phosphobetaine monomer 2-(methacryloyloxy)ethyl phosphorylcholine (MPC).^{121,122,124,125} MPC is especially interesting given its well-documented biocompatibility.^{187,190,274-281} Most recently the direct,²⁸² and indirect,²⁸³ synthesis of well-defined polysulfo- and polycarboxybetaines was accomplished by ring-opening metathesis polymerization (ROMP). Rankin and Lowe²⁸² described the rapid, direct, controlled homo- and copolymerization of *exo*-7-oxanorbornene sulfo- and carboxybetaine derivatives employing a novel 2,2,2-trifluoroethanol/CH₂Cl₂ solvent combination in conjunction with Grubbs first generation catalyst RuCl₂(PCy₃)₂CHPh. The only requirement for successful (co)polymerization was that the carboxybetaine be polymerized in the free acid form to prevent competitive complexation of carboxylate functional groups to the Ru metal center. Colak and Tew²⁸³ disclosed the synthesis of oxa- and methylene bridged norbornene-based polycarboxybetaines employing protecting group chemistry. Polymerizations of ammonium monomers with *tert*-butyl ester groups were performed in THF/methanol at 60°C employing the third generation Grubbs catalyst RuCl₂PCy₃(3-BrPy)₂CHPh. The free carboxybetaines were obtained post-polymerization

by treatment with neat trifluoroacetic acid.

Reversible addition-fragmentation chain transfer (RAFT) radical polymerization^{234,235-237,284,285} is, arguably, the most versatile of the controlled radical polymerization techniques facilitating the controlled polymerization of the broadest range of monomer families. For example, aside from the common monomer families such as styrenics,^{82,86,87,156,246,250} (meth)acrylates,^{241,244} and (meth)acrylamides,^{87,156,208,239,240,246,247,249,286} RAFT is suitable for non-activated substrates such as vinyl esters,²⁸⁷ vinyl amides,^{287,288} and diallylammonium species.²⁸⁹ RAFT has also been employed in the (co)polymerization of betaine monomers. The first report highlighting the application of RAFT in the synthesis of polybetaines was that of Laschewsky et al.,²⁹⁰ and was shortly followed by reports from Donovan and co-workers^{91,291} who described the direct homopolymerization of styrenic, methacrylic, and acrylamido sulfopropylbetaine derivatives in aqueous media as well as AB diblock and ABA triblock copolymers with *N,N*-dimethylacrylamide. MPC has also been (co)polymerized by RAFT - Yusa et al.²⁹² described a detailed study of the synthesis and self-association of AB diblock copolymers of MPC with *n*-butyl methacrylate. In addition to MPC, Stenzel et al.²⁹³ reported the RAFT polymerization of 2-(acryloyloxy)ethyl phosphorylcholine and the ability to form biocompatible nanocontainers.

While MPC has been copolymerized via RAFT with a hydrophobic comonomer

this technique has not been utilized in the preparation of new water-soluble stimulus-responsive block copolymers. To address this, we describe herein the synthesis of a new pH-responsive monomer and the block copolymerization of MPC with a variety of stimulus-responsive, or “smart”, neutral, ionic, and sulfobetaine comonomers. The comonomers were chosen to yield a range of materials exhibiting pH, temperature, or salt responsive properties that were anticipated to undergo reversible self-assembly in aqueous media as a function of such applied stimuli.

2. Experimental

All reagents were purchased from the Aldrich Chemical Company at the highest available purity and used as received unless noted otherwise. *N,N*-Diethylacrylamide was purchased from Polysciences Inc. and purified by distillation. The sulfobetaine monomer, *N*-(3-sulfopropyl)-*N*-methacryloxyethyl-*N,N*-dimethylammonium betaine (**DMAPS**), was prepared from the reaction between 2-(dimethylamino)ethyl methacrylate and 1,3-propanesultone in THF at ambient temperature.²⁹ 4-Cyanopentanoic acid dithiobenzoate,⁸⁵ 2-(methacryloyloxy)ethyl phosphorylcholine,¹⁸⁹ and 4-vinylbenzoic acid⁸⁵ were prepared according to literature procedures. 4,4'-Azobis(4-cyanovaleric acid) (V-501) was purified by recrystallization from MeOH and stored at -20°C until needed.

Synthesis of N,N-di-n-propyl-4-vinylbenzylamine (DnPBVA)

A mixture of 4-vinylbenzyl chloride (29.54 g, 0.194 mol), di-*n*-propylamine amine (50.0 g, 0.387 mol), methanol (50.0 mL, HPLC grade), and a small amount of phenothiazine were added to a 500 mL round bottom flask equipped with a magnetic stirring bar and a western condenser. The solution was then refluxed for 14 h.

Subsequently, methanol was removed using a rotary evaporator. The residue was then dissolved in 4.0 M HCl (100 mL) and this solution washed three times with diethyl ether (3 x 100 mL). NaOH was then added to the aqueous phase until the solution became slightly basic, after which it was washed three times with diethyl ether (3 x 100 mL).

The ether washings were combined and the solvent removed using a rotary evaporator to give a crude product yield of 76 %. The target monomer was purified via fractional distillation (bp of ~80 °C at ~1 mbar).

Homopolymerization of 2-(methacryloyloxy)ethyl phosphorylcholine (MPC)

To a Schlenk flask, equipped with a magnetic stir bar were added MPC (3.0 g, 10.2 mmol), 4-cyanopentanoic acid dithiobenzoate (CTP) (28 mg, 0.10 mmol), V-501 (5.6 mg, 2.0×10^{-2} mmol), deionized H₂O (15.0 g), and 5 wt% NaHCO₃ solution (336 mg). The mixture was then stirred for at least 4 h in an ice-bath to ensure complete dissolution of CTP and V-501. The solution was then purged with nitrogen prior to immersion in a preheated oil-bath at 70°C. After 2 h the polymerization was stopped via rapid cooling

and exposure to air. The polymerization solution was then dialyzed against deionized water for 12 h with 3 changes of the deionized water. Homopolymer was then recovered by freeze-drying yielding 1.7 g of material (yield of 56.7 %).

Synthesis of poly(MPC-block-4-vinylbenzoic acid), 50:50

All AB diblock copolymers were prepared using the same general approach. Any differences in reaction medium or polymerization temperature are noted in Table IV-1. Below is detailed the synthesis of a poly(MPC-*block*-4-vinylbenzoic acid) with a target molar composition of 50:50 as a representative example.

A mixture of polyMPC (0.5g, 1.69 mmol), 4-vinylbenzoic acid (VBZ) (0.251 g, 1.69 mmol), V-501 (2.8 mg, 9.93×10^{-3} mmol), Na_2CO_3 (180 mg, 1.70 mmol), and deionized H_2O (6.8 g) were added to a Schlenk flask equipped with a magnetic stir bar. The mixture was then stirred for at least 4 h in an ice-bath to ensure complete dissolution of V-501 and VBZ. The solution was then purged with nitrogen prior to immersion in a preheated oil-bath at 80 °C for 12 h. The polymerization was stopped by rapid cooling and exposure to air. The copolymer solution was then dialyzed against deionized H_2O for 6 h with 3 changes of the deionized water. The polymer was recovered by freeze-drying.

Sample preparation for dynamic light scattering experiments

Samples for dynamic light scattering were prepared as follows:

1.0 wt% solutions were prepared in 5 mL scintillation vials using the appropriate aqueous solution. The solution was then filtered through a Millex syringe filter with a pore size of 0.45 μm and 0.35 mL of the filtered solution was transferred to a polystyrene cuvette using a Rainin P1000 micro Pipette.

General instrumentation

^1H (300 MHz) NMR and ^{13}C (75 MHz) NMR spectra were recorded on a Bruker 300 53 nm spectrometer in appropriate deuterated solvents or solvent mixtures. Aqueous size exclusion chromatography experiments were conducted on a Viscotek system comprised of a Viscotek VE1122 pump, Viscotek VE3580 RI detector, a Viscotek viscoGEL PW_{XL} guard column followed by a series of two viscoGEL columns (G5000PW_{XL}+G4000 PW_{XL}), in 0.25 M NaBr solution which was degassed prior to use at a flow rate of 1.0 mL/min. The columns were calibrated with a series of narrow molecular weight distribution PEO/PEG standards. Data was manipulated using the Omnisec V4.1 software. Dynamic light scattering (DLS) experiments were conducted on a Malvern Instruments Zetasizer Nano-ZS (red badge) instrument operating with a 633nm laser. Data was collected and processed with the Dispersion Technology software V5.10.

3. Results and Discussion

With the aim of preparing and examining a range of new water-soluble, stimulus-responsive block copolymers based on the biocompatible building block 2-(methacryloyloxy)ethyl phosphorylcholine (MPC) a new pH-responsive styrenic monomer was initially prepared, Figure IV-1. *N,N*-Di-*n*-propyl-4-vinylbenzylamine (**DnPBVA**) was prepared in a straightforward manner from the reaction between 4-vinylbenzylchloride and di-*n*-propylamine and isolated in good yield. The structure of the product was confirmed via a combination of $^1\text{H}/^{13}\text{C}$ NMR and FTIR spectroscopies. Figure IV-2 shows the ^1H (a) and ^{13}C (b) NMR spectra of **DnPBVA**, recorded in CDCl_3 , with peak assignments, verifying structure and purity.

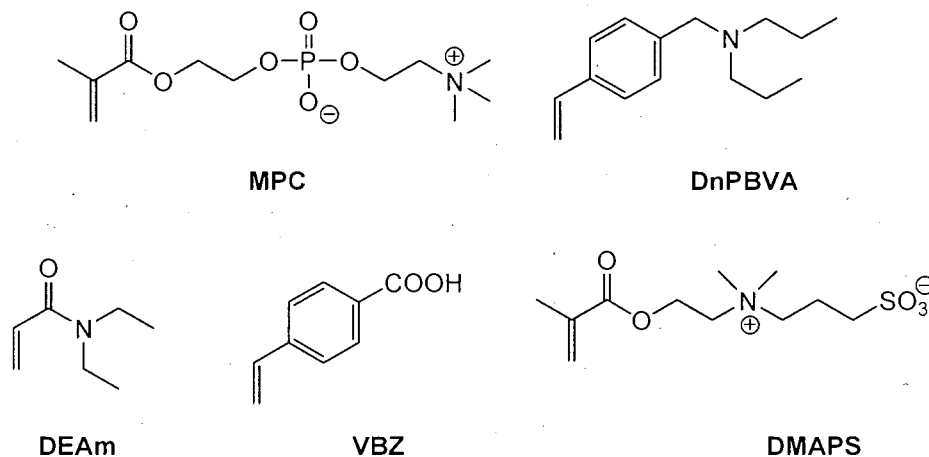


Figure IV-1. Chemical structures of monomers used in this study.

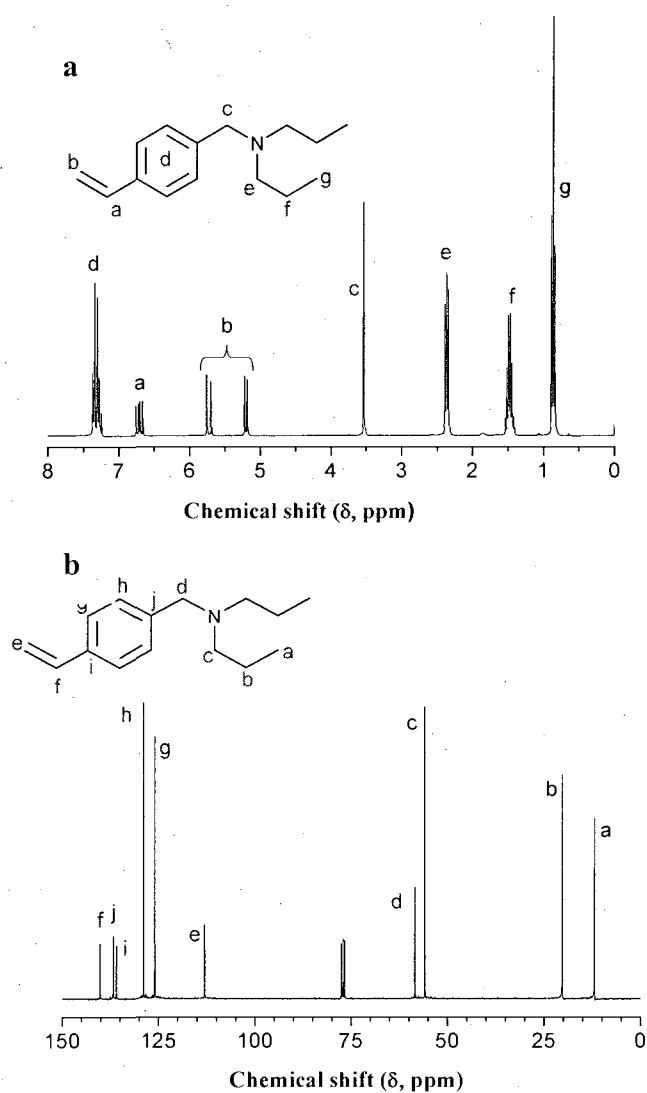
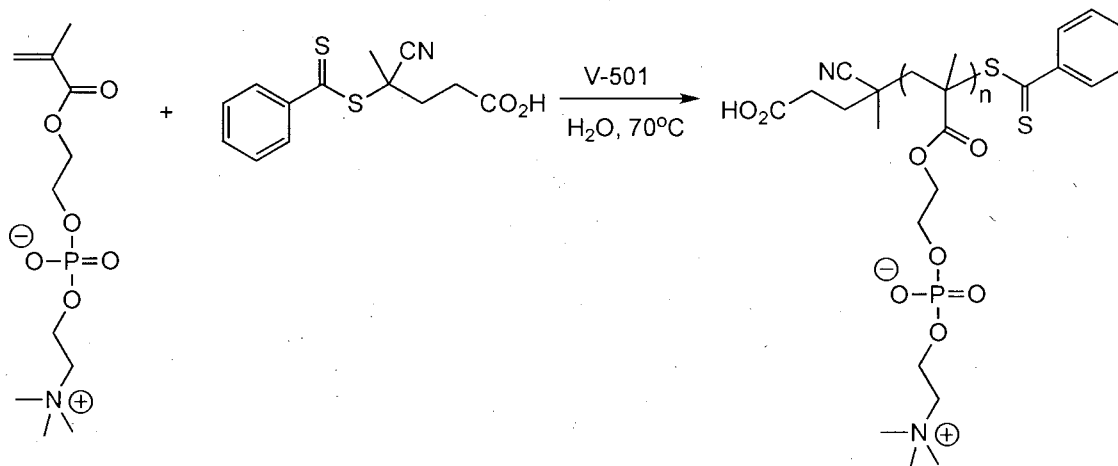


Figure IV-2. ^1H (a) and ^{13}C (b) NMR spectra, recorded in CDCl_3 , of N,N -di-*n*-propylbenzylvinylamine.

With the exception of N,N -diethylacrylamide (**DEAm**) all other monomers were prepared according to established literature procedures. With all monomers in hand a polyMPC (PMPC) homopolymer was prepared according to the method of Yusa et al.,²⁹² Scheme IV-1.



Scheme IV-1. Synthetic outline for the preparation of an MPC homopolymer.

Homopolymerization was conducted in water for 2 h at 70°C using the CTP/V-501 RAFT chain transfer agent (CTA)/initiator combination, with a target M_n of 30,000 at quantitative conversion. The resulting homopolymer was purified by dialysis against deionized water for 12 h and subsequently analyzed via a combination of NMR spectroscopy and aqueous size exclusion chromatography (ASEC).

Figure IV-3a shows the ASEC trace of the purified MPC homopolymer. The chromatogram is unimodal and symmetric and the homopolymer has an experimentally determined M_n , relative to narrow molecular weight poly(ethylene oxide) standards, of 12,100 with a corresponding polydispersity index (M_w/M_n) of 1.12. Figure IV-3b shows the ^1H NMR spectrum, recorded in D_2O of the same MPC homopolymer. Importantly, the resonances associated with the phenyl group of the dithioester end-group are visible and therefore facilitates the determination of the absolute molecular weight. Assuming one phenyl group per polymer chain, a comparison of the integral associated with the

phenyl hydrogens with those labeled c yields a calculated absolute M_n of 25,400.

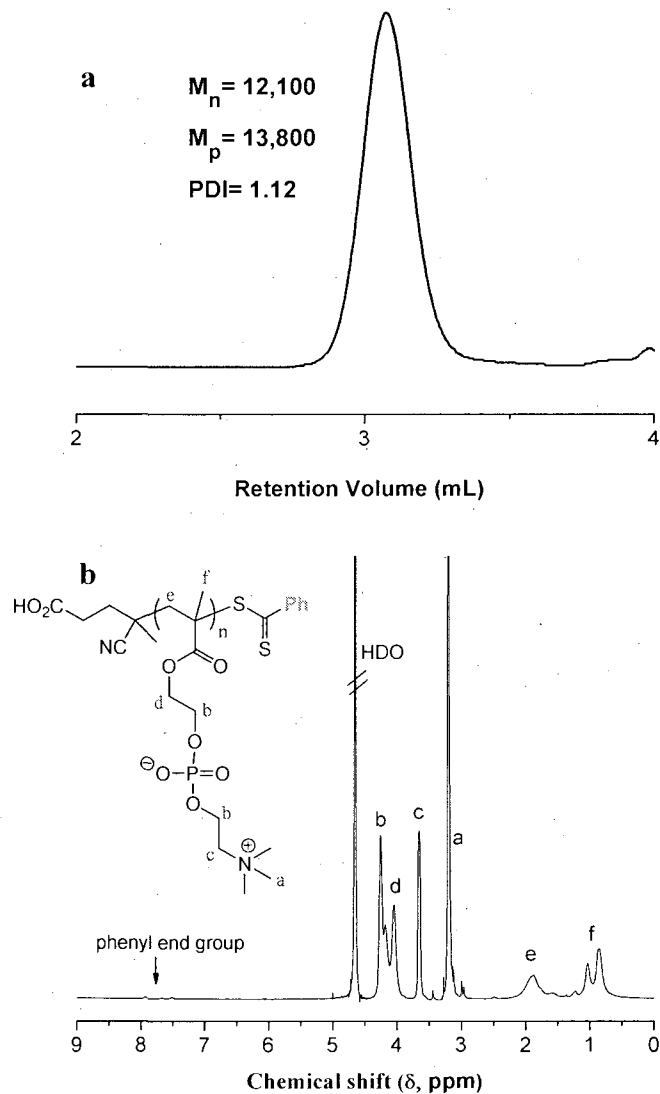


Figure IV-3. Aqueous size exclusion chromatogram (a) (RI signal) of a polyMPC homopolymer, and the ^1H NMR spectrum (b) of the same homopolymer recorded in D_2O , with peak assignments.

Having verified the ability to prepare PMPC in a controlled manner directly in aqueous media, AB diblock copolymers of varying molar composition were prepared with a range of comonomers from different monomer families with different aqueous solution characteristics. For example, homopolymers prepared from **DEAm** are readily

soluble in water at ambient temperature but possess a lower critical solution temperature (LCST) of ca. 32°C – essentially identical to the more commonly studied poly(*N*-isopropylacrylamide). Homopolymers derived from 4-vinylbenzoic acid (**VBZ**) are pH-responsive. Specifically, when ionized, i.e. at intermediate-to-high solution pH, homopolymers of **VBZ** are readily water-soluble. However, in the free acid form, at low pH, such materials undergo a distinct hydrophilic-to-hydrophobic phase transition and become insoluble. We, and others, have previously taken advantage of this pH-trigger in the synthesis of copolymers capable of undergoing pH-induced reversible self-assembly.^{82,85,87,294} Homopolymers of **DnPBVA** likewise exhibit pH-dependent solubility characteristics although it is opposite to that exhibited by materials containing **VBZ**, i.e. such materials are hydrophilic at low pH when the amine residues are protonated but become hydrophobic when deprotonated. Such behavior is entirely consistent with the structurally similar monomer *N,N*-dimethylvinylbenzylamine.⁸⁵ Finally, homopolymers derived from the sulfobetaine monomer **DMAPS** possess electrolyte responsive features in water.^{269,273} Generally, polymeric betaines exhibit limited-to-zero solubility in pure water due to the formation of an ionically crosslinked network-like structure. The addition of a small molecule electrolyte, such as NaCl, at some critical concentration effectively screens these ionic interactions resulting in dissolution. Once in solution, the addition of further salt results in a second, less pronounced conformational effect. In contrast to polyelectrolytes, which undergo chain contraction with added electrolyte, polymeric betaines undergo chain expansion – a phenomena referred to as the

anti-polyelectrolyte effect.¹⁹⁹ With respect to **DMAPS**, it is the former, more pronounced, effect that is of interest.

Table IV-1 gives a summary of the AB diblock copolymers that were prepared, their targeted and measured molar compositions, and M_n and polydispersity indices. Several points are worth highlighting. The varied, and sensitive, aqueous solution behavior of the target comonomers/polymers requires careful identification of suitable conditions for effective block copolymerization. The polymerization conditions noted were those found to give acceptable control/kinetics, conversions, and low PDIs. In all instances V-501 was used as the source of primary radicals at a ratio of 3:1 thiocarbonylthio end-group:initiator. In the case of block copolymers with **DEAm**, Table IV-1 entries 1 and 2, copolymerizations were performed at 60°C in MeOH at a total concentration of 25 wt%. In fact, MeOH is a convenient solvent for MPC and its copolymers and is commonly employed in ATRP syntheses.^{124,125,295} **DEAm** can also be copolymerized in water although this requires a low temperature initiator since, as noted above, **PDEAm** has an LCST of ca. 32°C. Similar polymerization conditions were used for one of the block copolymers with **DMAPS**, Table IV-1 entry 6, thus negating the need for added electrolyte in the case of aqueous based polymerization although this is also a feasible approach, Table IV-1 entry 7. In the case of **VBZ** block copolymers, Table IV-1 entries 3 and 4, syntheses were performed in water under slightly basic conditions although at a lower concentration of 10 wt%, and slightly higher reaction temperature of

80°C. In the case of the block copolymer with **DnPBVA**, Table IV-1 entry 5, copolymerization proceeded smoothly in 2,2,2-trifluoroethanol (TFE) at a concentration of 10 wt% and 70°C. While these synthetic conditions are varied, each of the resulting block copolymers presents a symmetric, unimodal ASEC trace with the final polydispersity indices in the range 1.10-1.24. As representative examples, Table IV-4 shows the ASEC traces for the MPC-*block-DEAm*, Table IV-1 entry 1, and MPC-*block-DMAPS*, Table IV-1 entry 7, copolymers.

Table IV-1. Summary of M_n experimental, M_p experimental, polydispersity index, and composition of synthesized AB diblock copolymers based on MPC.

Entry	Block copolymer	M_n expt	M_p expt ^f	M_w/M_n ^f	Theoretical Molar composition ^g	Measured molar composition ^h
1	MPC-DEAm ^a	12,400	12,900	1.10	80:20	82:18
2	MPC-DEAm ^a	10,700	12,500	1.24	50:50	56:44
3	MPC-VBZ ^b	10,400	11,100	1.10	80:20	89:11
4	MPC-VBZ ^b	10,200	11,800	1.16	50:50	50:50
5	MPC-DnPBVA ^c	11,000	11,700	1.18	50:50	70:30
6	MPC-DMAPS ^d	12,000	13,300	1.13	70:30	76:24
7	MPC-DMAPS ^e	12,000	13,500	1.17	50:50	58:42

- a. Polymerization conducted at 60°C with thiocarbonylthio end-group:V-501 = 3:1 at a concentration of 25 wt% in MeOH.
- b. Polymerization conducted at 80°C with thiocarbonylthio end-group:V-501 = 3:1 at a concentration of 10 wt% in deionized water with 1 molar equivalent of Na₂CO₃ based on VBZ to aid in the dissolution of the styrenic monomer.
- c. Polymerization conducted at 70°C with thiocarbonylthio end-group:V-501 = 3:1 at a concentration of 10 wt% in 2,2,2-trifluoroethanol.
- d. Polymerization conducted at 60°C with thiocarbonylthio end-group:V-501 = 3:1 at a concentration of 25 wt% in methanol.
- e. Polymerization conducted at 80°C with thiocarbonylthio end-group:V-501 = 3:1 at a concentration of 10 wt% in 0.25 M NaBr.
- f. As determined by aqueous size exclusion chromatography, in 0.25 M NaBr, calibrated with narrow molecular mass poly(ethylene oxide) standards.
- g. Assuming 100% conversion of the second block.
- h. As determined by ¹H NMR spectroscopy.

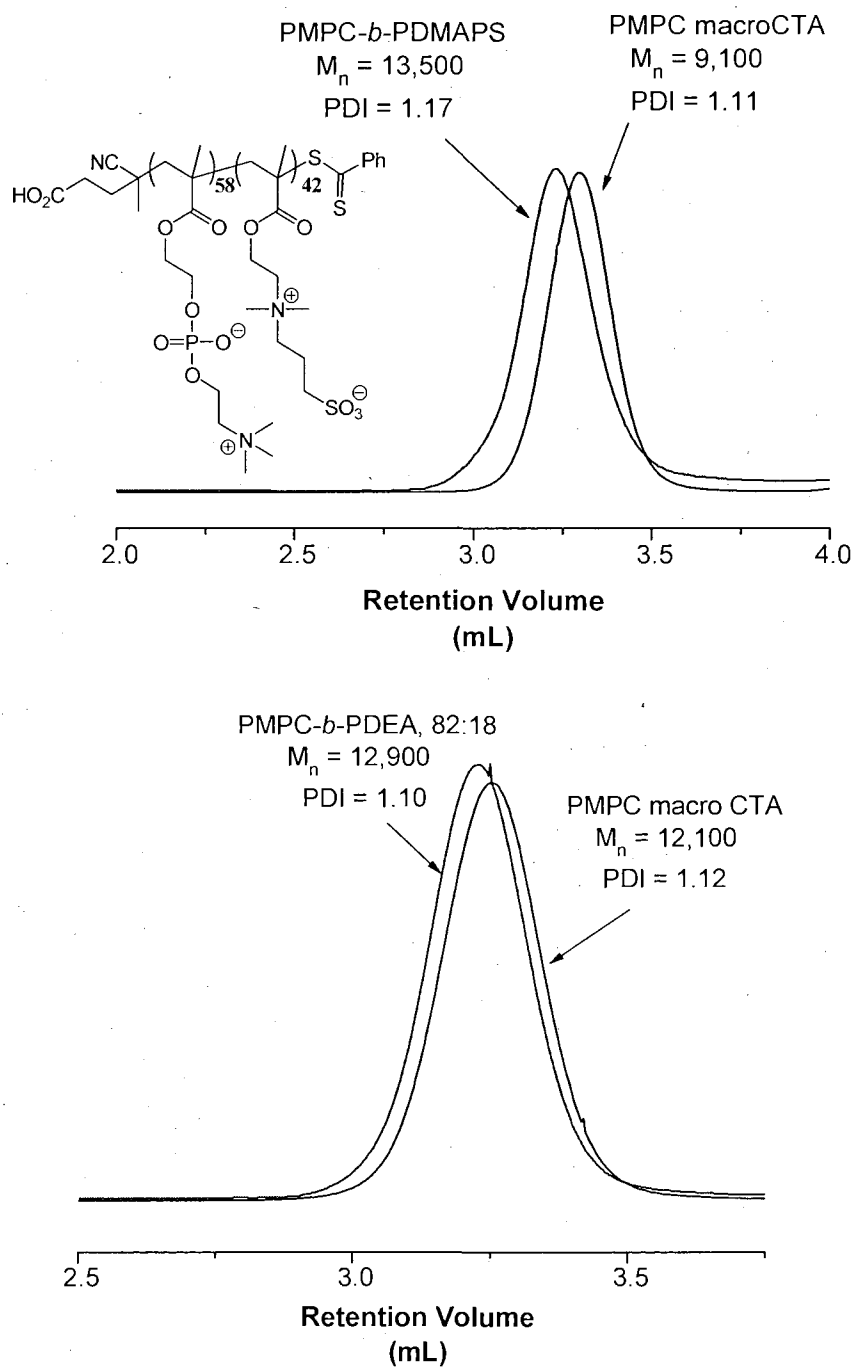
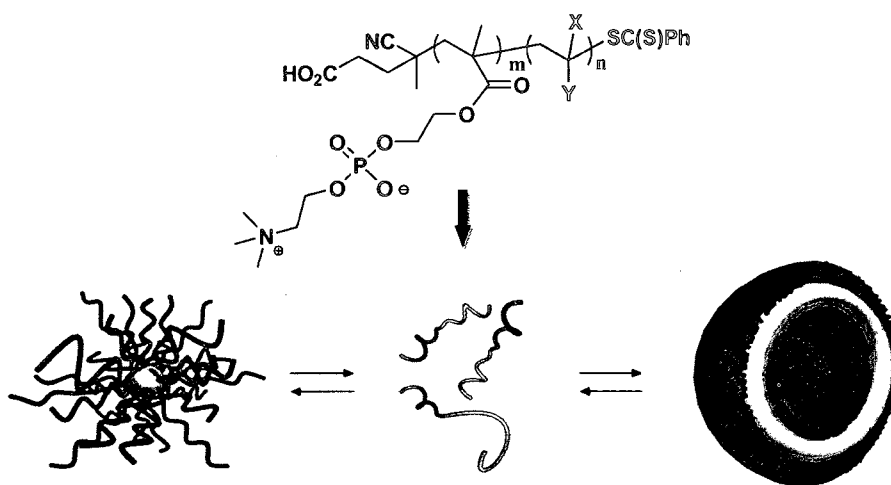


Figure IV-4. Aqueous size exclusion chromatograms (RI signal) of examples of PMPC-based AB diblock copolymers. P(MPC₅₈-*b*-DMAPS₄₂) (a) and P(MPC₈₂-*b*-DEAm₁₈) (b) demonstrating successful block copolymer formation.

With a series of MPC-based AB diblock copolymers in hand the aqueous solution properties of specific samples were briefly examined using a combination of ^1H NMR spectroscopy and dynamic light scattering (DLS). NMR is particularly useful for monitoring the change in solvation of a particular block under different solution conditions, while DLS is a fast and convenient method for measuring the hydrodynamic properties of copolymers, and aggregates thereof. Figure IV-5 shows the ^1H NMR spectra of the P(MPC-*b*-DEAm) copolymer with a molar composition of 56:44, Table IV-1 entry 2, at ambient temperature. All the resonances associated with the MPC and DEAm blocks are clearly present. With respect to the DEAm block, the major resonances are those labeled d, e, and f and are associated with the backbone hydrogens, the aza-methylene group, and the methyl hydrogens respectively. Heating the P(MPC₅₆-*b*-DEAm₄₄) copolymer solution in the NMR spectrometer to 50°C results in an NMR spectrum, Figure IV-6, devoid of any signals associated with the DEAm block. Specifically, there are three distinct changes. Firstly, the signals labeled d and e in 5a are completely absent while there is also a significant decrease in the intensity of the signal at $\delta \sim 1.1$ ppm. These changes are completely consistent with desolvation of the DEAm block. Since there is no evidence of macroscopic precipitation, and given the block architecture of the material such changes are entirely consistent with a self-assembly process yielding, for example, spherical polymeric micelles, Scheme IV-2. The formation of aggregate structures under these conditions was verified by dynamic light scattering (DLS). Figure IV-7 shows the measured size distributions for a 1 wt% aqueous solution

(0.1 M NaCl) of the P(MPC₅₆-*b*-DEAm₄₄) copolymer employed in the NMR study at 22 and 50°C. At the lower temperature DLS indicates an average hydrodynamic diameter (D_h) of ~ 6.0 nm which is entirely consistent with molecularly dissolved polymer chains (unimers) of the measured average molecular weight. In contrast, after heating the solution to 50°C the size distribution shifts significantly indicating the presence of a species with an average D_h of ~ 180 nm. Such a dramatic change in the D_h certainly indicates that the AB diblock copolymer is undergoing self-assembly forming an aggregate structure such as a micelle, vesicle or higher ordered structure. We have not, at this time, attempted to elucidate the exact nature of the aggregate species. However, such assembly is completely reversible. Cooling the solution back down to room temperature results in the disappearance of the large aggregates and the reappearance of the smaller, unimer population. Similarly, temperature cycling in the NMR spectrometer confirms the reversible solvation-desolvation of the **DEAm** residues (data not shown).



Scheme IV-2. Idealized, reversible self-assembly, with the possible formation of either micelles or vesicles, of 'smart' AB diblock copolymers based on MPC.

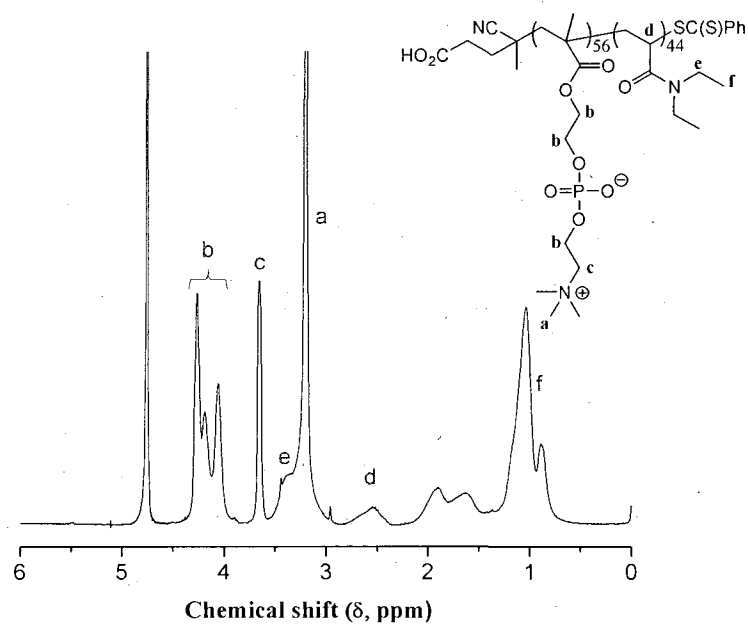


Figure IV-5. ^1H NMR spectra of the $\text{P}(\text{MPC}_{56}\text{-}b\text{-DEAm}_{44})$ at ambient temperature recorded in D_2O .

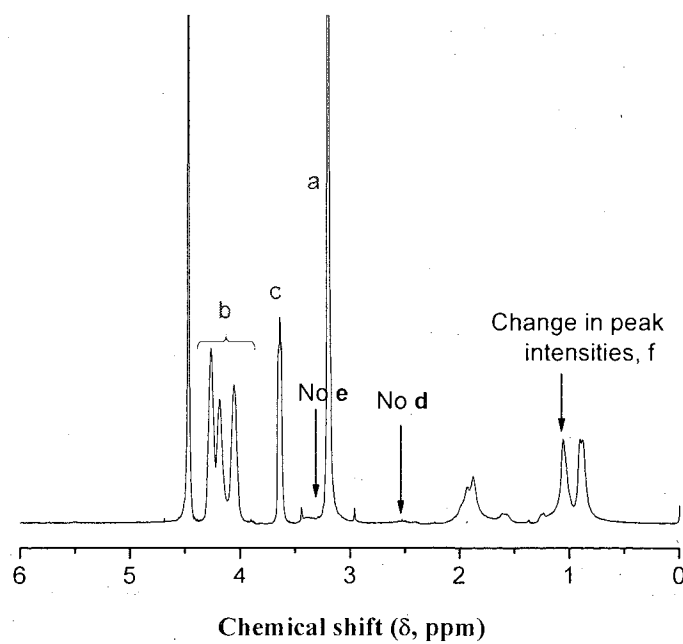


Figure IV-6. ^1H NMR spectra of the $\text{P}(\text{MPC}_{56}\text{-}b\text{-DEAm}_{44})$ at 50°C recorded in D_2O .

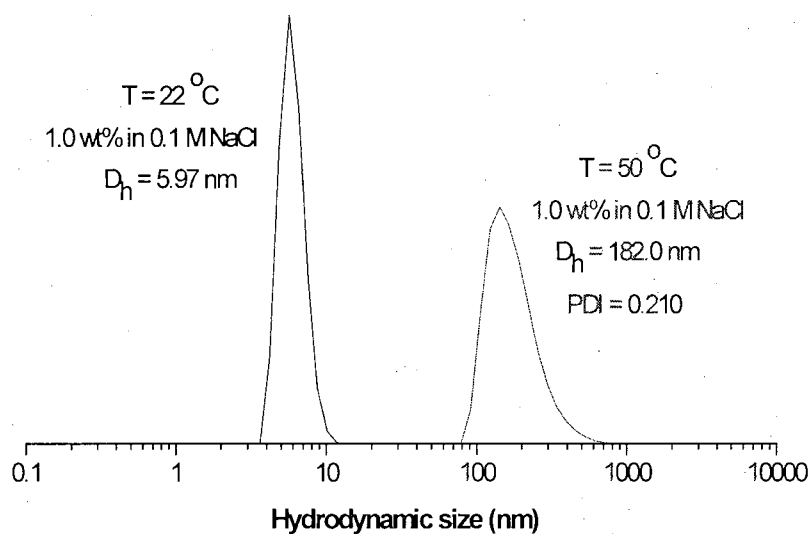


Figure IV-7. Size distributions measured by dynamic light scattering as a function of temperature highlighting the formation of aggregates

Figure IV-8 - Figure IV-14 show the results from the same series of experiments for the P(MPC₅₀-*b*-**VBZ**₅₀), P(MPC₇₀-*b*-**DnPBVA**₃₀), and the P(MPC₇₆-*b*-**DMAPS**₂₄) copolymers, Table IV-1 entries 4, 5 and 6.

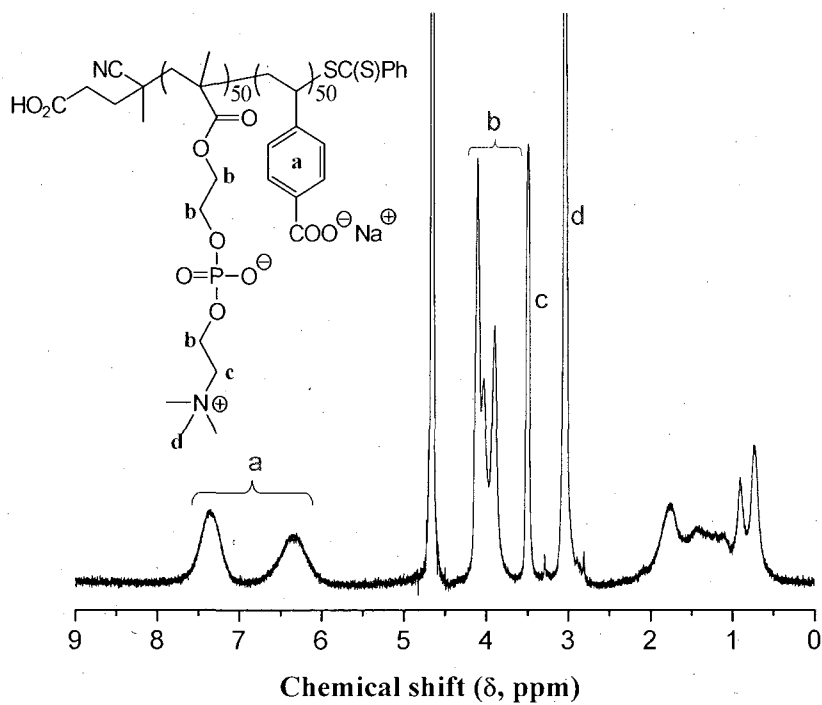


Figure IV-8. ¹H NMR spectra, recorded in D₂O, of the P(MPC₅₀-*b*-VBZ₅₀) at ambient temperature under basic conditions.

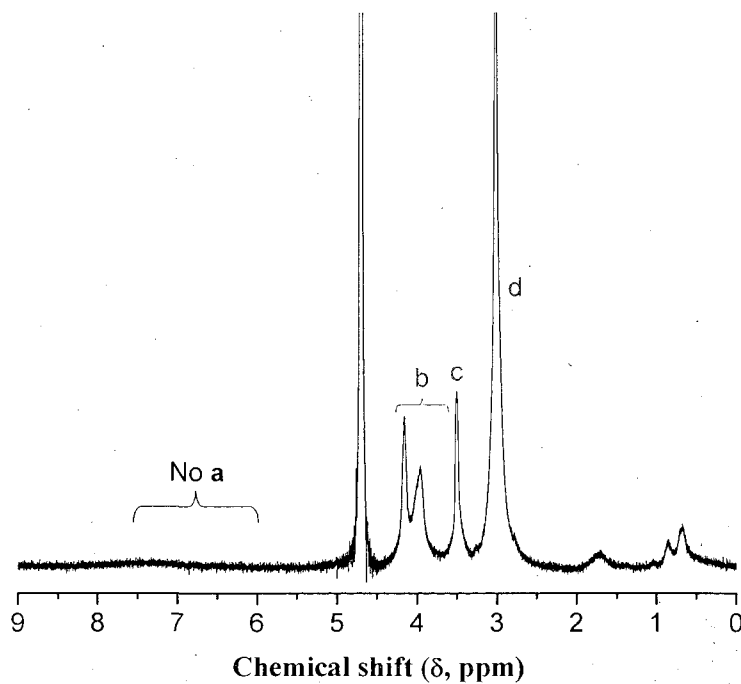


Figure IV-9. ¹H NMR spectra, recorded in D₂O, of the P(MPC₅₀-*b*-VBZ₅₀) at ambient temperature under acidic conditions.

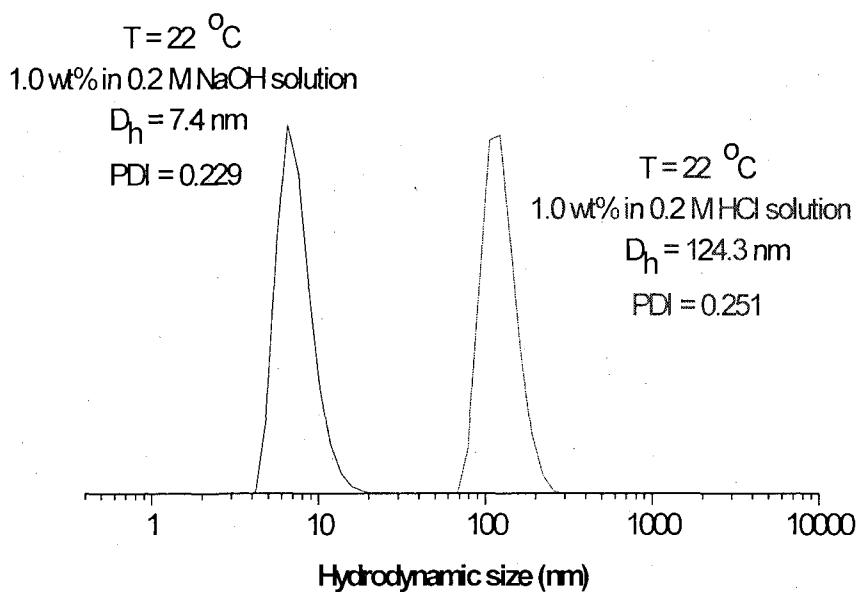


Figure IV-10. Size distributions of the P(MPC₅₀-*b*-VBZ₅₀) measured by dynamic light scattering as a function of pH highlighting the formation of aggregates.

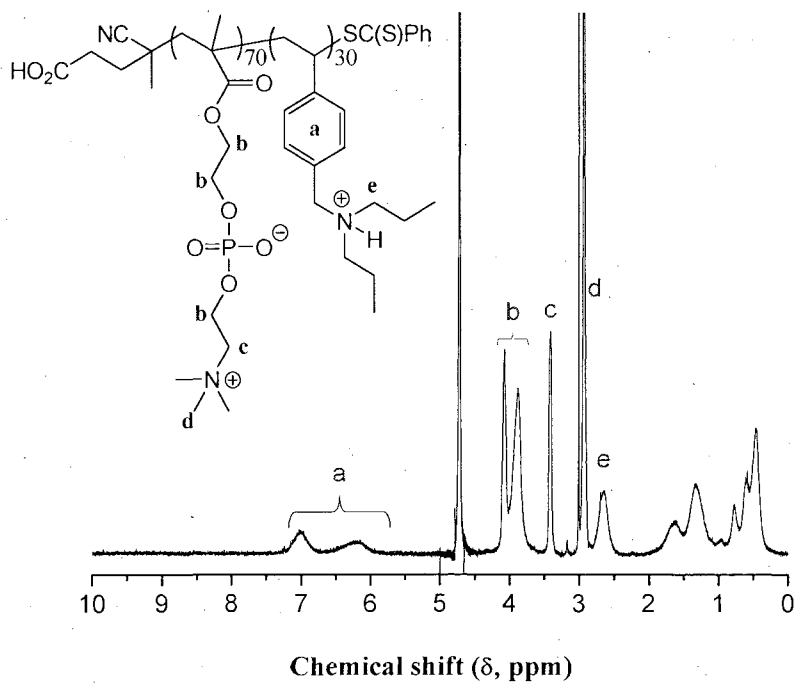


Figure IV-11. ^1H NMR spectra, recorded in D_2O , of the P(MPC₇₀-*b*-DnPBVA₃₀) at ambient temperature under acidic conditions.

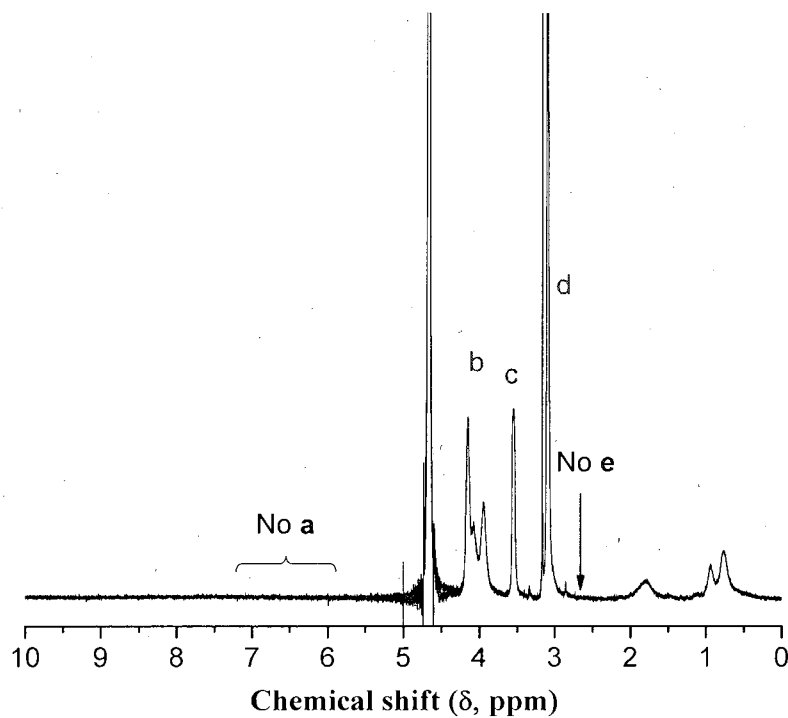


Figure IV-12. ^1H NMR spectra, recorded in D_2O , of the $\text{P}(\text{MPC}_{70}\text{-}b\text{-DnPBVA}_{30})$ at ambient temperature under basic conditions.

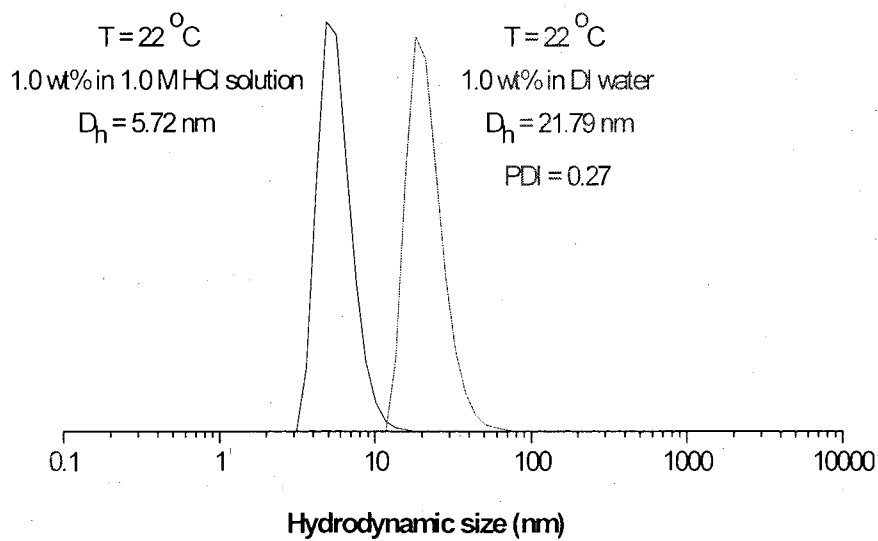


Figure IV-13. Size distributions of the $\text{P}(\text{MPC}_{70}\text{-}b\text{-DnPBVA}_{30})$ measured by dynamic light scattering as a function of pH highlighting the formation of aggregates.

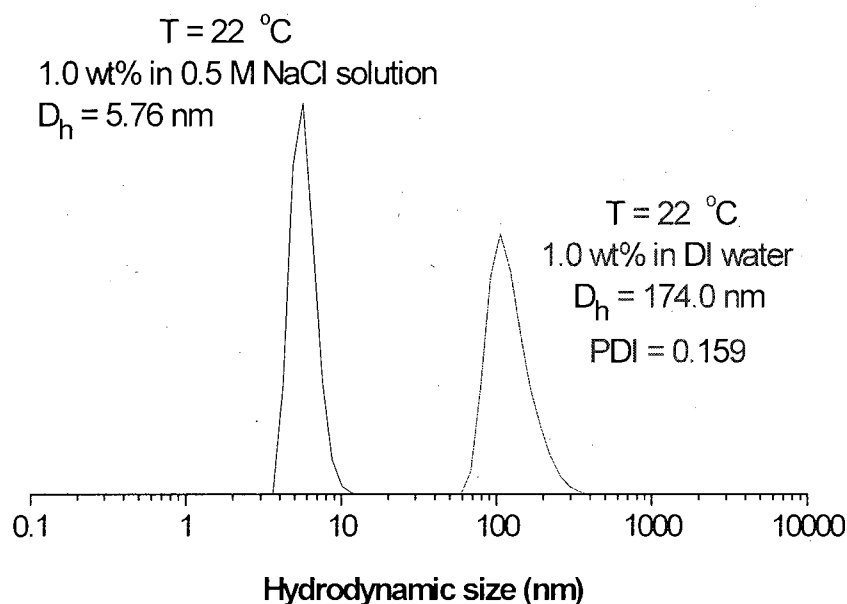


Figure IV-14. Experimentally determined hydrodynamic size distributions of a 1 wt% solution of the P(MPC₇₆-*b*-DMAPS₂₄) copolymer in 0.5 M NaCl and deionized water demonstrating the ability to form self-assembled aggregates.

Consider first the P(MPC₅₀-*b*-VBZ₅₀) copolymer. Figure IV-8 shows the ¹H NMR spectrum of the block copolymer under conditions in which both the MPC and VBZ blocks are hydrophilic and thus solvated, i.e. under basic solution conditions in which the VBZ block is ionized. The key signals associated with MPC are again clearly visible as well as the key resonance for the VBZ block – the two signals spanning $\sim \delta = 6 - 7.5$ ppm associated with the four hydrogens of the benzene ring. Acidification of this solution with DCl results in Figure IV-9. The signals associated with MPC are still present but those associated with VBZ are absent. As with the temperature-induced desolvation observed for the P(MPC₅₆-*b*-DEAm₄₄) copolymer, this pH-induced change also leads to the formation of nanosized aggregates as evidenced by DLS. Figure IV-10

shows the measured DLS size distributions for the MPC-**VBZ** block copolymer at a concentration of 1 wt%, 22°C, in 0.2 M NaOH and 0.2 M HCl. Under basic conditions, when both blocks are hydrophilic, DLS indicates the presence of unimers with an average D_h of ~ 7.0 nm. However, under acidic conditions a rather broad size distribution comparable to that observed for the P(MPC₅₆-*b*-**DEAm**₄₄) copolymer is seen with an average D_h of ~124 nm and a corresponding polydispersity of 0.25. Again, such a size may indicate the presence of vesicles or higher ordered structures as opposed to spherical micelle-like species. Given the similar block copolymer compositions and molecular weights of these P(MPC₅₆-*b*-**DEAm**₄₄) and P(MPC₅₀-*b*-**VBZ**₅₀) copolymers it is perhaps not surprising that they behave similarly in their amphiphilic forms even though such behavior is induced by a different external stimulus. The P(MPC₇₀-*b*-**DnPBVA**₃₀) copolymer also exhibits pH-induced self-assembly characteristics although the pH-trigger is reversed. As noted above the **DnPBVA** residues are hydrophilic at low pH but hydrophobic at intermediate-to-high pH. Figure IV-11 shows the ¹H NMR spectrum of the P(MPC₇₀-*b*-**DnPBVA**₃₀) under acidic conditions where both blocks are hydrophilic and solvated. The main, identifiable, signals associated with the **DnPBVA** block are those associated with the aromatic ring at ~ $\delta = 6-7.2$ ppm as well as the signal at ~ $\delta = 2.7$ ppm. Under basic conditions both of these key signals disappear consistent with the pH-induced hydrophilic-hydrophobic transition of the **DnPBVA** residues. DLS again confirms the occurrence of a self-assembly process with this change in solution pH. For a 1 wt% solution of the P(MPC₇₀-*b*-**DnPBVA**₃₀) at 22°C a unimers distribution with an

average D_h of ~ 6 nm is observed. Deprotonation of the **DnPBVA** residues renders them hydrophobic and self-assembly occurs yielding aggregates with a D_h of ~ 22 nm. This size is much smaller than those observed for either the P(MPC₅₆-*b*-**DEAm**₄₄) or P(MPC₅₀-*b*-**VBZ**₅₀) copolymers, although it must be noted that the copolymer composition is significantly different. Finally, the P(MPC₇₆-*b*-**DMAPS**₂₄) copolymer was examined with respect to the effect of electrolyte on solubility/self-assembly. In the case of the NMR experiments little-to-no change was observed in peak intensities when spectra were recorded in the presence and absence of electrolyte indicating that the **DMAPS** block was still in a solvated, although perhaps somewhat reduced, state. In contrast, DLS experiments did indicate the presence of aggregate structures for the block copolymer in deionized water. Figure IV-14 shows the measured size distributions for the P(MPC₇₆-*b*-**DMAPS**₂₄) copolymer in 0.5 M NaCl and deionized water at a concentration of 1 wt% at 22°C. In the electrolyte solution unimers are observed with an average D_h of ~ 6 nm. In contrast, when dissolved directly in deionized water aggregates are observed with an average D_h of 174 nm. A more detailed, fundamental study of the effect of block copolymer composition on the self-assembly properties of these copolymers is currently underway.

4. Summary and Conclusions

We have demonstrated herein that reversible addition-fragmentation chain transfer (RAFT) radical polymerization is a convenient method for the synthesis of a range of AB diblock copolymers based on the phosphobetaine 2-(methacryloyloxy)ethyl phosphorylcholine (MPC) with a range of 'smart' comonomers. Employing an MPC macro-CTA well defined AB diblock copolymers of varying molar composition and narrow molecular weight distribution with *N,N*-diethylacrylamide, 4-vinylbenzoic acid, *N*-(3-sulfopropyl)-*N*-methacryloxyethyl-*N,N*-dimethylammonium betaine and *N,N*-di-*n*-propylbenzylvinylamine, were prepared in protic media. These comonomers were chosen to yield block copolymers that were capable of undergoing stimulus induced self-assembly in aqueous media. Indeed, we demonstrated that such MPC-based block copolymers are able to undergo self-assembly processes as a functional of either a change in solution temperature, pH, or electrolyte concentration. Preliminary evaluation of the self-assembly properties using a combination of ¹H NMR spectroscopy and dynamic light scattering showed that when molecularly dissolved the block copolymers had average hydrodynamic diameters in of ~ 6-7 nm. In contrast, and under the appropriate applied external stimulus, aggregates in the range ~ 22-180 nm. Such self assembly is completely reversible and removal of the applied stimulus results in a return to the unimeric state.

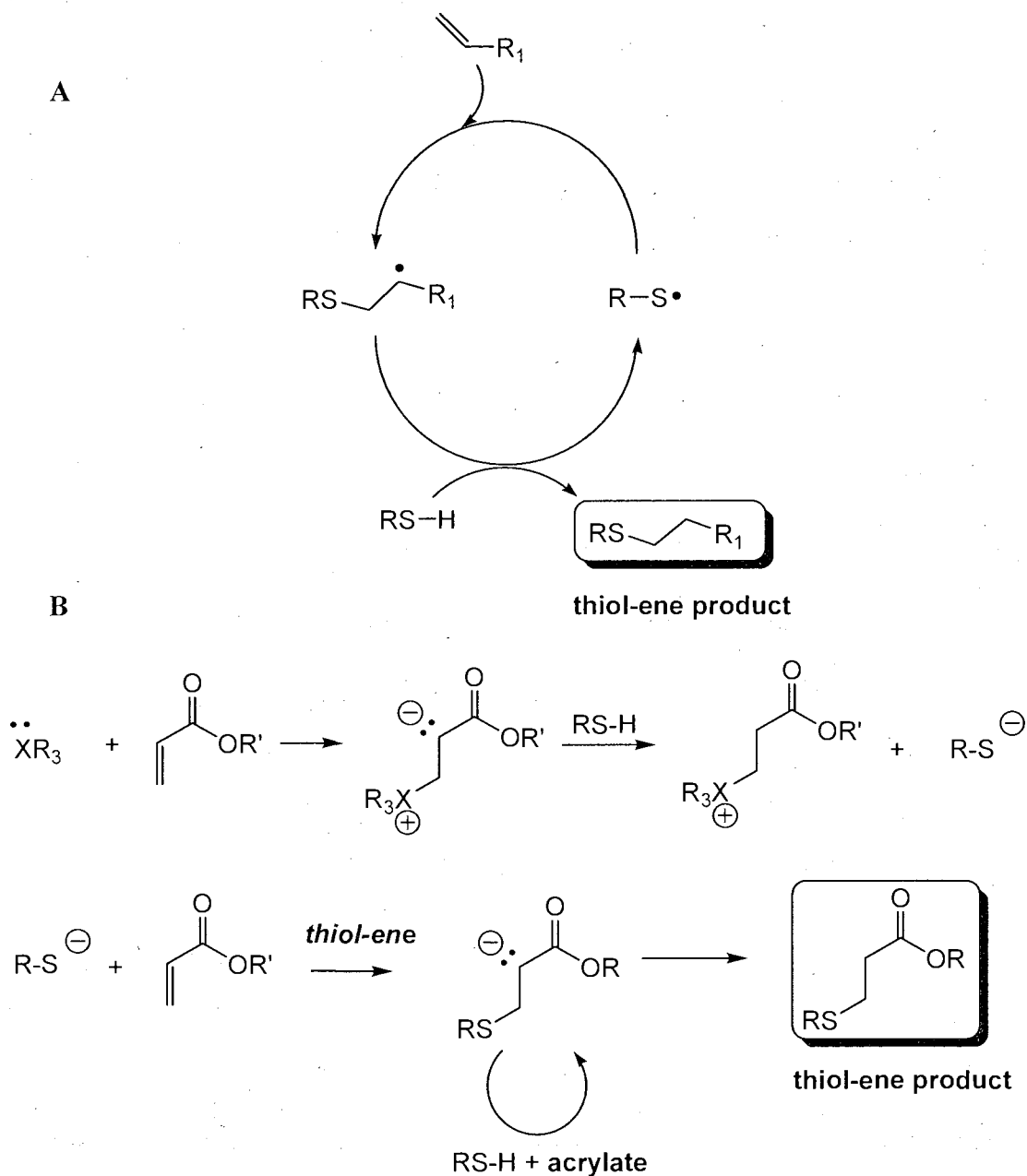
CHAPTER V

SEQUENTIAL THIOL-ENE/THIOL-ENE AND THIOL-ENE/THIOL-YNE
REACTIONS AS A ROUTE TO WELL-DEFINED MONO AND BIS
END-FUNCTIONALIZED POLY(N-ISOPROPYLACRYLAMIDE)

1. Introduction

The thiol-ene reaction²⁰³ (the hydrothiolation of a C=C bond) has recently attracted significant attention in the materials arena²⁰⁴ since it displays many of the attributes of click chemistry.²⁰⁵ Such additions can be accomplished under a variety of experimental methodologies including acid/base catalysis,²¹⁰ nucleophile-mediated catalysis,^{208,296} radical-mediated chain reactions (most induced photochemically),^{204,206,207} and via a solvent promoted process.^{297,298} However, the reaction is most commonly performed under radical conditions where it is applicable to any ene substrate, or under nucleophilic conditions, with activated enes via an anionic chain process, Scheme V-1. A real synthetic strength of the thiol-ene reaction is its versatility with respect to ene substrates that can be employed and include both activated and non-activated species such as norbornenes, (meth)acrylates, maleimides, and allyl ethers to name but a few.²⁰⁵ Recent examples describing the application of the thiol-ene reaction in the polymer/materials field include dendrimer synthesis,²²⁶ convergent star synthesis,²⁰⁸ modification of side chains in poly[2-(3-butenyl)-2-oxazoline],²⁹⁹ synthesis of multifunctional branched organosilanes,³⁰⁰ synthesis of materials for soft imprint

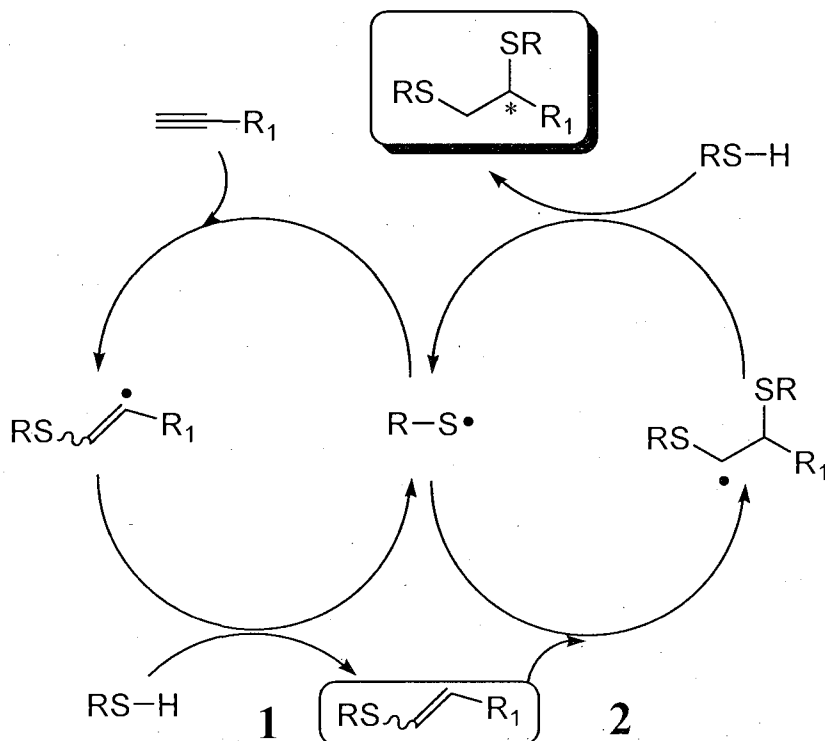
lithography,³⁰¹ functionalization of poly(ester)s,³⁰² and synthesis of functional telechelics and a modular approach to block copolymers.³⁰³



Scheme V-1. (A) Mechanism for the radical mediated thiol-ene reaction with a terminal ene, and (b) anionic chain mechanism for the amine/phosphine mediated nucleophilic thiol-ene reaction with an acrylate.

The *radical*-mediated addition of a thiol to an *yne*^{304,305} was reported over 50 years ago. The radical thiol-yne reaction should be considered a sister reaction to the radical thiol-ene reaction, possessing many similar characteristics both kinetically and mechanistically. As with the thiol-ene reaction, the thiol-yne reaction, in general, proceeds rapidly under a variety of experimental conditions selectively yielding the mono and/or bis-addition products, depending on the chemical nature of the thiol species, the reaction conditions, and the thiol and yne component ratios.²¹³⁻²¹⁸ In the case of the double addition products formed under radical conditions the reaction of 2 equivalents of thiol with a terminal alkyne is itself a two-step process, Scheme V-2. The first, slower, step (1) involves the regiospecific anti-Markovnikov-like addition of a thiyl radical across the C≡C bond yielding the intermediate vinylic radical as a mixture of the cis and trans diastereoisomers. This vinylic radical subsequently undergoes chain transfer to additional thiol, yielding the cis/trans vinylthioether concomitantly generating a new thiyl radical. The vinylthioether product is able to undergo a second, faster, regiospecific (2), formally thiol-ene, reaction with the newly generated thiyl radical yielding the intermediate bithioether radical that undergoes chain transfer with another thiol molecule thereby producing quantitatively the target bithioether with exclusive 1,2-orientation.³⁰⁶ However, one important difference between the radical thiol-ene and radical thiol-yne reactions, at least in the case of the double addition products, is that the thiol-yne reaction of a terminal acetylene results in the generation of a stereocenter. Thus the final 1,2-addition product is a mixture of (*R*) and (*S*) enantiomers, and as such the

radical thiol-yne reaction is not stereoselective.



Scheme V-2. Proposed mechanism for the radical mediated thiol-yne reaction with a terminal alkyne.

Like the radical-mediated thiol-ene reaction, the radical initiated thiol-yne reaction can proceed extremely rapidly yielding products *quantitatively* under facile conditions and with little-to-no clean up required, i.e. reactions can be easily performed in an air atmosphere at ambient temperature and humidity. While also known since the first half of the last century,^{304,305} the thiol-yne reaction has been essentially overlooked in the polymer/materials field. However, researchers have recently begun to evaluate this potentially highly versatile reaction in the context of network film. Fairbanks et al.³⁰⁶

described radical-mediated thiol-yne step-growth polymerization as a route to highly crosslinked networks, and conducted a detailed kinetic analysis of the process simultaneously noting the similarities with the radical thiol-ene process. Chan et al.³⁰⁷ reported the synthesis and physical properties of high refractive index polysulfide networks formed via the photopolymerization of a range of alkyldithiols with a series of alkyldiynes, and most recently, Chan, Hoyle, and Lowe²⁹⁶ described the first example of a sequential, quantitative nucleophilic thiol-ene/radical thiol-yne process for the synthesis of a range of branched structures including examples with potential biomedical significance.

Reversible addition-fragmentation chain transfer (RAFT) radical polymerization^{94,234,236,308} is a powerful synthetic tool mediated by thiocarbonylthio compounds that is simple to perform, highly functional group tolerant process that is readily applicable to a wide range of monomeric substrates and experimental conditions. It facilitates the synthesis of (co)polymers with narrow molecular weight distributions, predetermined molecular weights, and advanced architectures.^{82,87,235,239-241,247,251,257,309} As a consequence of the degenerative chain transfer mechanism, (co)polymers prepared by RAFT bear very specific end-groups, the chemical nature of which is dependent on the structure of the chain transfer agent (CTA) and, to a lesser extent, the CTA/initiator pair. Assuming no undesirable side reactions, the α terminus of a (co)polymer chain will be chemically identical to the R-group of the RAFT CTA while the ω terminus bears a

thiocarbonylthio functional group. The exact chemical structure of R group will be dependent of the class of RAFT CTA employed, i.e. dithioester vs. xanthate vs. trithiocarbonate etc. As such, RAFT offers an attractive, and convenient, route to making telechelic (co)polymers simply by using functional RAFT agents.²⁴⁴ In addition, the thiocarbonylthio end-groups are easily modified post-polymerization to a variety of species including cleavage to a thiol, typically with a primary or secondary amine,^{208,245,310} cleavage to a thiolate,^{142,147} thermolysis to an ene,^{98,311} or radical-induced reduction to a saturated species with, for example, Bu_3SnH .³¹² Importantly, the presence of the reactive thiol, or thiolate, at the ω chain terminus allows for further modification reactions to be performed via versatile thiol-ene and thiol-yne chemistry. Thiol-ene reactions include both free-radical and nucleophilic induced processes that proceed by chain processes to quantitative conversion.

Described herein is a facile sequential route to either mono or bis end-functionalized poly(*N*-isopropylacrylamide) employing tandem nucleophilic thiol-ene/radical thiol-ene and nucleophilic thiol-ene/radical thiol-yne reactions. These reaction sequences take advantage of the click characteristics of the thiol-ene reaction and the similar, rapid and quantitative radical mediated reaction of thiols with alkynes. This represents the first time such sequential thiol-ene/thiol-ene and thiol-ene/thiol-yne reactions proceeding by inherently different mechanistic pathways have been employed in polymer synthesis/modification. It represents a totally new and highly efficient

methodology for the site specific modification of RAFT-prepared polymers. That opens up the potential for attaining polymers with controlled molecular weights that are functionalized with virtually any types of end group desired.

2. Experimental

All reagents were purchased from the Aldrich Chemical at the highest available purity and used as received unless stated otherwise. 1-Cyano-1-methylethyl dithiobenzoate (CPDB) was prepared according to a literature procedure.⁹⁴ 2,2'-Azobis(2-methylpropionitrile) (AIBN) was recrystallized from methanol, and stored in a freezer at -20 °C until needed. *N*-Isopropylacrylamide (NIPAm) was purified by recrystallization from hexane and stored in a freezer at -20 °C until needed.

Homopolymerization of N-isopropylacrylamide

A mixture of NIPAm (15.0 g, 133 mmol), CPDB (388 mg, 1.75 mmol), AIBN (58 mg, 0.353 mmol), and DMF (10.0 g) were added to a Schlenk flask equipped with a magnetic stirring bar. The mixture was stirred for at least 30 min while submerged in an ice bath to ensure complete dissolution of CPDB and AIBN. The flask was then purged by repeatedly evacuating and refilling with N₂ at least 3 times prior to immersion in a preheated oil bath at 70 °C. After 48 hours, the reaction was quenched by rapid cooling in liquid N₂ and exposure to air. The homopolymer was isolated by precipitation into a large

excess of hexanes cooled in an ice-bath followed by dialysis against methanol for 8 h with the solvent changed every 2 hours. The purified polymer was then dried in a vacuum oven at room temperature overnight.

Synthesis of propargyl end functionalized poly(N-isopropylacrylamide)

(PNIPAm-S-PROPA)

PolyNIPAm (PNIPAm) (2.5 g, 0.424 mmol), propargyl acrylate (551 mg, 5.0 mmol), dimethylphenylphosphine (10 mg, 0.072 mmol), and CH_2Cl_2 (7.5 g) were added to a 50-ml round bottom flask equipped with a magnetic stirring bar. After purging the mixture with N_2 for 15 min with moderate stirring, octylamine (969 mg, 7.5 mmol) was added with a 1-mL syringe. The mixture was purged for another 15 min, and then left to stir overnight at room temperature. The product was isolated by precipitation into a large excess of hexanes cooled in an ice-bath followed by dialysis against methanol for 8 h with the solvent changed every 2 hours. The purified polymer was then dried in a vacuum oven at room temperature overnight.

Synthesis of allyl end functionalized poly(N-isopropylacrylamide) (PNIPAm-S-ALMA)

The synthesis of PNIPAm-S-ALMA was achieved following exactly the same protocol as described above for the preparation of PNIPAm-S-PROPA except allyl methacrylate was used in place of propargyl acrylate.

General procedure for the photochemical, radical thiol-ene and thiol-yne reactions

To a 20-mL scintillation vial was added either PNIPAm-S-ALMA or PNIPAm-S-PROPA (0.2 g), 100% excess of target thiol (based on the molarity of “ene” or “yne”), benzil dimethyl ketal (Irgacure 651) photoinitiator (15.0 mg), and the appropriate volume of THF to give a total weight of 1.5 g. The vial was gently swirled to ensure complete dissolution of added reagents prior to being placed in a UV reactor. The reaction was allowed to proceed for 2 h prior to removal from the UV reactor. The sample was immediately dialyzed against MeOH for a period of 8 h with the MeOH being changed every 2 h. The product was isolated by drying overnight *in vacuo* at room temperature.

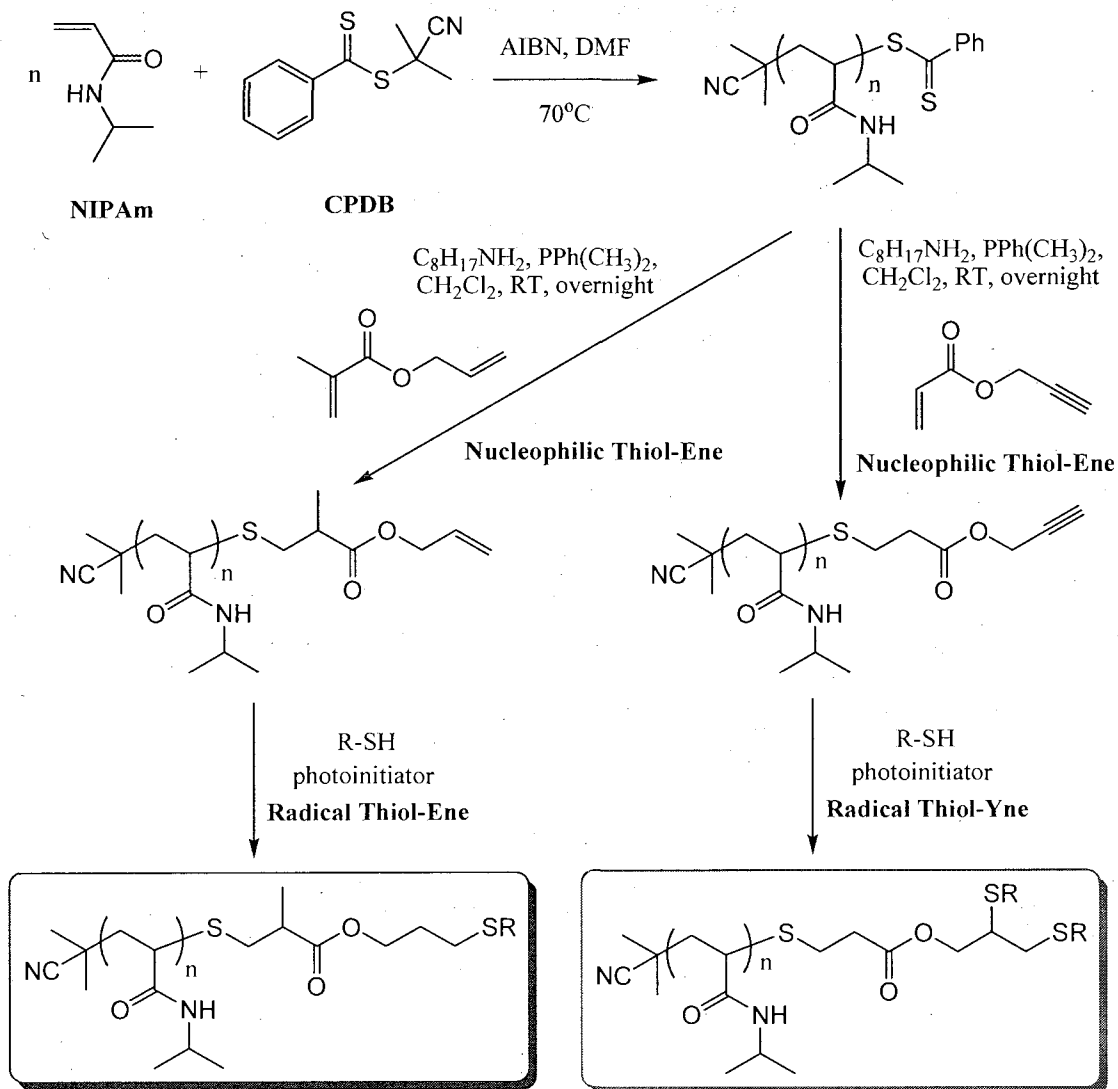
General Instrumentation

^1H and ^{13}C NMR spectra were recorded on a Bruker 300 53 mm spectrometer in appropriate deuterated solvents. Size exclusion chromatographic analysis was performed on a Waters system comprised of a Waters 515 HPLC pump, Waters 2487 Dual λ absorbance detector, and Waters 2410 RI detector equipped with a PolymerLabs PLgel 5 μm guard column and a PolymerLabs PLgel 5 μm MIXED-C column (molecular weight range: 200-2,000,000 g/mol), in THF stabilized with 281 ppm BHT at a flow rate of 1.0 mL/min. The column was calibrated with a series of narrow molar mass distribution poly(methyl methacrylate) standards. The digital thermometer used in solution studies was a Traceable[®] expanded range thermometer. pH measurements was performed on a

Accument[®] AR15 pH meter calibrated with three pH buffers (pH = 4.00, 7.00, and 10.00). Photochemical reactions were performed on a Rayonet RPR-100 photochemical reactor with 350 nm broadband lamps. Dynamic light scattering (DLS) experiments were conducted on a Malvern Instruments Zetasizer Nano-ZS (red badge) instrument operating with a 633nm laser. Data was collected and processed with Dispersion Technology software V5.10.

3. Results and Discussion

The reversible addition-fragmentation chain transfer (RAFT) radical polymerization of *N*-isopropylacrylamide (NIPAm) was accomplished with 1-cyano-1-methylethyl dithiobenzoate (CPDB) as the RAFT chain transfer agent in conjunction with AIBN in DMF at 70 °C, Scheme V-3, with a targeted M_n of 8,800 at 100% conversion.



Scheme V-3. Reversible addition-fragmentation chain transfer polymerization of N-isopropylacrylamide and subsequent end-group modifications, via a combination of nucleophilic thiol-ene/radical thiol-ene and nucleophilic thiol-ene/radical thiol-yne pathways.

The homopolymerization was intentionally terminated early in an effort to preserve thiocarbonylthio end-groups and minimize the presence of terminated products derived from coupling reactions. The resulting homopolymer was characterized using a combination of size exclusion chromatography (SEC) and ^1H NMR spectroscopy. SEC,

Figure V-1A, indicated an M_n of 3,100 with a corresponding polydispersity index of 1.18.

The low targeted molecular weight of the NIPAm homopolymer allowed for a more accurate determination of M_n by ^1H NMR spectroscopic end-group analysis, which indicated a degree of polymerization of 50 (PNIPAm₅₀), equivalent to an absolute M_n of 5,880 assuming quantitative α,ω -functionalization of the PNIPAm₅₀ with cyanoisopropyl and dithiobenzoate functional groups respectively, Figure V-1B.

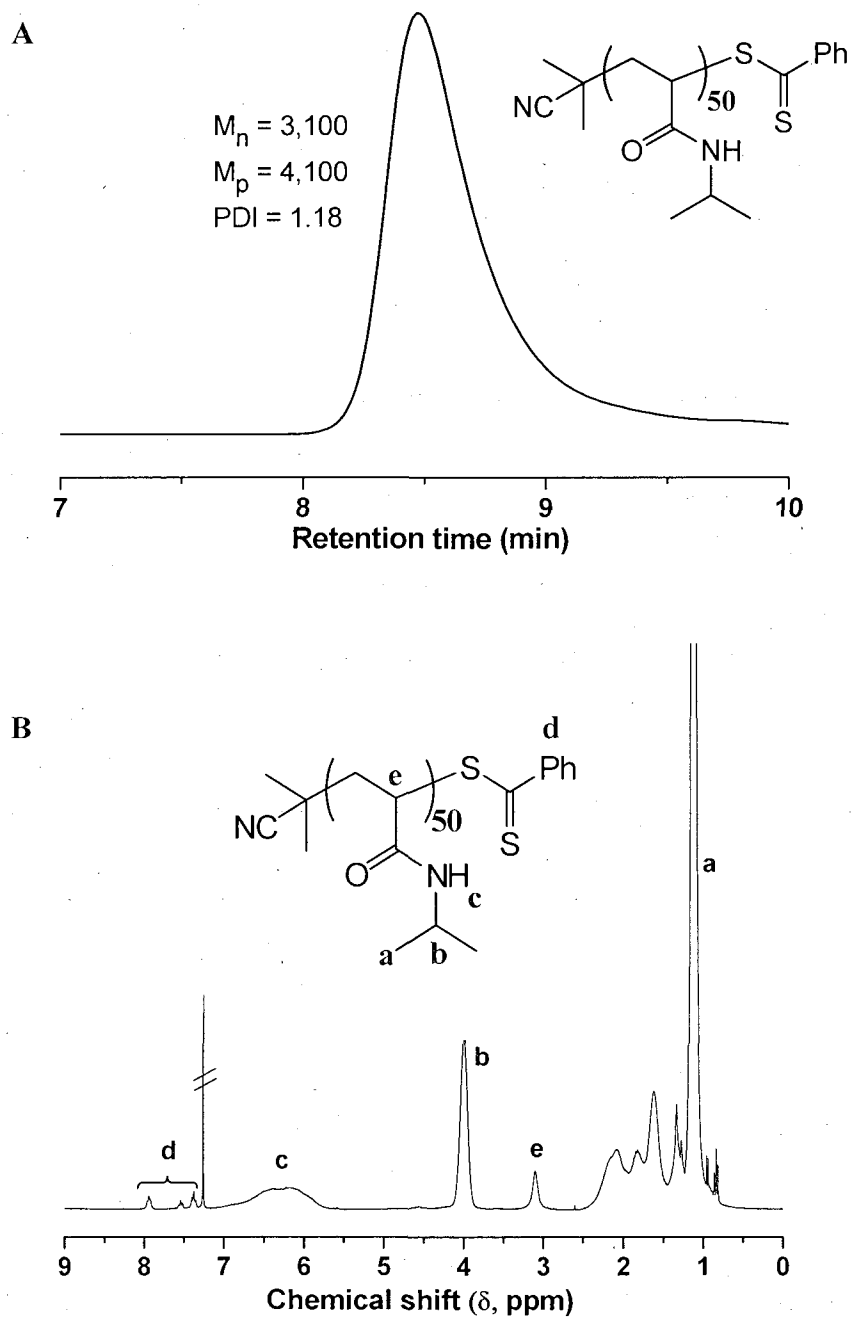


Figure V-1. (A) Size exclusion chromatographic (SEC) trace of the parent poly(N-isopropylacrylamide) homopolymer and (B) 1H NMR spectrum, recorded in $CDCl_3$, of the parent poly(N-isopropylacrylamide) homopolymer highlighting the presence of the phenyl end-group and the calculation of the absolute degree of polymerization.

With the well-defined PNIPAm₅₀ in-hand, the thiocarbonylthio end-groups were modified to allylic and propargylic species. The transformations were accomplished via tandem aminolysis/thiol-Michael (thiol-ene) reactions with allyl methacrylate (ALMA) and propargyl acrylate (PROPA), respectively. This one-pot conversion was achieved employing a combination of octylamine (OctAM) and dimethylphenylphosphine (Me₂PPh). OctAM was specifically employed to cleave the thiocarbonylthio end-groups yielding PNIPAm₅₀-SH, while Me₂PPh served two important roles. Firstly, it prevented the formation of macromolecular disulfide formed by the aerial oxidation of PNIPAm₅₀-SH and secondly it served as an extremely potent catalyst for the subsequent nucleophilic thiol-ene reaction.²⁰⁸ Indeed, the reducing capabilities of phosphines as well as their ability to serve as initiators/catalysts for Michael conjugate addition reactions is well documented.^{211,212,313} The products from the thiol-ene reaction, PNIPAm₅₀-S-ALMA and PNIPAm₅₀-S-PROPA, were characterized using a combination of ¹H NMR spectroscopy and SEC, Figure V-2 and Table V-1. Figure V-2A shows the ¹H NMR spectrum of PNIPAm₅₀-S-PROPA recorded in CDCl₃ with the corresponding SEC trace shown inset. Several key features are evident. Firstly, when comparing the NMR spectrum in 2A with 1B it is clear that the resonances of the phenyl hydrogens associated with the phenyl ring of the dithiobenzoate end-group of PNIPAm₅₀ are completely absent indicating quantitative cleavage. Additionally, a new resonance, labeled a, is observed in 2A and is assigned to the propargylic methylene hydrogens of the end group in PNIPAm₅₀-S-PROPA. Interestingly, a can be used to calculate the average degree of

polymerization (DP), simultaneously verifying quantitative reaction. The ratio of a to b, the resonance associated with the methine group of the isopropyl side chains, indicates a DP of 52. This agrees almost exactly with the previously calculated value of 50 determined using the phenyl end-group as noted above, and is within the error associated with NMR spectroscopy. This excellent agreement not only confirms the high efficacy of the macromolecular, Me₂PPh-mediated nucleophilic thiol-ene reaction but also serves to verify the beneficial effect of the Me₂PPh in preventing disulfide formation, since any significant oxidative coupling of the macromolecular thiols would result in a calculated DP that differs significantly from that calculated prior to end-group cleavage. The absence of any polymeric disulfide was also confirmed by SEC, see inset in Figure V-2A. The SEC trace is unimodal, symmetric, and narrow with no evidence of any coupled products that are most commonly observed as a shoulder at lower retention times on the main distribution. Indeed, the measured polydispersity index for PNIPAm₅₀-S-PROPA is identical to the precursor PNIPAm₅₀ with $M_w/M_n = 1.18$.

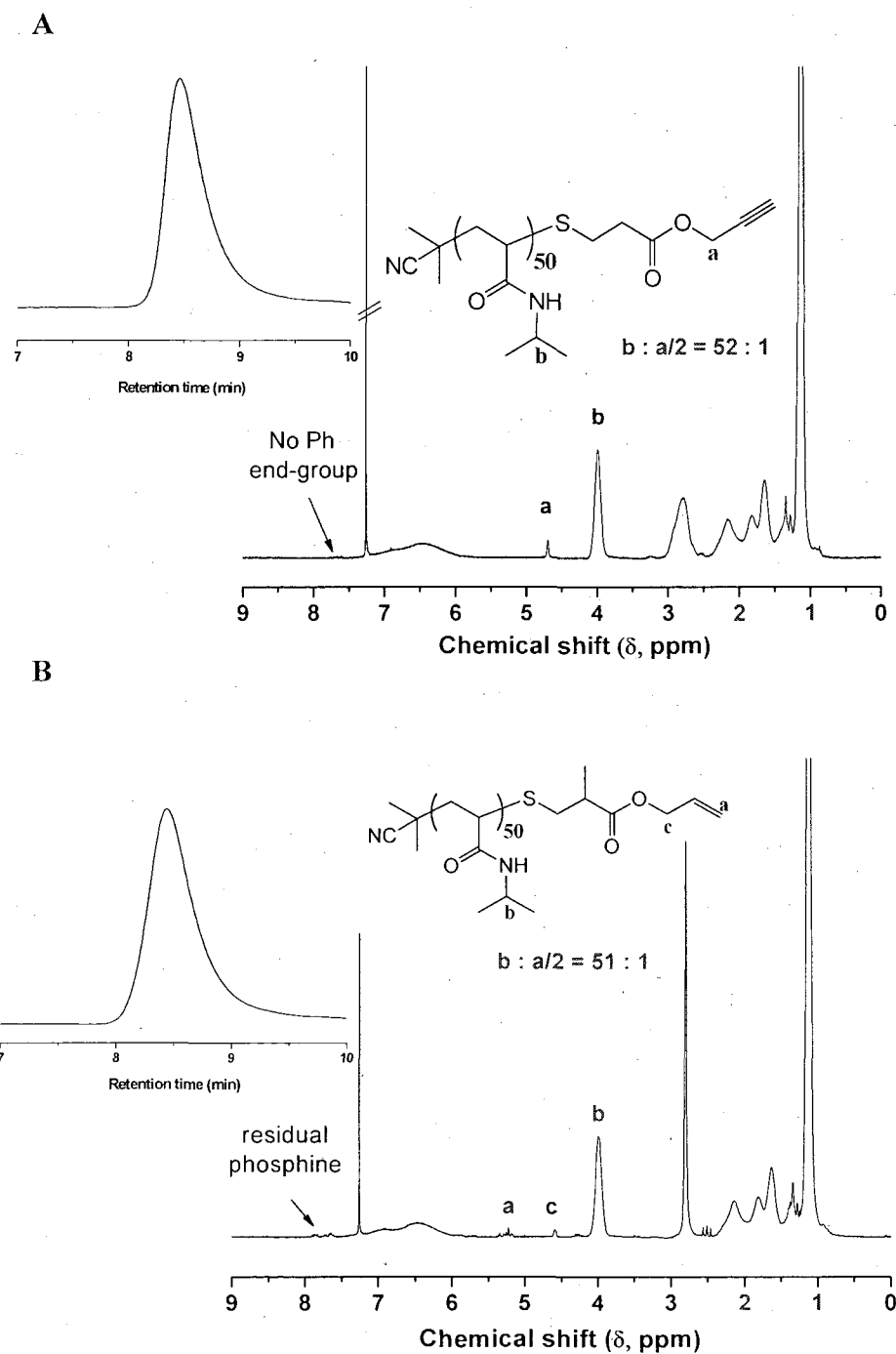


Figure V-2. (A) ^1H NMR spectrum, recorded in CDCl_3 , of the propargyl-end functionalized PNIPAM_{50} verifying quantitative end-group modification with the SEC trace shown inset, and (B) ^1H NMR spectrum, recorded in CDCl_3 , of the allyl-end functionalized PNIPAM_{50} verifying quantitative end-group modification with the resulting SEC trace shown inset.

Table V-1. Summary of the number average molecular weights determined by size exclusion chromatography and NMR spectroscopy, the polydispersity indices, average calculated degrees of polymerization, and lower critical solution temperatures as determined optically and by dynamic light scattering for the precursor PNIPAm₅₀ homopolymer and the series of end-modified PNIPAm homopolymers.

Polymer	M_n SEC ^a	M_n NMR ^b	M_w/M_n ^a	Calculated DP ^b	LCST ^c (°C)	LCST ^e (°C)
PNIPAm	3,100	5,880	1.18	50	29.0	29.0
PNIPAm-S-ALMA	3,300	-	1.22	51	30.0	29.0
PNIPAm-S-PROPA	3,200	-	1.18	52	29.0	34.0
PNIPAm-S-ALMA-(S-HexOH)	3,000	-	1.17	53	33.0	26.0
PNIPAm-S-PROPA-(S-HexOH) ₂	2,800	-	1.14	56	32.0	-
PNIPAm-S-ALMA-(S-Hex)	2,800	-	1.18	-	27.0	26.0
PNIPAm-S-PROPA-(S-Hex) ₂	2,700	-	1.17	-	27.0	26.0
PNIPAm-S-ALMA-(S-POSS)	3,700	-	1.22	47	35.0	35.0
PNIPAm-S-PROPA-(S-POSS) ₂	3,800	-	1.23	58	- ^d	- ^d

- determined by size exclusion chromatography with a MIXED-C column (molecular weight range: 200-2,000,000 g/mol), in THF stabilized with 281 ppm BHT at a flow rate of 1.0 mL/min. The column was calibrated with a series of narrow molar mass distribution poly(methyl methacrylate) standards
- determined by ¹H NMR spectroscopy
- determined visually with a temperature probe and gentle heating with a heat gun
- insoluble, even at temperatures approaching 0°C.
- determined by dynamic light scattering with 1 wt % solutions and heating from 5-40°C. Temperature was increased in 1°C increments and allowed to equilibrate for 2 min. prior to a measurement being made.

Similar observations were made in the case of the ALMA modified PNIPAM₅₀, likewise prepared via an OctAM/Me₂PPh-mediated nucleophilic thiol-ene reaction, Figure V-2B. Resonances associated with the allylic end-group are clearly present in the region $\delta \sim 4.5$ -5.3 ppm and are labeled a and c. A simple ratio of a to b indicates a DP of 51, a value entirely consistent with those determined for PNIPAM₅₀ and PNIPAM₅₀-S-PROPA, and likewise indicates successful and quantitative formation of PNIPAM₅₀-S-ALMA. SEC analysis of PNIPAM₅₀-S-ALMA, Table V-1, indicated a very small difference in the polydispersity index, from 1.18 to 1.22. However, the chromatogram was unimodal and symmetric.

With the PNIPAM₅₀-S-PROPA and PNIPAM₅₀-S-ALMA polymers in-hand the allylic and propargylic end-groups were modified with three different small molecule thiols via both radical-mediated thiol-ene and thiol-yne reactions. Specifically, the unsaturated end-groups were reacted with 6-mercaptohexan-1-ol (S-HexOH), hexane-1-thiol (S-Hex), and a 3-mercaptopropyl polyhedral oligomeric silsesquioxane (S-POSS) with R = *iso*-butyl, Figure V-3, under photochemical conditions at ambient temperature, humidity and under a normal air atmosphere.

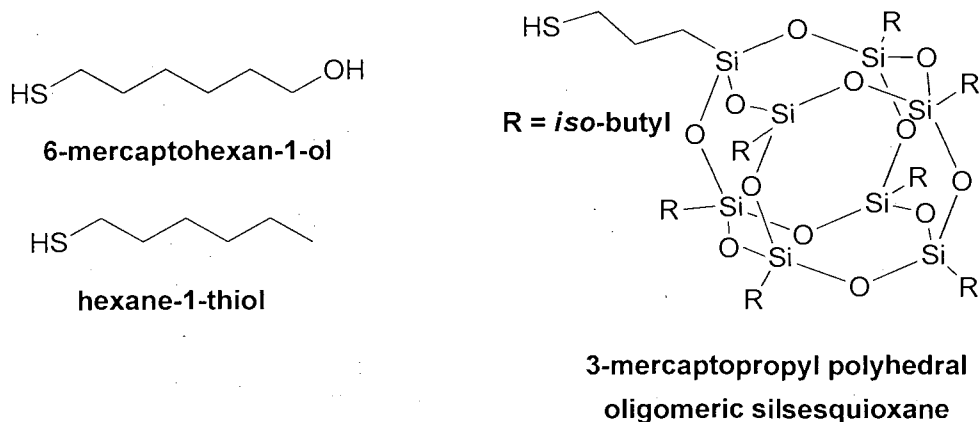


Figure V-3. Chemical structures of the three representative, commercially available, thiols employed in the radical thiol-ene and radical thiol-yne end-group reactions.

These thiols were chosen as common commercially available species with hydrophobic and hydrophilic character. However, this chemistry is not limited to these molecules, and a range of other, functional thiols, including those of potential biomedical importance, can be employed in such thiol-ene and thiol-yne radical reactions.^{206,296,314}

Figure V-4 A-F shows the ^1H NMR spectra, recorded in CDCl_3 , of the products obtained from the reaction of $\text{PNIPAm}_{50}\text{-S-PROPA}$ and $\text{PNIPAm}_{50}\text{-S-ALMA}$ with the three thiols.

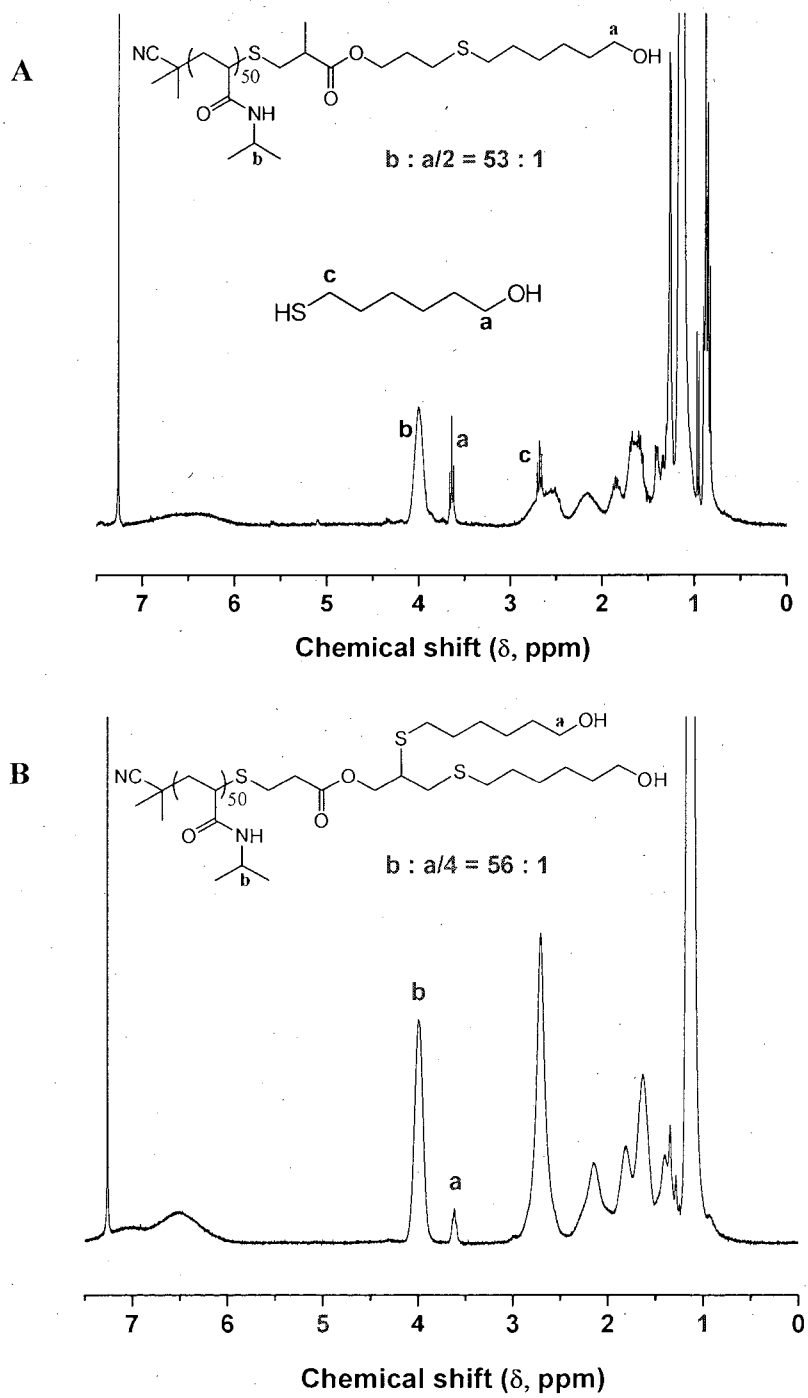


Figure V-4. ^1H NMR spectra, recorded in CDCl_3 for (A) PNIPAm₅₀-S-ALMA-S-HexOH), (B) PNIPAm₅₀-S-PROPA-(S-HexOH)₂.

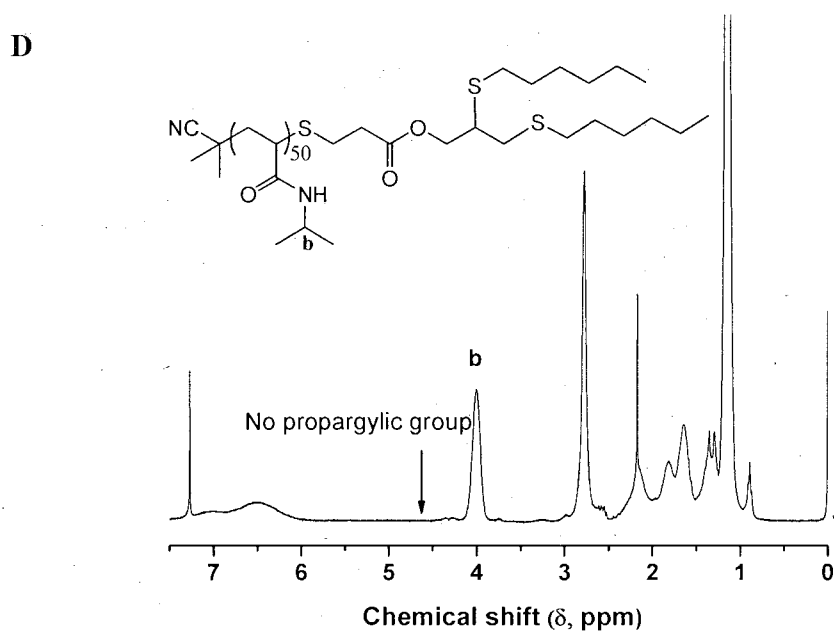
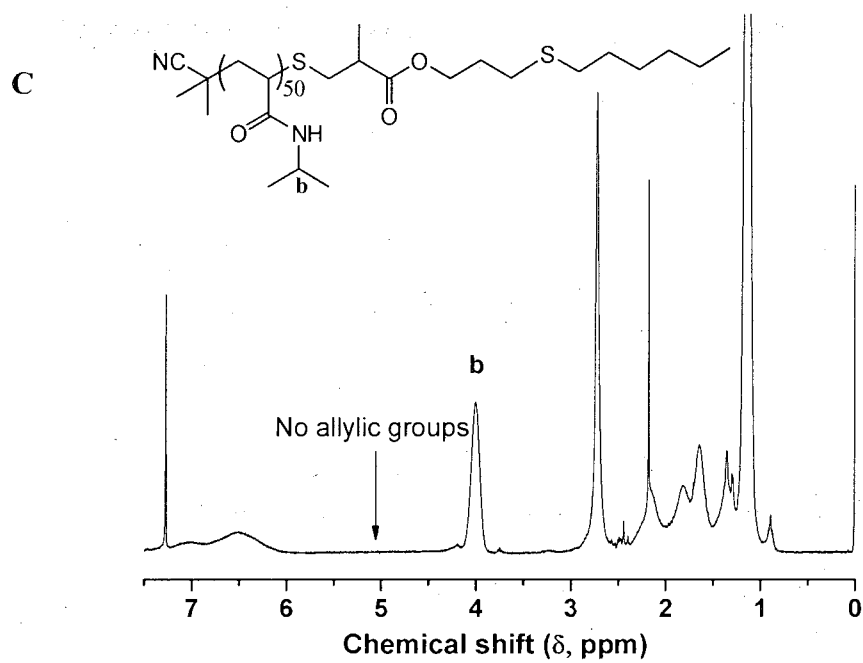


Figure V-4. (continued) ¹H NMR spectra, recorded in CDCl₃ for (C) PNIPAm₅₀-S-ALMA-S-Hex, (D) PNIPAm₅₀-S-PROPA-(S-Hex)₂.

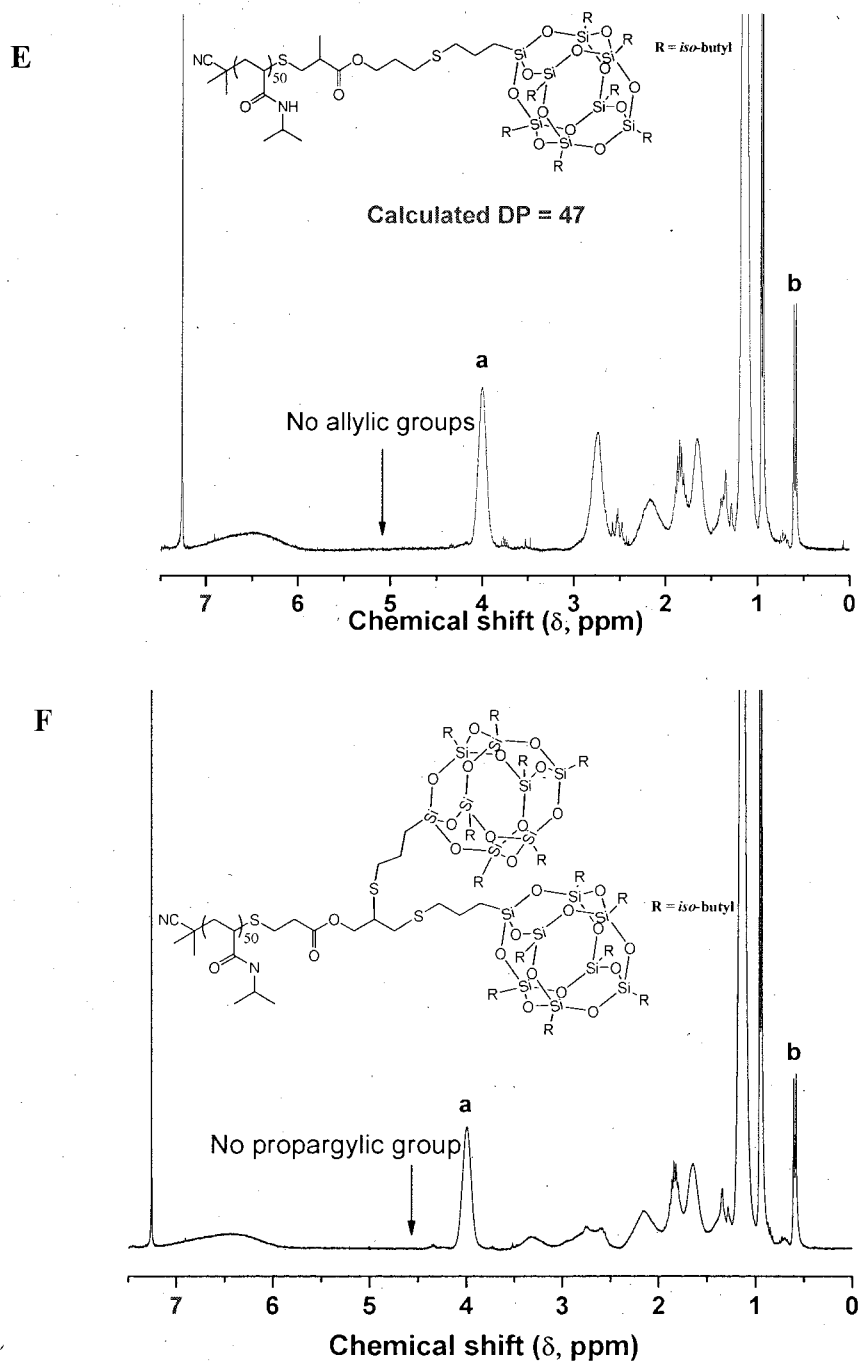


Figure V-4. (continued) ^1H NMR spectra, recorded in CDCl_3 for (E) PNIPAm₅₀-S-ALMA-S-POSS, and (F) PNIPAm₅₀-S-PROPA-(S-POSS)₂.

Figure V-4A and Figure V-4B show the ^1H NMR spectra for PNIPAm₅₀-S-PROPA-(S-HexOH)₂ and PNIPAm₅₀-S-ALMA-(S-HexOH). In the case of the thiol-ene reaction on PNIPAm₅₀-S-ALMA two important differences between Figure V-4A and Figure V-2B are evident. Firstly, the resonances associated with the allylic end-group, previously observed at $\delta \sim 4.5\text{-}5.3$ ppm, have completely disappeared while new resonances due to the S-HexOH are evident. The resonance of the $-\text{CH}_2-$ group alpha to the OH group is clearly visible at $\delta \sim 3.6$ ppm while that associated with the $-\text{CH}_2-$ alpha to S is visible at $\delta \sim 2.7$ ppm, but overlaps with another polymer-related resonance. A ratio of the integrals of the signals labeled a and b indicates a DP of 53 which agrees almost exactly with the DP values calculated for the PNIPAm homopolymer and the ALMA end-modified species and, again, suggests a quantitative thiol-ene reaction. Similar observations were made in the case of the radical thiol-yne reaction of PNIPAm₅₀-S-PROPA with S-HexOH. The resonance associated with the propargylic hydrogens, observed at $\delta \sim 4.6$ ppm (Figure V-2A), is completely absent while the resonance of the methylene hydrogens alpha to the OH group is again present at $\delta \sim 3.6$ ppm. In this instance, a ratio of a with b indicates a DP of 56, slightly higher than that determined for PNIPAm₅₀-S-PROPA, but still indicating essentially quantitative reaction. The reaction of PNIPAm₅₀-S-ALMA and PNIPAm₅₀-S-PROPA with hexane-1-thiol, Figure V-4C and 4D, proved difficult to quantify since no distinct, non-overlapping, resonances associated with S-Hex were observed. However, after reaction the key allylic and propargylic resonances were completely absent, qualitatively indicating successful

and complete reaction. Finally, the allylic and propargylic end-groups of the NIPAm homopolymer were modified by radical reaction with S-POSS yielding novel polymer-nanomaterial hybrid structures. As with the previous reactions, the reaction was monitored via a combination of ^1H NMR spectroscopy and SEC. Figure V-4E and 4F show the ^1H NMR spectra, recorded in CDCl_3 , for the S-POSS modified NIPAm homopolymers. Consistent with the previous two thiols, following the radical thiol-ene and thiol-yne reactions neither the allylic nor propargylic resonances are observable in the ^1H NMR spectra qualitatively indicating complete consumption of the unsaturated bonds. In both instances resonances associated with the S-POSS moiety are clearly present although most overlap with polymer signals. One signal that can be integrated with reasonable accuracy is the doublet at $\delta \sim 0.6$ ppm that is assigned to the methylene group of the *iso*-butyl alkyl groups on the POSS cage and is labeled b in Figure V-4E. In the case of the reaction with PNIPAm₅₀-S-ALMA a ratio of a with b indicates a DP of 47, again a value that agrees extremely well with that calculated for the precursor PNIPAm homopolymer. For the thiol-yne reaction on PNIPAm₅₀-S-PROPA, Figure V-4F, a ratio of the same two resonances indicates a DP of 58. This value would seem to indicate that the radical thiol-yne reaction did not go to completion, although assuming that the initial DP of 50 for the NIPAm homopolymer is correct this value indicates a yield $\geq 90\%$. Given the fact that the signals associated with b are not fully baseline resolved, the error inherently associated with these integral values, and the large bulky nature of the S-POSS *iso*-butyl molecule, this value is still in reasonable agreement with the expected, ideal

value of 50. In all instances, the polydispersity indices for the mono- and bis-end modified PNIPAm₅₀ homopolymers remained essentially the same as the parent homopolymer with values in the range $M_w/M_n = 1.14-1.23$.

One reason PNIPAm attracts significant attention is due to its readily accessible lower critical solution temperature (LCST). It is well documented that the LCST of PNIPAm is ~ 32 °C,³¹⁵⁻³¹⁸ close to physiological temperature. While varying the degree of polymerization,¹⁵⁴ and topology,³¹⁹ offers some degree of control and tunability of the LCST in NIPAm homopolymers, for materials with low molecular weights the effect on the LCST of end-groups can become important.^{320,321} As such, and given the relatively low molecular weight of the parent NIPAm homopolymer, it was anticipated that the introduction of either one or two S-HexOH, S-Hex, or S-POSS groups, all with differing hydrophilicities/hydrophobicities, at the PNIPAm ω chain terminus would have an effect on the LCST, and general aqueous solution behavior of the PNIPAm₅₀-based materials. Indeed, and as clearly noted by Kujawa et al.,¹⁵⁴ the introduction of hydrophobic end-groups can affect the aqueous phase behavior of PNIPAm in two distinct ways. Firstly, the general miscibility of the homopolymer in water is worsened due to the interactions between water and the hydrophobic end-groups, and secondly, sufficiently large hydrophobic species at the chain end can lead to aggregation/micellization reducing the mixing entropy of the polymer chains, although this does not really effect the hydration of the main polymer chains. Both of these factors tend to favor phase

separation, and in the case of PNIPAm, should lead to a lowering of the LCST.

The LCSTs of the parent NIPAm₅₀ homopolymer, PNIPAm₅₀-S-ALMA, PNIPAm₅₀-S-PROPA and the six mono/bis modified materials were evaluated using a combination of simple optical measurements and dynamic light scattering (DLS). For the optical measurements, 1 wt% solutions were gently heated and the temperature at which the starting water-white solutions became noticeably opaque was recorded as the LCST. In the case of DLS measurements, samples were heated from 5 to 40°C with a measurement taken at each 1 °C increment after equilibrating for 2 minutes. The temperature at which an abrupt change in the hydrodynamic diameter (D_h) was observed was taken as the LCST.

Consider the optical measurements. In the case of the NIPAm₅₀ homopolymer, Figure V-5A, the cloud point (T_{cp}) was determined to be 29°C. This value is very close to the generally quoted value of 32 °C for the coil-to-globule-to-precipitate transition associated with PNIPAm. Given the low molecular weight of this sample ($M_n \sim 5,900$) this observed difference of three degrees may be a direct result of the hydrophobic phenyl dithioester end-group reducing the generally solubility of the PNIPAm chains. However, as noted by Kujawa,⁵⁸ there is a clear molecular weight dependence on the LCST for NIPAm homopolymers. For example, in their studies of octadecyl α,ω -end-functionalized PNIPAm's of varying molecular weights (with M_n values ranging from 12,000 to 49,000),

at a constant concentration of 1.0 g/L, the LCST was observed to fall from 30.7°C for the highest molecular weight species down to 25.1°C for the lowest molecular weight species. Therefore, this observed value of 29°C may, simply, be a direct result of the low molecular weight of the precursor PNIPAm homopolymer. Essentially identical observations were made in the case of the PNIPAm₅₀-S-ALMA and PNIPAm₅₀-S-PROPA homopolymers, Figure V-5B and 5C, with observed T_{cp} values of 30.0 and 29.0°C respectively. In the case of the PNIPAm₅₀-S-ALMA-S-HexOH and PNIPAm₅₀-S-PROPA-(S-HexOH)₂ polymers, Figure V-5D, the T_{cp} values were observed to be 33 and 32°C, respectively, identical to the commonly reported LCST for PNIPAm. Presumably, these elevated T_{cp} values are due to the presence of the terminal, hydrophilic, H-bonding OH functional groups that offset any hydrophobic effect of the precursor ALMA/PROPA segments as well as the C6 fragment associated with S-HexOH. There appears to be little, if any, effect of having two vs. one OH groups. This proposed beneficial effect of the hydrophilic OH groups is supported by the observation that in the case of the PNIPAm₅₀-S-ALMA-S-Hex and PNIPAm₅₀-S-PROPA-(S-Hex)₂ polymers, Figure V-5E, the measured T_{cp} values are both 27°C, several degrees lower than for the precursor PNIPAm₅₀-S-ALMA and PNIPAm₅₀-S-PROPA species. This lowering of the LCST is attributed to the increase in hydrophobicity associated with the introduction of the hexyl end-groups. Again, however, there appears to be no distinguishable effect upon the introduction of one vs. two hexyl chains. Finally, in the case of the POSS modified PNIPAm's there was a clear effect with respect to the introduction of one or two POSS

cages at the ω -terminus. In the case of the di-functional species,

PNIPAm₅₀-S-PROPA-(S-POSS)₂ Figure V-5F, the end-modified PNIPAm was not

water-soluble at the examined concentration of 1 wt% even at temperatures approaching 0°C. This is consistent with the highly bulky and hydrophobic nature of the POSS cage.

In the case of the mono-POSS species, PNIPAm₅₀-S-ALMA-S-POSS, the modified

polymer was soluble at the specified concentration and at ambient temperature, and also

clearly exhibited LCST behavior. However, repeated measurements indicated an LCST of

~35°C – a value higher than expected given the low molecular weight of the parent

PNIPAm homopolymer and the hydrophobic nature of POSS. We currently have no

explanation for this anomalously high value of T_{cp} .

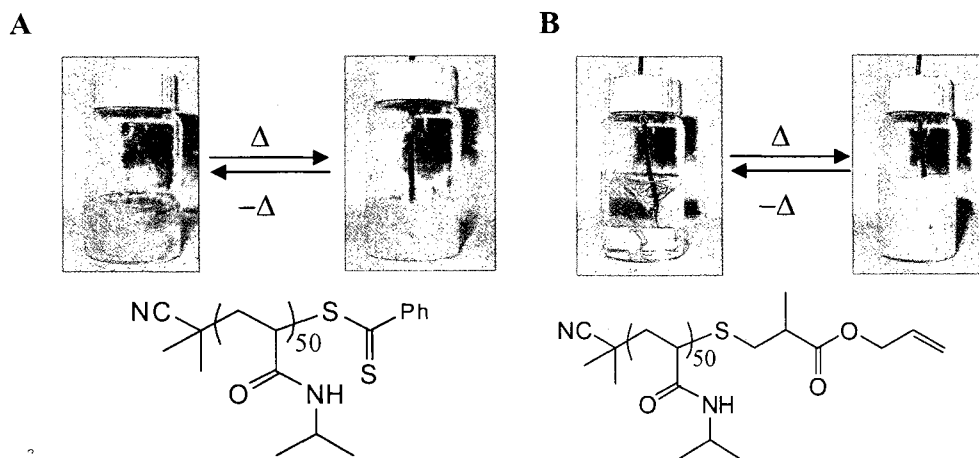


Figure V-5. Digital pictures demonstrating the reversible temperature-induced phase separation and chemical structures of 1 wt% solutions of (A) PNIPAm₅₀ (B) PNIPAm₅₀-S-ALMA.

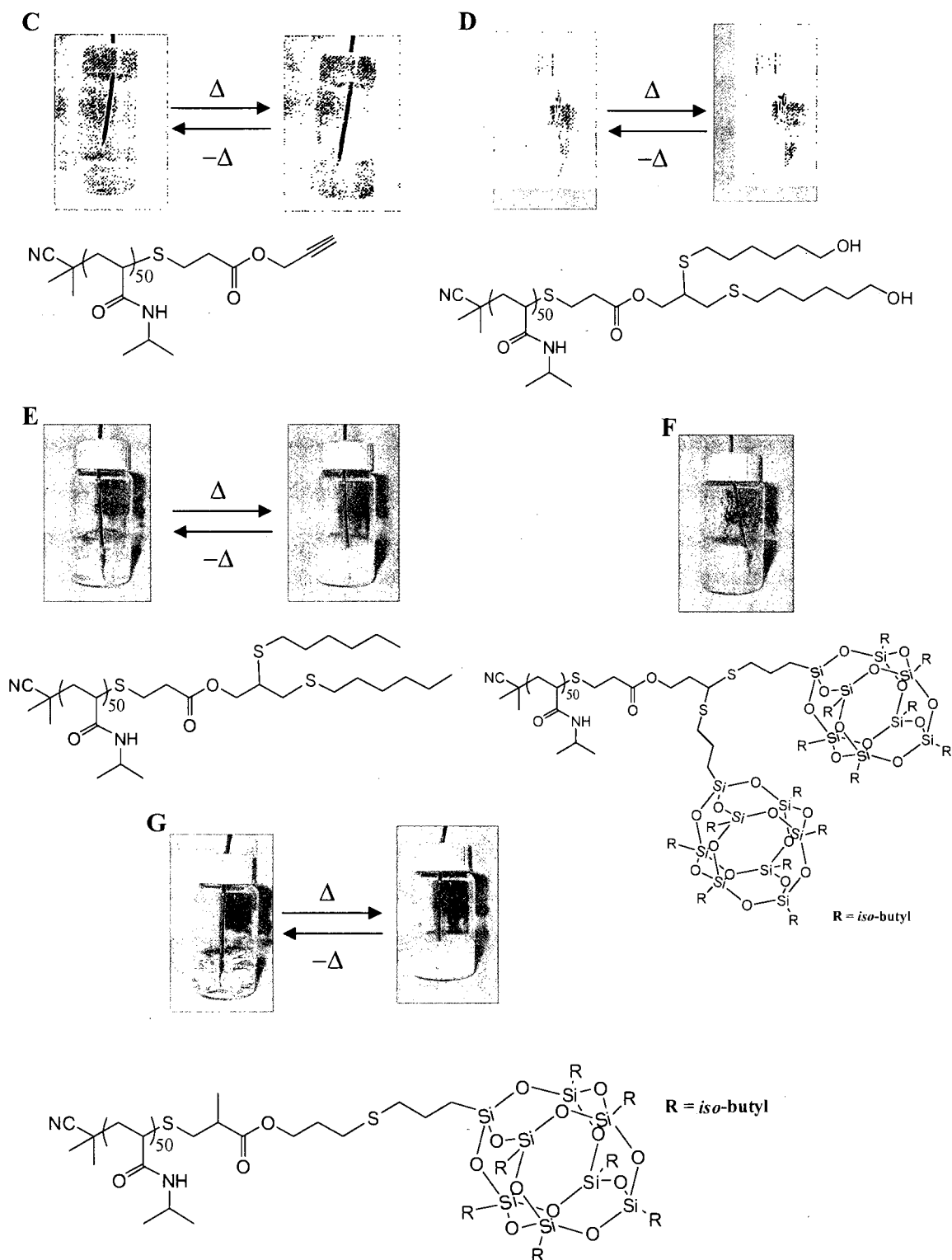


Figure V-5. (continued) Digital pictures demonstrating the reversible temperature-induced phase separation and chemical structures of 1 wt% solutions of (C) PNIPAM₅₀-S-PROPA (D) PNIPAM₅₀-S-PROPA-(S-HexOH)₂ (E) PNIPAM₅₀-S-PROPA-(S-Hex)₂ (F) PNIPAM₅₀-S-PROPA-(S-POSS)₂, and (G) PNIPAM₅₀-S-ALMA-S-POSS.

The LCSTs as estimated by DLS measurements generally agreed very well with those determined optically. For example, in the case of PNIPAm₅₀ and PNIPAm₅₀-S-ALMA the determined T_{cp} values were, in both instances, 29 °C, identical to those measured optically. The T_{cp} value for PNIPAm₅₀-S-PROPA was found to be several degrees higher than that determined optically. In all three instances, however, the DLS data, see Figure V-6 for an example, indicated some type of aggregation process with the formation of species, prior to macroscopic phase separation, with hydrodynamic sizes in the micron range. While the soluble-to-insoluble transition in PNIPAm, and other thermoresponsive polymers, is often very sharp, as highlighted in the cooperative dehydration mechanism,³²² Wu and co-workers³²³ noted that in dilute solutions of hydrophobically modified PNIPAm it is possible for chains to collapse and associate to form a stable mesoglobular phase between single chain globules and macroscopic precipitate. While the exact mode of ‘self-assembly’ of these end-group modified PNIPAm’s is unclear there certainly appears to be a colloiddally stable species present prior to macroscopic phase separation. However, given the micron size of these aggregates it is highly unlikely that these species are well-defined micelle-like structures that can, and have, been observed with end-group modified PNIPAm’s bearing larger hydrophobic end-group species.¹⁵⁴ Good agreement between the T_{cp} values obtained by DLS and optical measurements was also observed in the case of the PNIPAm₅₀-S-ALMA-S-Hex, PNIPAm₅₀-S-PROPA-(S-Hex)₂, and PNIPAm₅₀-S-ALMA-S-POSS polymers with the S-Hex-based polymers yielding T_{cp}

values of 26°C by DLS, versus 27°C optically. DLS indicated an identical, but still anonymously high value, of 35°C for the S-POSS derivative. In the case of PNIPAm₅₀-S-ALMA-S-HexOH the DLS T_{cp} was significantly lower, at 26°C, than that determined optically (33°C).

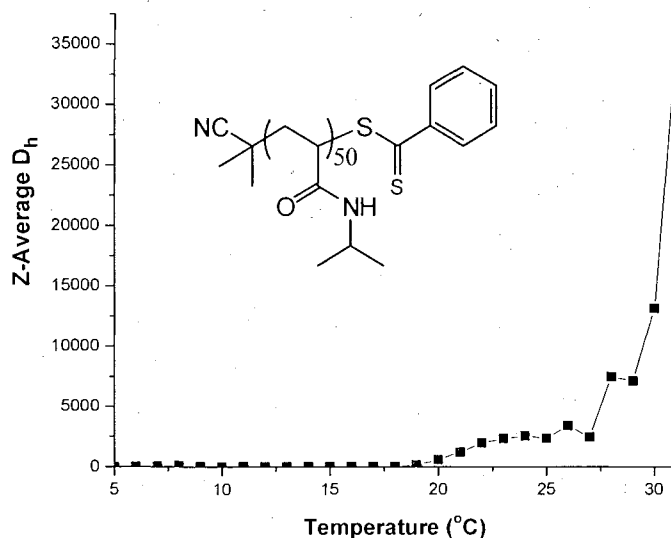


Figure V-6. Plot of Z-average hydrodynamic diameter vs. temperature for a 1 wt% aqueous solution of PNIPAm₅₀ demonstrating the determination of the LCST.

4. Summary and Conclusions

The synthesis of a range of well-defined, end-group modified poly(*N*-isopropylacrylamide)s (PNIPAm_s) is described and the effect of end-group modification on the lower critical solution temperature noted. The end-group modifications were accomplished on a RAFT-prepared PNIPAm via a sequential process involving tandem amine-mediated dithioester end-group cleavage/phosphine-mediated

thiol-ene reactions with allyl methacrylate and propargyl acrylate followed by radical-mediated thiol-ene and thiol-yne reactions to yield the mono and bis-end functionalized species. This is the first time the sequential thiol-ene/thiol-ene and thiol-ene/thiol-yne reactions, proceeding via inherently different mechanisms, have been applied in polymer synthesis. We highlight the high efficiency of the radical and nucleophile click thiol-ene reactions as well as its sister radical-mediated thiol-yne reaction. End group modifications were shown to be quantitative yielding novel modified PNIPAMs. The lower critical solution temperatures of the precursor PNIPAM and the end-group modified species were examined using a combination of dynamic light scattering and optical measurements, yielding cloud point values that were generally in good agreement. The observed differences in the cloud points was rationalized in terms of the hydrophilicity/hydrophobicity of the introduced end-groups.

CHAPTER VI

SUMMARY AND CONCLUSIONS

Three novel methacrylic monomers containing 2 or 3 tertiary amine functional groups, 1,3-bis(dimethylamino)propan-2-yl methacrylate (**M1**), 1-(bis(3-(dimethylamino)propyl)amino)propan-2-yl methacrylate (**M2**) and 2-((2-(2-(dimethylamino)ethoxy)ethyl)methylamino)ethyl acrylate (**M3**), were successfully synthesized via a straightforward acylation of methacryloyl chloride and aminoalcohols. Among these three monomers, **M1** has been reported previously while both **M2** and **M3** are completely new. However, none of them has been polymerized under controlled conditions. The homopolymerization of **M1-M3** were conducted under standard RAFT conditions and the living nature is proven by a combination of linear pseudo-first order kinetic plot and well-defined molecular weight profiles. The CTA:Initiator ratio affects the polymerization process as predicted by the RAFT mechanism. For all of the three monomer, the lower CTA:Initiator ratio leads to a faster polymerization rate due to the higher radical concentration. And a longer induction period was observed for the higher CTA:Initiator ratio homopolymerization due to the lower radical concentration. Both **M1** and **M3** were successfully copolymerized with hexyl and lauryl methacrylates to yield well-defined statistical copolymers with predetermined composition. All three homopolymers were observed possessing reversible stimuli-responsive properties in aqueous solution, temperature-responsive and

pH-responsive. Poly**M1** shows a lower critical solution temperatures (LCST) of 23 °C, for poly**M2** the LCST is 33 °C, and for poly**M3** the LCST is 63 °C. All three homopolymers phase separate at pH near 13.

A series of water-soluble, stimuli-responsive AB diblock copolymers based on the biocompatible 2-(methacryloyloxy)ethyl phosphorylcholine (MPC) was successfully synthesized via RAFT polymerization in either water or protic organic solvent, or a mixture of both. The chosen comonomers, *N,N*-diethylacrylamide (DEAm), 4-vinylbenzoic acid (VBZ), *N,N*-di-*n*-propylbenzylvinylamine (DnPVBA), and *N*-(3-sulfopropyl)-*N*-methacryloxyethyl-*N,N*-dimethylammonium betaine (DMAPS), exhibit corresponding stimuli-responsive properties as expected based on the ¹H NMR spectroscopy and dynamic light scattering experiments. Such diblock copolymers are able to self-assemble upon the application of corresponding stimulus, and disassemble upon removal of the stimulus. The unimer sizes of these copolymers are consistent 6-7 nm. However, the sizes of the aggregates formed vary from 22-182 nm, indicating the formation of micelles or vesicles, or higher ordered structures.

Due to the high efficiency of thiol-ene click chemistry, end group modifications of RAFT-synthesized homopolymer with either allyl methacrylate or propargyl acrylate were accomplished with near quantitative conversion. In the subsequent radical thiol-ene and thiol-yne addition, the ene and yne end groups were quantitatively modified to mono-

and bis-end functions, respectively, with 6-mercaptohexan-1-ol, hexane-1-thiol, and POSS-thiol. The LCSTs for these homopolymers of NIPAm were determined by a combination of optical measurement and dynamic light scattering. The results show that the LCSTs are dependent on the nature of the end-groups. The poly(NIPAm) with dithioester, propargyl acrylate, and allyl methacrylate end-groups have very close LCST, 29-30 °C. The introduction of hydrophobic end-groups causes a decrease of the LCST, while the introduction of hydrophilic end-groups causes an increase of the LCST. This is in agreement with the LCSTs of the NIPAm homopolymers with hexane and hexanol end-groups. However, the introduction of one or two end-groups does not affect the LCST since the NIPAm homopolymers with mono- and bis-hexane (or mono- and bis-hexanol) end-groups have almost identical LCSTs.

CHAPTER VII

FUTURE WORK

Polybetaines are well-known for their biocompatibility anti-adherent properties. The dimethylamino functional groups in **M1-M3** are ready to be converted to difunctional betaine species by reaction with betainizing agent, such as 1,3-propanesultone and lactones. The prepared betaine monomers can be directly polymerized via aqueous RAFT polymerization to yield well-defined polybetaines materials, or as an alternative method, post-polymerization betainization of the polymer containing **M1-M3** may yield the corresponding polybetaines as well. The biocompatibility and anti-adherent properties of such well-defined di-functional polybetaines can be compared with mono-functional species and give useful function-structure information.

The synthesized MPC-based AB diblock copolymers exhibit stimuli-responsive properties as expected. However, the nature of the formed aggregates with varied size has not been elucidated. In the future, we will explore the nature of these aggregates (micelles, vesicles, or higher ordered structures) employing transmission electron microscopy (TEM) which offers visual images of the target aggregates. With the synthesized diblock copolymers, it is possible to prepare tri-block copolymers by using these diblock copolymers as macro-CTAs in RAFT polymerizations with other stimuli-responsive comonomers to yield materials responsive to additional stimuli. For example, the

prepared P(MPC-*b*-DEAm) can be used as a macro-CTA mediating the RAFT polymerization of VBZ monomer yielding a P(MPC-*b*-DEAm-*b*-VBZ) triblock, which responds to both thermal and pH changes of the solution. Again, these stimuli-responsive properties could be thoroughly studied by a combination of ^1H nuclear magnetic resonance (NMR) spectroscopy, dynamic light scattering (DLS) and TEM.

To better understand the effect of end-group structures on the lower critical solution temperatures (LCST), more NIPAm polymers with different end-groups should be prepared via the established sequential thiol-ene/thiol-ene and thiol-ene/thiol-yne click reactions. The LCST will be studied by a combination of optical measurement and DLS at varied temperatures.

REFERENCES

1. Jagur-Grodzinski, J. *Living and Controlled Polymerization* **2005**,
2. Odian, G. *Principles of Polymerization* **4th edition**
3. Yamago, S., Lida, K., Yoshida, J. *J.Am.Chem.Soc.* **2002**, *124*, 2874
4. *IUPAC Compendium of Chemical Terminology* **1996**, *68*, 2308
5. Quirk, R. P., Lee, B. *Polym.Int.* **1992**, *27*, 359
6. Szwarc, M. *Nature* **1956**, *178*, 1168
7. Szwarc, M., Levy, M., Milkovich, R. *J.Am.Chem.Soc.* **1956**, *78*, 2656
8. Hirao, A., Nagawa, T., Hatayama, T., Yamaguchi, K., Nakahama, S. *Macromolecules* **1985**, *18*, 2101
9. Aoshima, S., Uesugi, N., Sawamoto, M., Higashimura, T. *Macromolecules* **1985**, *18*, 2097
10. Miyamoto, M., Sawamoto, M., Higashimura, T. *Macromolecules* **1984**, *17*, 2228
11. Szwarc, M. *J.J.Polym.Sci., Part A: Polym.Chem.* **1998**, *36*, v
12. Szwarc, M. *Adv.Polym.Sci.* **1983**, *49*, 1
13. Young, R. N., Quirk, R. P., Fetters, L. J. *Adv.Polym.Sci.* **1984**, *56*, 1
14. Szwarc, M. *Adv.Polym.Sci.* **1960**, *2*, 275
15. Webster, O. W., Hertler, W. R., Sogah, D. Y., Farnham, W. B., Rajanbabu, T. V. *J.Am.Chem.Soc.* **1983**, *105*, 5706
16. Miyamoto, M., Sawamoto, M., Higashimura, T. *Macromolecules* **1984**, *17*, 265
17. Higashimura, T., Miyamoto, M., Sawamoto, M. *Macromolecules* **1985**, *18*, 611
18. Faust, R., Kennedy, J. P. *Polym.Bull.* **1986**, *15*, 317
19. Sawamoto, M., Kennedy, J. P. *J.Macromol.Sci.,Chem.* **1982**, *A18*, 1275
20. Toman, L., Spevacek, J., Vlcek, P., Holler, P. *J.Polym.Sci., Part A: Polym.Chem.* **2000**, *38*, 1568

21. Bossaer, P. K., Goethals, E. J., Hackett, P. J., Pepper, D. C. *Eur.Polym.J.* **1979**, *13*, 489
22. Gandini, A., Plesch, P. H. *J.Chem.Soc.* **1965**, 4826
23. Sawamoto, M., Fujimoro, J., Hgashimura, T. *Macromolecules* **1987**, *20*, 916
24. Allcock, H. R., Nelson, J. M., Morrissey, C. T., Crane, C. A., Reeves, S. D., Honeyman, H. H., Manners, I. *Macromolecules* **1996**, *29*, 7740
25. Schrock, R. R., DePue, R. T., Feldmen, J., Schaverian, J. C., Dewan, J. C., Liu, A. H. *J.Am.Chem.Soc.* **1988**, *110*, 1423
26. Trnka, T. M., Grubbs, R. H. *Acc.Chem.Res.* **2001**, *34*, 18
27. Ostu, T., yoshida, M., Kuriyama, A. *Makromol.Chem.Rapid Commun.* **1982**, *3*, 133
28. Otsu, T., Yoshida, M., Tazaki, T. *Makromol.Chem.Rapid Commun.* **1982**, *3*, 127
29. Lowe, A. B., Billingham, N. C., Armes, S. P. *Chem.Commun.* **1996**, 1555
30. Georges, M. K., Veregin, P. M., Kazmaier, P. M., Hamer, G. K. *Macromolecules* **1993**, *26*, 2987
31. Fischer, H. *J.Polym.Sci., Part A: Polym.Chem.* **1999**, *37*, 1885
32. Souailler, M., Fischer, H. *Macromolecules* **2000**, *33*, 7378
33. Solomon, D. H., Rizzardo, E., Cacioli, P. *U.S.Patent* 4581429, **1986**
34. Hawker, C. J., Bosman, A. W., Harth, E. *Chem.Rev.* **200**, *101*, 3661
35. Benoit, D., Chaplinski, V., Braslau, R., Hawker, C. J. *J.Am.Chem.Soc.* **1999**, *121*, 3904
36. Wang, J. S., Matyjaszewski, K. *J.Am.Chem.Soc.* **1995**, *117*, 5614
37. Wang, J. S., Matyjaszewski, K. *Macromolecules* **1995**, *28*, 1721
38. Kato, M., Kamigaito, M., Sawamoto, M., Higashimura, T. *Polym.Prep.Jpn.* **1994**, *43*, 1792
39. Kato, M., Kamigaito, M., Sawamoto, M., Higashimura, T. *Macromolecules* **1995**, *28*, 1721
40. Ando, T., Kato, M., Kamigaito, M., Sawamoto, M. *Macromolecules* **1996**, *29*, 1070
41. Kotani, Y., Kamigaito, M., Sawamoto, M. *Macromolecules* **1999**, *32*, 2420

42. Ando, T., Kamigaito, M., Sawamoto, M. *Macromolecules* **1997**, *30*, 4507
43. Percec, V., Barboiu, B., Neumann, A. *Macromolecules* **1996**, *29*, 3665
44. Brandts, J. A. M., van de Geijn, P., van Faassen, E. E., Boersma, J., van Koten, G. *J.Org.Chem.* **1999**, 246
45. Kickelbick, G., Matyjaszewski, K. *Makromol.Chem.Rapid Commun.* **1999**, *20*, 341
46. Matyjaszewski, K., Patten, T. E., Xia, J. *J.Am.Chem.Soc.* **1997**, *119*, 974
47. Matyjaszewski, K., Wei, M., Xia, J., McDermott, N. E. *Macromolecules* **1997**, *30*, 8161
48. Davis, K., Paik, H., Matyjaszewski, K. *Macromolecules* **1999**, *32*, 1767
49. Simal, F., Demonceau, A., Noels, A. F. *Angew.Chem.* **1999**, *38*, 538
50. Teodorescu, M., Gaynor, S. G., Matyjaszewski, K. *Macromolecules* **2000**, *33*, 2335
51. Grimaud, T., Matyjaszewski, K. *Macromolecules* **1997**, *30*, 2216
52. Granel, C., Dubois, P., Jerome, R., Teyssie, P. *Macromolecules* **1998**, *31*, 6756
53. Huang, X., Wirth, M. J. *Macromolecules* **1999**, *32*, 1694
54. Li, D., Brittain, W. *Macromolecules* **1998**, *31*, 3852
55. Rademacher, J. T., Baum, M., Pallack, M. E., Brittain, W. J., Simonsick, W. J. *Macromolecules* **2000**, *33*, 284
56. Senoo, M., Kotani, Y., Kamigaito, M., Sawamoto, M. *Macromolecules* **1999**, *32*, 8005
57. Matyjaszewski, K., Beers, K. L., Muhlebach, A., Coca, S., Zhang, X., Gaynor, S. G. *Polym.Mater.Sci.Eng.* **1998**, *79*, 429
58. Matyjaszewski, K., Jo, S. M., Paik, H., Shipp, D. A. *Macromolecules* **1999**, *32*, 6431
59. Matyjaszewski, K., Jo, S. M., Paik, H., Gaynor, S. G. *Macromolecules* **1997**, *30*, 6398
60. Xia, J., Matyjaszewski, K. *Macromolecules* **1997**, *30*, 7692
61. Wang, J. S., Matyjaszewski, K. *Macromolecules* **1995**, *28*, 7572
62. Le, T. P., Moad, G., Rizzardo, E., Thang, S. H. *WO Patent* 9801478, **1998**
63. Corpart, P., Charmot, D., Biadatti, T., Zard, S. Z., Michelet, D. *WO Patent* 9858974, **1998**

64. Charmot, D., Corpart, P., Adam, H., Zard, S. Z., Biadatti, T., Bouhadir, G. *Macromol.Symp.* **2000**, *23*, 150
65. Lowe, A. B., McCormick, C. L. *Aust.J.Chem.* **2002**, *55*, 367
66. Perrier, S., Takolpuckdee, P. *J.Polym.Sci., Part A: Polym.Chem.* **2005**, *43*, 5348
67. Monteiro, M. J., de Brouwer, H. *Macromolecules* **2001**, *34*, 349
68. Barner-Kowollik, C., Quinn, J. F., Nguyen, T. L. U., Heuts, J. P. A., Davis, T. P. *Macromolecules* **2001**, *34*, 7849
69. Barner-Kowollik, C., Quinn, J. F., Morsley, D. R., Davis, T. P. *J.Polym.Sci., Part A: Polym.Chem.* **2001**, *39*, 1353
70. Barner-Kowollik, C., Coote, M. L., Davis, T. P., Radom, L., Vana, P. *J.Polym.Sci., Part A: Polym.Chem.* **2003**, *41*, 2828
71. Hawthorne, D. G., Moad, G., Rizzardo, E., Thang, S. H. *Macromolecules* **1999**, *32*, 5457
72. Coote, M. L., Henry, D. J. *Macromolecules* **2005**, *38*, 1415
73. Dureault, A., Gnanou, Y., Taton, D., Destarac, M., Leising, F. *Angew.Chem.Int.Ed.* **2003**, *42*, 2869
74. Bouhadir, G., Legrand, N., Quiclet-Sire, B., Zard, S. Z. *Tetrahedron.Lett.* **1999**, *40*, 277
75. Thang, S. H., Chong, Y. K., Mayadunne, R. T. A., Moad, G., Rizzardo, E. *Tetrahedron.Lett.* **1999**, *40*, 2435
76. Vosloo, J. J., De Wet-Roos, D., Tonge, M. P., Sanderson, R. D. *Macromolecules* **2002**, *35*, 4894
77. Destarac, M., Charmot, D., Franck, X., Zard, S. Z. *Makromol.Chem.Rapid Commun.* **200**, *21*, 1035
78. March, J. *Advanced Organic Chemistry, Reactions, Mechanisms, and Structure* 4th Edition, John Wiley & Sons: New York, **1992**
79. Mayadunne, R. T. A., Moad, G., Rizzardo, E. *Tetrahedron.Lett.* **2002**, *43*, 6811
80. Zheng, G., Pan, C. *Polymer* **2005**, *46*, 2802
81. Xiong, Q., Ni, P., Zhang, F., Yu, Z. *Polym.Bull.* **2004**, *53*, 1

82. Wang, R., Lowe, A. B. *J.Polym.Sci., Part A: Polym.Chem.* **2007**, *45*, 2468
83. Vasilieva, Y. A., Thomas, D. B., Scales, C. W., McCormick, C. L. *Macromolecules* **2004**, *37*, 2728
84. Thomas, D. B., Vasilieva, Y. A., Armentrout, R. S., McCormick, C. L. *Macromolecules* **2003**, *36*, 9710
85. Mitsukami, Y., Donovan, M. S., Lowe, A. B., McCormick, C. L. *Macromolecules* **2001**, *34*, 2248
86. Lowe, A. B., Wang, R., Tiriveedhi, V., Butko, P., McCormick, C. L. *Macromol.Chem.Phys.* **2007**, *208*, 2339
87. Lowe, A. B., Torres, M., Wang, R. *J.Polym.Sci., Part A: Polym.Chem.* **2007**, *45*, 5864
88. Lord, H. T., Quinn, J. F., Angus, S. D., Whittaker, M. R., Stenzel, M. H., Davis, T. P. *J.Mater.Chem.* **2003**, *13*, 2819
89. Laus, M., Papa, R., Sparnacci, K., Alberti, A., Benaglia, M., Macciantelli, D. *Macromolecules* **2001**, *34*, 7269
90. Kanagasabapathy, S., Sudalai, A., Benicewicz, B. C. *Macromol.Rapid.Commun.* **2001**, *22*, 1076
91. Donovan, M. S., Sumerlin, B. S., Lowe, A. B., McCormick, C. L. *Macromolecules* **2002**, *35*, 8663
92. Destarac, M., Brochon, C., Catala, J. M., Wilczewska, A., Zard, S. Z. *Macromol.Chem.Phys.* **2002**, *203*, 2281
93. Davies, M. C., Dawkins, J. V., Hourston, D. J. *Polymer* **2005**, *46*, 1739
94. Chiefari, J., Chong, Y. K., Ercole, F., Krstina, J., Jeffery, J., Le, T. P. T., Mayadunne, R. T. A., Meijs, G. F., Moad, C. L., Moad, G., Rizzardo, E., Thang, S. H. *Macromolecules* **1998**, *31*, 5559
95. Barner, L., Li, C. E., Hao, X., Stenzel, M. H., Barner-Kowollik, C., Davis, T. P. *J.Polym.Sci., Part A: Polym.Chem.* **2004**, *42*, 5067
96. Alstrum-Acevedo, J. H., DeSimone, J. M., Schauer, C. K., Papaniolas, J. *Polym.Mater.Sci.Eng.* **2004**, *91*, 721
97. Chong, Y. K., Moad, G., Rizzardo, E., Skidmore, M. A., Thang, S. H. *Macromolecules* **2007**, *40*, 9262

98. Chong, Y. K., Moad, G., Rizzardo, E., Skidmore, M., Thang, S. H. *Aust.J.Chem.* **2006**, *59*, 755
99. Ladaviere, C., Dorr, N., Claverie, J. P. *Macromolecules* **2001**, *34*, 5370
100. Llauro, M. L. J., Boisson, F., Delolme, F., Ladaviere, C., Claverie, J. *J.Polym.Sci., Part A: Polym.Chem.* **2004**, *42*, 5349
101. Taton, D., Welczewska, A. Z., Destarac, M. *Makromol.Chem.Rapid Commun.* **2001**, *22*, 1497
102. Ferguson, C. J., Hughes, R. J., Nguyen, D., Pham, B. T. T., Gilbert, R. G., Serelis, A. K., Such, C. H., Hawket, B. S. *Macromolecules* **2005**, *38*, 2191
103. Ferguson, C. J., Hughes, R. J., Pham, B. T. T., Hawket, B. S., Gilbert, R. G., Serelis, A. K., Such, C. H. *Macromolecules* **2002**, *35*, 9243
104. Quinn, J. F., Davis, T. P., Rizzardo, E. *Chem.Commun.* **2001**, 1044
105. Perrier, S., Takolpuckdee, P., Westwood, J., Lewis, D. M. *Macromolecules* **2004**, *37*, 2709
106. Perrier, S., Barner-Kowollik, C., Quinn, J. F., Vana, P., Davis, T. P. *Macromolecules* **2002**, *35*, 8300
107. McLeary, J. B., McKenzie, J. M., Tonge, M. P., Sanderson, R. D., Klumperman, B. *Chem.Commun.* **2004**, 1950
108. Barner, L., Barner-Kowollik, C., Davis, T. P., Stenzel, M. H. *Aust.J.Chem.* **2004**, *57*, 19
109. Jesberger, M., Barner, L., Stenzel, M. H., Malmstroem, E., Davis, T. P., Barner-Kowollik, C. J. *J.Polym.Sci., Part A: Polym.Chem.* **2003**, *41*, 3847
110. Chong, Y. K., Krstina, J., Le, T. P. T., Moad, G., Postma, A., Rizzardo, E., Thang, S. H. *Macromolecules* **2003**, *36*, 2256
111. Venkatesh, R., Staal, B. B. P., Klumperman, B., Monteiro, M. J. *Macromolecules* **2004**, *37*, 7906
112. Dereault, A., Taton, D., Destarac, M., Leising, F., Gnanou, Y. *Macromolecules* **2004**, *37*, 5513
113. Zhu, J., Zhu, X., Zhou, D. J. *Macromol.Sci., Part A* **2004**, *41*, 827
114. Zhu, J., Zhu, X., Cheng, Z., Lu, J., Liu, F. *J.Macromol.Sci., Chem.* **2003**, *40*, 963

115. Hu, Y. C., Liu, Y., Pan, C. Y. *J. Macromol. Sci., Chem.* **2004**, *42*, 4862
116. Ma, Z., Lacroix-Desmazes, P. *J. Macromol. Sci., Chem.* **2004**, *53*, 349
117. Tichagwa, L., Gotz, C., Tonge, M., Sanderson, R., Pasch, H. *Macromol. Symp.* **2003**, *193*, 251
118. Albertin, L., Stenzel, M., Barner-Kowollik, C., Foster, L. J. R., Davis, T. P. *Macromolecules* **2004**, *37*, 7530
119. Hao, X., heuts, J. P. A., Barner-Kowollik, C., Davis, T. P., Evans, E. *J. Polym. Sci., Part A: Polym. Chem.* **2003**, *41*, 2949
120. Hao, X., Stenzel, M. H., Barner-Kowollik, C., Davis, T. P., Evans, E. *Polymer* **2004**, *45*, 7401
121. Licciardi, M., Tang, Y., Billingham, N. C., Armes, S. P., Lewis, A. L. *Biomacromolecules* **2005**, *6*, 1085
122. Lobb, E. J., Ma, I., Billingham, N. C., Armes, S. P., Lewis, A. L. *J. Am. Chem. Soc.* **2001**, *123*, 7913
123. Lowe, A. B., Sumerlin, B. S., McCormick, C. L. *Polymer* **2003**, *44*, 6761
124. Ma, I., Lobb, E. J., Billingham, N. C., Armes, S. P., Lewis, A. L., Lloyd, A. W. *Macromolecules* **2002**, *35*, 9306
125. Ma, Y., Tang, Y., Billingham, N. C., Armes, S. P., Lewis, A. L., Lloyd, A. W., Salvage, J. P. *Macromolecules* **2003**, *36*, 3475
126. Mayadunne, R. T. A., Rizzardo, E., Chiefari, J., Chong, Y. K., Moad, G., Thang, S. H. *Macromolecules* **1999**, *32*, 6977
127. Mayadunne, R. T. A., Rizzardo, E., Chiefari, J., Krstina, J., Moad, G., Postma, A., Thang, S. H. *Macromolecules* **2000**, *33*, 243
128. Rzayev, J., Penelle, J. *Angew. Chem. Int. Ed.* **2004**, *43*, 1691
129. Shinoda, H., Matyjaszewski, K. *Makromol. Chem. Rapid Commun.* **2001**, *22*, 1176
130. Shinoda, H., Matyjaszewski, K., Okrasa, L., Mierzwa, M., Pakula, T. *Macromolecules* **2003**, *36*, 4772
131. Uzulina, I., Kanagasabapathy, S., Claverie, J. *Macromol. Symp.* **2000**, *150*, 33

132. Venketesh, R., Yajjou, L., Koning, C. E., Klumperman, B. *Macromol.Chem.Phys.* **2004**, *205*, 2161
133. Xu, X., Huang, J. *J.Polym.Sci., Part A: Polym.Chem.* **2004**, *42*, 5523
134. Zhu, J., Di, Z., Zhu, X., Chen, G. *J.Polym.Sci., Part A: Polym.Chem.* **2004**, *42*, 2558
135. Zhu, J., Zhou, D., Zhu, X., Cheng, Z. *J.Macromol.Sci.Pure Appl.Chem.* **2004**, *41*, 1059
136. Rizzardo, E., Chiefari, J., Mayadunne, R. T. A., Moad, G., Thang, S. H. *ACS Symp.Ser.* **2000**, *768*, 278
137. Stenzel, M., Cummins, L., Roberts, G. E., Davis, T. P., Vana, P., Barner-Kowollik, C. *Macromol.Chem.Phys.* **2003**, *204*, 1160
138. Stenzel, M., Davis, T. P., Barner-Kowollik, C. *Chem.Commun.* **2004**, 1546
139. Stenzel-Rosenbaum, M., Davis, T. P., Chen, V., Fane, A. G. *J.Polym.Sci., Part A: Polym.Chem.* **2001**, *39*, 2777
140. Mayadunne, R. T. A., Jeffery, J., Moad, G., Rizzardo, E. *Macromolecules* **2003**, *36*, 1505
141. Schilli, C., Lanzendoerfer, M. G., Mueller, A. H. E. *Macromolecules* **2002**, *35*, 6819
142. Lowe, A. B., Sumerlin, B. S., Donovan, M. S., McCormick, C. L. *J.Am.Chem.Soc.* **2002**, *124*, 11526
143. Depuy, C. H. K. R. W. *Chem.Rev.* **1960**, *60*, 444
144. Llauro, M. L. J., Boisson, F., Delolme, F., Ladaviere, C., Claverie, J. *J.Polym.Sci., Part A: Polym.Chem.* **2004**, *42*, 5439
145. Mori, K. S. T., Masuda, S. *Tetrahedron.Lett.* **1978**, *37*, 3477
146. Rizzardo, E. C. J., Chong, B. Y. K., Ercole, F., Krstina, J., Jeffery, J., Le, T. P. T., Mayadunne, R. T. A., Meijs, G. F., Moad, C. L., Moad, G., Thang, S. H. *Macromol.Symp.* **1999**, *143*, 291
147. Sumerlin, B. S., Lowe, A. B., Stroud, P. A., Urban, M. W., McCormick, C. L. *Langmuir* **2003**, *19*, 5559
148. Vana, P., Albertin, L., Barner, L., Davis, T. P., Barner-Kowollik, C. *J.Polym.Sci., Part A: Polym.Chem.* **2002**, *40*, 4032
149. Yamago, S., Lida, K., Yoshida, J. *J.Am.Chem.Soc.* **2002**, *124*, 13666

150. Yamago, S. *J. Polym. Sci., Part A: Polym. Chem.* **2005**, *44*, 1
151. Blecher, L., Lorez, D. H., Lowd, H. L., Wood, A. S., Wyman, D. P. *Handbook of Water-Soluble Gums and Resins* McGraw-Hill Book Co., Inc., New York, **1980**,
152. Forder, C., Patrickios, C. S., Armes, S. P., Billingham, N. C. *Macromolecules* **1996**, *29*, 8160
153. Forder, C., Patrickios, C. S., Billingham, N. C., Armes, S. P. *Chem. Commun.* **1996**, 883
154. Kujawa, P., Segui, F., Shaban, S., Diab, C., Okada, Y., Tanaka, F., Winnik, F. M. *Macromolecules* **2006**, *39*, 341
155. Kulicke, W. M., Kniewske, R., Klein, J. *Prog. Polym. Sci.* **1982**, *8*, 373
156. Sumerlin, B. S., Lowe, A. B., Thomas, D. B., Convertine, A. J., Donovan, M. S., McCormick, C. L. *J. Polym. Sci., Part A: Polym. Chem.* **2004**, *42*, 1724
157. Alfrey, T., Fuoss, R. M., Morawetz, H., Pinner, H. *J. Am. Chem. Soc.* **1952**, *74*, 438
158. Armemtrout, R. S., McCormick, C. L. *Macromolecules* **2000**, *33*, 419
159. Armemtrout, R. S., McCormick, C. L. **2000**, *33*, 2994
160. Baumann, M., Schmidt-Naake, G. *Macromol. Chem. Phys.* **1999**, *201*, 2751
161. Bütün, V., Armes, S. P., Billingham, N. C. *Polymer* **2001**, *42*, 5993
162. Bütün, V., Bennett, C. E., Vamvakaki, M., Lowe, A. B., Billingham, N. C., Armes, S. P. *J. Mater. Chem.* **1997**, *7*, 1693
163. Bütün, V., Billingham, N. C., Armes, S. P. *Chem. Commun.* **1997**, 671
164. Bütün, V., Billingham, N. C., Armes, S. P. *J. Am. Chem. Soc.* **1998**, *120*, 11818
165. Chalari, I., Pispas, S., Hadjichristidis, N. *J. Polym. Sci., Part A: Polym. Chem.* **2001**, *39*, 2889
166. Chen, Z., Cai, J., Jiang, X., Yang, C. **2001**, *37*, 33
167. Convertine, A. J., Sumerlin, B. S., Thomas, D. B., McCormick, C. L. *Macromolecules* **2003**, *36*, 4679
168. Davis, K. A., Matyjaszewski, K. *Macromolecules* **2001**, *34*, 2101
169. De Paz Banez, M. V., Robinson, K. L., Bütün, V., Armes, S. P. *Polymer* **2001**, *42*, 29

170. Fischer, A., Jonquieres, A., Brembilla, A., Lochon, P. *Macromolecules* **1999**, *32*, 6069
171. Gan, L., Ravi, P., Mao, B. W., Tam, K. *J.Polym.Sci., Part A: Polym.Chem.* **1997**, *35*, -2035
172. McCormick, C. L., Blackmon, K. P., Elliott, D. L. *Polymer* **1986**, *27*, 1976
173. McCormick, C. L., Salazar, L. C. *J.Polym.Sci., Part A: Polym.Chem.* **1993**, *31*, 1099
174. Shi, L., Chapman, T. M., Beckman, E. J. *Macromolecules* **2003**, *36*, 2563
175. Shyluk, W. P. *J.Polym.Sci., Part A: Polym.Chem.* **1964**, *2*, 2191
176. Simmons, M. R., Patrickios, C. S. *Macromolecules* **1998**, *31*, 9075
177. Simmons, M. R., Patrickios, C. S. *J.Polym.Sci., Part A: Polym.Chem.* **2003**, *41*, 2688
178. Thomas, D. B., Vasilieva, Y. A., Armentrout R.S. *Macromolecules* **2003**, *36*, 9710
179. Tsitsiliani, C., Voyiatzis, G. A., Kallitsis, J. K. *Makromol.Chem.Rapid Commun.* **2000**, *21*, 1130
180. Varsheny, S. K., Zhong, X. F., Eisenbert, A. *Macromolecules* **1993**, *26*, 701
181. Salamone, J. C., Volksen, W., Israel, S. C., Olson, A. P., Raia, D. C. *Polymer* **1977**, *18*, 1058
182. Monroy Soto, V. M., Galin, J. C. *Polymer* **1984**, *25*, 121
183. Kathmann, E. E., White, L. A., McCormick, C. L. *Polymer* **1997**, *38*, 871
184. Kathmann, E. E., White, L. A., McCormick, C. L. *Polymer* **1997**, *38*, 879
185. Favresse, P., Laschewsky, A. *Polymer* **2001**, *42*, 2755
186. Bonte, N., Laschewsky, A. *Polymer* **1996**, *37*, 2011
187. Hasegawa, T., Iwasaki, Y., Ishihara, K. *J.Biomed.Mater.Res.* **2002**, *63*, 333
188. Ishihara, K., Iwasaki, Y., Fiujiike, A., Kurita, K., Nakabayashi, N. *J.Polym.Sci., Part A: Polym.Chem.* **1996**, *34*, 199
189. Ishihara, K., Ueda, T. *Polym.J.* **1990**, *22*, 355
190. Ishihara, K., Ziats, N. P., Tierney, B. P., Nakabayashi, N., Anderson, J. M. *J.Biomed.Mater.Res.* **1991**, *25*, 1397

191. Kros, A., Gerritsen, M., Murk, J., Jansen, J. A., Sommerdijk, N. A. J. M. *J.Polym.Sci., Part A: Polym.Chem.* **2001**, *39*, 468
192. Oishi, T., Fukuda, T., Uchiyama, H., Kondou, F., Hoe, H., Tsutsumi, H. *Polymer* **1997**, *38*, 3109
193. Sugiyama, K., Ohga, K., Aoki, H. *Macromol.Chem.Phys.* **1995**, *196*, 1907
194. Chrisment, J., Galin, M., Galin, J. C. *New J.Chem.* **1995**, *19*, 303
195. Galin, J. C., Galin, M. *J.Polym.Sci., Part B: Polym.Phys.* **1995**, *33*, 2033
196. Grassl, B., Francois, J., Billon, L. *Polym.Int.* **2001**, *50*, 1162
197. Pujol-Fortin, M.-L., Galin, J. C. *Macromolecules* **1991**, *24*, 4523
198. Pujol-Fortin, M.-L., Galin, J. C. *Polymer* **1994**, *35*, 1462
199. Lowe, A. B., McCormick, C. L. *Chem.Rev.* **2002**, *102*, 4177
200. Nagaya, T., Li, Y.-J. *Prog.Polym.Sci.* **1999**, *24*, 143
201. Tuzar, Z., Popisil, H., Plestil, J., Lowe, A. B., Baines, F. L., Billingham, N. C., Armes, S. P. *Macromolecules* **1997**, *30*, 2509
202. Riess, G. *Prog.Polym.Sci.* **2003**, *28*, 1107
203. Posner, T. *Ber. Chem. Ges.* **1905**, *38*, 646
204. Hoyle, C. E., Lee, T. Y., Roper, T. *J.Polym.Sci., Part A: Polym.Chem.* **2004**, *42*, 5301
205. Kolb, H. C., Finn, M. G., Sharpless, K. B. *Angew.Chem.Int.Ed.* **2001**, *40*, 2004
206. Brummelhuis, N. T., Diehl, C., Schlaad, H. *Macromolecules* **2008**, *41*, 9946
207. Dondoni, A. *Angew.Chem.Int.Ed.* **2008**, *47*, 2
208. Chan, J. W., Yu, B., Hoyle, C. E., Lowe, A. B. *Chem.Commun.* **2008**, 4959
209. Kumar, A., Akanksha. *Tetrahedron* **2007**, *63*, 11086
210. Dix, L. R., Ebdon, J. R., Hodge, P. *Eur.Polym.J.* **1995**, *31*, 653
211. Methot, J. L., Roush, W. R. *Adv.Synth.Catal.* **2004**, *346*, 1035
212. Gimbert, C., Lumbierres, M., Marchi, C., Moreno-Manas, M., Sebastien, R. M.,

- Vallribera, A. *Tetrahedron* **2005**, *61*, 8598
213. Ananikov, V. P., Orlov, N. V., Beletskaya. *Organomet.* **2006**, *25*, 1970
214. Manarin, F., Roehrs, J. A., Prigol, M., Alves, D., Nogueira, C. W., Zeni, G. *Tetrahedron.Lett.* **2007**, *48*, 4805
215. Ogawa, A., Ikeda, T., Kimura, K., Hirao, T. *J.Am.Chem.Soc.* **1999**, *121*, 5108
216. Shoai, S., Bichler, P., Kang, B., Buckley, H., Love, J. A. *Organomet.* **2007**, *26*, 5778
217. Yadav, J. S., Subba Reddy, B. V., Raju, A., Ravindar, K., Baishya, G. *Chem.Lett.* **2007**, *36*, 1474
218. Kondoh, A., Takami, K., Yorimitsu, H., Oshima, K. *J.Org.Chem.* **2005**, *70*, 6468
219. Kuniyasu, H., Ogawa, A., Sato, K. *J.Am.Chem.Soc.* **1992**, *114*, 5902
220. Backvall, J. E., Ericsson, A. *J.Org.Chem.* **1994**, *59*, 5850
221. Han, L. b., Zhang, C., Yazawa, H., Shimada, S. *J.Am.Chem.Soc.* **2004**, *126*, 5080
222. Jethmalani, J., Dreher A.W., Abdel-Sadek, G., Chomyn, J., Li, J. M., Qaddoura, M. *U.S.PatentAppl Publ* 20060052547, **2006**
223. Smith, R. A., Herold, R. D., Okoroafor, M. O. *PCTInt Appl* WO 0064964, **2000**
224. Lu, H., Carioscia, J. A., Stansbury, J. W., Bowman, C. N. *Dent.Mater.* **2005**, *21*, 1129
225. Khire, V. S., Lee, T. Y., Bowman, C. N. *Macromolecules* **2007**, *40*, 5669
226. Killops, K. L., Campos, L. M., Hawker, C. J. *J.Am.Chem.Soc.* **2008**, *130*, 5062
227. Bütün, V., Billingham, N. C., Armes, S. P. *J.Am.Chem.Soc.* **1998**, *120*, 12135
228. Bütün, V., Armes, S. P., Billingham, N. C., Tuzar, Z., Rankin, A., Eastoe, J., Heenan, R. K. *Macromolecules* **2001**, *34*, 1503
229. Liu, S., Weaver, J. V. M., Tang, Y., Billingham, N. C., Armes, S. P. *Macromolecules* **2002**, *35*, 6121
230. Sonawane, N. D., Szoka Jr, F. C., Verkman, A. S. *J.Biol.Chem.* **2003**, *278*, 44826
231. Gu, T., Hasebe, Y. *Anal.Chim.Acta.* **2004**, *525*, 191
232. Pelta, J., Livolant, F., Sikorav, J.-L. *J.Biol.Chem.* **1996**, *271*, 5656

233. Igarashi, K., Kashiwagi, K. *Biochem.Biophys.Res.Commun.* **2000**, 271, 559
234. Moad, G., Rizzardo, E., Thang, S. H. *Aust.J.Chem.* **2005**, 58, 379
235. Lowe, A. B., McCormick, C. L. *Prog.Polym.Sci.* **2007**, 32, 283
236. Barner-Kowollik, C., Buback, M., Charleuz, B., Coote, M. L., Drache, M., Fukuda, T., Goto, A., Klumperman, B., Lowe, A. B., McCleary, J. B., Moad, G., Monteiro, M. J., Sanderson, R. D., Tonge, M. P., Vana, P. J. *J.Polym.Sci., Part A: Polym.Chem.* **2006**, 44, 5809
237. Favier, A., Charreyre, M.-T. *Macromol.Rapid.Commun.* **2006**, 27, 653
238. Stenzel, M. *Chem.Commun.* **2008**, 3468
239. Scales, C. W., Vasilieva, Y. A., Convertine, A. J., Lowe, A. B., McCormick, C. L. *Biomacromolecules* **2005**, 6, 1846
240. Vasilieva, Y. A., Scales, C. W., Thomas, D. B., Ezell, R. G., Lowe, A. B., Ayres, N., McCormick, C. L. *J.Polym.Sci., Part A: Polym.Chem.* **2005**, 43, 3141
241. Lowe, A. B., Wang, R. *Polymer* **2007**, 48, 2221
242. Ting, S. R. S., Granville, A. M., Quemener, D., Davis, T. P., Stenzel, M., Barner-Kowollik, C. *Aust.J.Chem.* **2007**, 60, 405
243. He, L., Read, E. S., Armes, S. P., Adams, D. J. *Macromolecules* **2007**, 40, 4429
244. Wang, R., McCormick, C. L., Lowe, A. B. *Macromolecules* **2005**, 38, 9518
245. Qui, X.-P., Winnik, F. M. *Macromol.Rapid.Commun.* **2006**, 27, 1648
246. Gondi, S. R., Vogt, A. P., Sumerlin, B. S. *Macromolecules* **2008**, 40, 474
247. Convertine, A. J., Lokitz, B. S., Lowe, A. B., Scales, C. W., Myrick, L. J., McCormick, C. L. *Macromol.Rapid.Commun.* **2005**, 26, 791
248. Heredia, K. L., Nguyen, T. H., Chang, C.-W., Bulmus, V., Davis, T. P., Maynard, H. D. *Chem.Commun.* **2008**, 3245
249. Li, M., De, P., Gondi, S. R., Sumerlin, B. S. *J.Polym.Sci., Part A: Polym.Chem.* **2008**, 46, 5093
250. Mitsukami, Y., Hashidzume, A., Yusa, S., Morishima, Y., Lowe, A. B., McCormick, C. L. *Polymer* **2006**, 47, 4333

251. Roy, D., Cambre, J. N., Sumerlin, B. S. *Chem. Commun.* **2008**, 2477
252. Zhou, D., Zhu, X., Zhu, J., Cheng, Z. *Polymer* **2008**, *49*, 3048
253. Zhang, H., Deng, J., Lu, L., Cai, Y. *Macromolecules* **2008**, *40*, 9252
254. Nicolay, R., Kwak, Y., Matyjaszewski, K. *Macromolecules* **2008**, *41*, 4585
255. Goldmann, A. S., Quemener, D., Millard, P.-E., Davis, T. P., Stenzel, M., Barner-Kowollik, C., Müller, A. H. E. *Polymer* **2008**, *49*, 2274
256. Mori, H., Kato, I., Matsuyama, M., Endo, T. *Macromolecules* **2008**, *41*, 5604
257. Boyer, C., Bulmus, V., Liu, J., Davis, T. P., Stenzel, M., Barner-Kowollik, C. *J. Am. Chem. Soc.* **2007**, *129*, 7145
258. Deng, Z., Boucekif, H., Babooram, K., Housni, A., Choytun, N., Narain, R. *J. Polym. Sci., Part A: Polym. Chem.* **2008**, *46*, 4984
259. Hu, Y. Q., Kim, M. S., Kim, B. S., Lee, D. S. *Polymer* **2007**, *48*, 3437
260. Chan, Y., Wong, T., Byrne, F., Kavallaris, M., Bulmus, V. *Biomacromolecules* **2008**, *9*, 1826
261. Assem, Y., Chaffey-Millar, H., Barner-Kowollik, C., Wegner, G., Agarwal, S. *Macromolecules* **2007**, *40*, 3907
262. Favier, A., Barner-Kowollik, C., Davis, T. P., Stenzel, M. *Macromol. Chem. Phys.* **2004**, *205*, 925
263. Scales, C. W., Convertine, A. J., McCleary, J. B. B. *Biomacromolecules* **2006**, *7*, 1389
264. Becer, R., Hahn, S., Fijten, M. W. M., Thijs, H. M. L., Hoogenboom, R., Schubert, U. S. *J. Polym. Sci., Part A: Polym. Chem.* **2008**, *46*, 7138
265. Albertin, L., Kohlert, C., Stenzel, M., Foster, L. J. R., Davis, T. P. *Biomacromolecules* **2004**, *5*, 255
266. Biegle, A., Mathis, A., Galin, J. C. *Macromol. Chem. Phys.* **1999**, *200*, 1393
267. Ward, M., Sanchez, M., Elasri, M. O., Lowe, A. B. *J. Appl. Polym. Sci.* **2006**, *101*, 1036
268. Lowe, A. B., Vamvakaki, M., Wassall, M. A., Wong, L., Billingham, N. C., Armes, S. P., Lloyd, A. W. *J. Biomed. Mater. Res.* **2000**, *52*, 88

269. Kudaibergenov, S., Jaeger, W., Laschewsky, A. *Adv. Polym. Sci.* **2006**, *201*, 157
270. Nagaya, J., Uzawa, H., Minoura, N. *Macromol. Rapid Commun.* **1999**, *20*, 573
271. Ladenheim, H., Morawetz, H. *J. Polym. Sci.* **1957**, *26*, 251
272. Hart, R., Timmerman, D. *J. Polym. Sci.* **1958**, *28*, 638
273. Lowe, A. B., Billingham, N. C., Armes, S. P. *Macromolecules* **1999**, *32*, 2141
274. Kimura, M., Takai, M., Ishihara, K. *J. Biomed. Mater. Res.* **2007**, *80*, 45
275. Sawada, S., Sakaki, S., Iwasaki, Y., Nakabayashi, N., Ishihara, K. *J. Biomed. Mater. Res.* **2003**, *64*, 611
276. Ueda, T., Oshida, H., Kurita, K., Ishihara, K., Nakabayashi, N. *Polym. J.* **1992**, *24*, 1259
277. Ishihara, K., Aragaki, R., Ueda, T., Watanabe, A., Nakabayashi, N. *J. Biomed. Mater. Res.* **1990**, *24*, 1069
278. Lewis, A. L., Hughes, P. D., Kirkwood, L. C., Leppard, S. W., Redman, R. P., Tolhurst, L. A., Stratford, P. W. *Biomaterials* **2000**, *21*, 1847
279. West, S. L., Salvage, J. P., Lobb, E. J., Armes, S. P., Billingham, N. C., Lewis, A. L., Hanlon, G. W., Lloyd, A. W. *Biomaterials* **2004**, *25*, 1195
280. Moro, T., Takatori, Y., Ishihara, K., Konno, T., Takigawa, Y., Matsushita, T. *Nature Materials* **2004**, *3*, 829
281. Fujii, K., Matsumoto, H., Koyama, Y., Iwasaki, Y., Ishihara, K., Takakuda, K. *J. Vet. Med. Sci.* **2008**, *70*, 167
282. Rankin, D. A., Lowe, A. B. *Macromolecules* **2008**, *41*, 614
283. Colak, S., Tew, G. N. *Macromolecules* **2008**, *41*, 8436
284. McCormick, C. L., Lowe, A. B. *Acc. Chem. Res.* **2004**, *37*, 312
285. Barner-kowollik, C., *Handbook of RAFT Polymerization* Wiley-VCH **2008**
286. Convertine, A. J., Lokitz, B. S., Vasilieva, Y., Myrick, L. J., W., S. C., Lowe, A. B., McCormick, C. L. *Macromolecules* **2006**, *39*, 1724
287. Pound, G., Aguesse, F., McCleary, J. B., Lange, R. F. M., Klumperman, B. *Macromolecules* **2007**, *40*, 8861

288. Mori, H., Ookuma, H., Endo, T. *Macromolecules* **2008**, *41*, 6925
289. Yasser, A., Andreas, G., Seema, A. *Macromol.Rapid Commun.* **2007**, *28*, 1923
290. Arotcarena, M., Heise, B., Ishaya, S., Laschewsky, A. *J.Am.Chem.Soc.* **2002**, *124*, 3787
291. Donovan, M. S., Lowe, A. B., Sanford, T. A., McCormick, C. L. *J.Polym.Sci., Part A: Polym.Chem.* **2003**, *41*, 1262
292. Yusa, S., Fukuda, K., Yamamoto, T., Ishihara, K., Morishima, Y. *Biomacromolecules* **2005**, *6*, 663
293. Stenzel, M. H., Barner-kowollik, C., Davis, T. P., Dalton, H. M. *Macromol.Biosci.* **2005**, *4*, 445
294. Gabaston, L. I., Furlong, S. A., Jackson, R. A., Armes, S. P. *Polymer* **1999**, *40*, 4505
295. Madsen, J., Armes, S. P., Lewis, A. L. *Macromolecules* **2006**, *39*, 7455
296. Chan, J. W., Hoyle, C. E., Lowe, A. B. *J.Am.Chem.Soc.*
297. Radu, L. C., Yang, J., Kopecek, J. *Macromol.Biosci.* **2009**, *9*, 36
298. Ghosh, S. S., Kao, P. M., McCue, A. W., L., C. H. *Bioconjugate.Chem.* **1990**, *1*, 71
299. Gress, A., Volkel, A., Schlaad, H. *Macromolecules* **2007**, *40*, 7928
300. Rissing, C., Son, D. Y. *Organomet.* **2008**, *27*, 5394
301. Campos, L. M., Meinel, I., Guino, R. G., Schierhorn, M., Gupta, N., Stucky, G. D., Hawker, C. J. *Adv.Mater.* **2008**, *20*, 3728
302. Pounder, R. J., Stanford, M. J., Brooks, P., Richards, S. P., Dove, A. P. *Chem.Commun.* **2008**, 5158
303. Li, M., De, P., Gondi, S. R., Sumerlin, B. S. *J.Polym.Sci., Part A: Polym.Chem.* **200**, *46*, 5093
304. Bader, H., Cross, L. C., Heilbron, I., Jones, E. R. H. *Chem.Soc.J.* **1949**, *1*, 619
305. Sauer, J. C. *J.Am.Chem.Soc.* **1957**, *79*, 5314
306. Fairbanks, B. D., Scott, T. F., Kloxin, C. J., Anseth, K. S., Bowman, C. N. *Macromolecules* **2009**, *42*, 211
307. Chan, J. W., Zhou, H., Hoyle, C. E., Lowe, A. B. *Chem.Mater.* In Press

308. Moad, G., Rizzardo, E., Thang, S. H. *Aust.J.Chem.* **2006**, *59*, 669
309. Vogt, A. P., Sumerlin, B. S. *Macromolecules* **2008**, *41*, 7368
310. Xu, J., He, J., Fan, D., Wang, X., Yang, Y. *Macromolecules* **2006**, *39*, 8616
311. Postma, A., Davis, T. P., Moad, G., O'Shea, M. S. *Macromolecules* **2005**, *38*, 5371
312. Moad, G., Chong, Y. K., Postma, A., Rizzardo, E., Thang, S. H. *Polymer* **2005**, *46*, 8458
313. Stewart, I. C., Bergman, R. G., Toste, F. D. *J.Am.Chem.Soc.* **2003**, *125*, 8696
314. Campos, L. M., Killops, K. L., Sakai, R., Paulusse, J. M. J., Dameron, D., Drockenmuller, E., Messmore, B. W., Hawker, C. J. *Macromolecules* **2008**, *41*, 7063
315. Boutris, C., Chatzi, E. G., Kiparissides, C. *Polymer* **1997**, *38*, 2567
316. Costa, R. O. R., Freitas, R. F. S. *Polymer* **2002**, *43*, 5879
317. Winnik, F. M., Ringsdorf, H., Venzmer, J. *Macromolecules* **1990**, *23*, 2415
318. Housni, A., Narain, R. *Eur.Polym.J.* **2007**, *43*, 4344
319. Satokawa, Y., Shikata, T., Tanaka, F., Qiu, X.-P., Winnik, F. M. *Macromolecules* **2009**, *42*, 4100
320. Xia, Y., TYin, X., Burke, N. A. D., Stver, H. D. H. *Macromolecules* **2005**, *38*, 5937
321. Xia, Y., Burke, N. A. D., Stver, H. D. H. *Macromolecules* **2006**, *39*, 2275
322. Okada, Y., Tanaka, F. *Macromolecules* **2005**, *38*, 4465
323. Wu, C., Li, W., Zhu, X. X. *Macromolecules* **2004**, *37*, 4989